

# Operational impact of quantum resources in chemical dynamics

Julia Liebert<sup>1</sup> and Gregory D. Scholes<sup>1,\*</sup>

<sup>1</sup>*Department of Chemistry, Princeton University, Princeton, NJ 08540, United States*

(Dated: March 10, 2026)

Quantum coherence and other non-classical features are widely discussed in chemical dynamics, yet it remains difficult to quantify when such resources are operationally relevant for a given process and observable. While quantum resource theories provide a comprehensive framework for comparing free and resourceful settings, existing approaches typically rely on resource monotones or on performance bounds under free operations, and do not directly quantify the maximal influence a chosen resource can exert on a fixed chemical dynamics. Here, we introduce task specific, process level quantifiers that upper bound the largest change a quantum resource can induce in a target figure of merit. Central is a resource impact functional  $\mathcal{C}_M(\Lambda)$ , defined by comparing a state with its paired resource-free counterpart under the same quantum channel  $\Lambda$ , which admits an operational interpretation in binary hypothesis testing. We derive variation and time bounds that constrain how rapidly a resource can modify a target signal, providing resource-aware analogues of quantum speed limits. Moreover, we show that open system dynamics can be decomposed into free and resourceful components such that only the resourceful component contributes to  $\mathcal{C}_M(\Lambda)$ , thereby isolating the parts of a generator responsible for resource-induced changes in the observable. We illustrate the framework exemplary for energy transfer in a donor-acceptor dimer in two analytically solvable regimes. Our results provide a general toolbox for diagnosing and benchmarking quantum resource effects in molecular processes.

## I. INTRODUCTION

The interface of quantum information science and chemistry offers a unique opportunity to advance quantum technologies while at the same time providing new insights into chemical mechanisms [1–5]. Quantum-information measures such as entanglement, quantum discord, and coherence have increasingly been used as descriptors of chemical structure and dynamics, including chemical bonding and bond formation [6–19], vibrational spectra [20, 21], and critical points on potential energy surfaces [22]. Moreover, experimental and theoretical evidence for long-lived electronic and vibronic coherences in molecular systems, such as photosynthetic complexes and other molecular aggregates [23–43], as well as spin-correlated radical pairs [44–46], has led to an ongoing debate over whether such coherences are functionally exploited or are merely by-products of the underlying dynamics. In all these settings, a central challenge is to distinguish the contribution of genuinely quantum effects from that of classical structure and environmental noise.

However, even when a positive correlation is observed between a quantum quantity, such as coherence or entanglement, and a chemical figure of merit, such as a yield or transport efficiency, this does not by itself establish that the quantum resource *causes* the observed enhancement as a third structural feature may influence both the resource and the observable. Using coherence or entanglement merely as static descriptors is therefore not sufficient to determine the *operational* role of quantum effects in chemical systems, in particular for dynamical

processes. A meaningful and comprehensive assessment requires comparing the effect of a given quantum feature to an appropriate “classical” baseline in which that feature has been removed.

Quantum resource theories (QRTs) provide a natural framework for such comparisons [47, 48]. In a QRT, both quantum states and operations are partitioned into free and resourceful ones: free objects model states and controls available at negligible cost, while resourceful ones correspond to genuinely quantum features such as coherence, asymmetry, or entanglement. A central theme in this literature is to identify resources via improved performance in operational tasks compared to the best free strategy. In particular, several works have shown that resourceful states, measurements, and channels can outperform all free counterparts in suitable state, sub-channel, or channel discrimination problems, and that standard resource monotones such as the (generalised) robustness or robustness of coherence quantitatively capture this advantage [49–54]. These results compare optimised resourceful and free strategies, typically via

$$\max_{\rho \in \mathcal{R}}(\text{task performance}) \quad \text{vs.} \quad \max_{\sigma \in \mathcal{F}}(\text{task performance}),$$

where  $\mathcal{R}$  and  $\mathcal{F}$  denote the resourceful and free sets, respectively. In contrast, to address the functional chemical question pursued here, namely, how sensitive a specific chemical figure of merit is to a quantum feature for a fixed process, it is important to keep each state paired with its own free counterpart. In QRTs, such a paired quantum-classical baseline is provided by resource-destroying maps  $\mathcal{G}$ , which map every state to a corresponding free state by “removing” the chosen resource [47, 55, 56]. In this setting, we compare the task performance of  $\rho$  directly with that of  $\mathcal{G}(\rho)$  under the same dynamics, rather than optimising independently over all resourceful and all free

---

\* gscholes@princeton.edu

inputs. As we will show, this paired comparison is crucial for quantifying the operational impact of quantum resources in concrete chemical processes.

Furthermore, recent works have begun to connect QRTs to concrete chemical scenarios, for example by linking non-stabilizerness to bond formation [57], or by deriving thermodynamic resource-theoretic bounds on photoisomerization yields [58, 59]. These approaches typically focus on characterising what free operations can achieve. In the photoisomerization case [58, 59], for instance, one asks for the maximal yield compatible with thermodynamic constraints, largely independent of the detailed molecular dynamics.

In contrast, in molecular settings the dynamics is often effectively fixed, for example by a specific open system Hamiltonian and its associated master equation, and is usually not a free operation for the resource under consideration. If one is interested in the functional role of a given quantum resource for a particular chemical process, analysing restrictions under free operations alone therefore does not directly address the relevant question. Instead, the central issue becomes: *for this fixed process, to what extent can a chosen quantum resource actually influence a chemically meaningful observable such as a yield or another figure of merit?* Answering this process-level question requires shifting the emphasis from optimising over free operations to analysing the impact of quantum resources for the actual dynamics. While not phrased in the language of resource theories, this type of resource-induced operational advantage already appears, for example, in enhanced coherent control via entangled reactant states [60, 61].

To address this question when and where quantum effects are operational in chemical processes and can be harnessed to improve target yields, we develop in this paper a theoretical framework tailored to the setting with specific processes and readouts. Building on the paired quantum-classical baseline provided by a resource-destroying map  $\mathcal{G}$ , we introduce a so-called resource impact functional that provides a rigorous upper bound on the maximal modification of a chosen figure of merit that a given process can draw from the resource. This functional satisfies pre- and post-processing properties and admits a clear operational meaning in terms of a binary state discrimination task. To bound how quickly a resource can modify a yield, we further define an instantaneous advantage rate whose time integral yields explicit minimal time guarantees to achieve a prescribed resource-induced change in the target yield, thus providing resource-aware analogues of quantum speed limits. In addition, we show that general open system dynamics can be decomposed into free and resourceful components relative to a resource-destroying map, with only the latter contributing to a resource-induced influence on the observable. This decomposition allows us to isolate those parts of the evolution that are genuinely responsible for changing the readout.

Returning to the role of coherence in molecular sys-

tems raised at the beginning of this section, we illustrate the calculation of the resource impact functional and the instantaneous advantage rate using donor-acceptor excitation transfer in the single excitation manifold. This setting allows for an analytic characterization of how the resource impact functional identifies the time windows over which the dynamics and, thus, the chosen readout, is most sensitive to coherence.

In the longer term, we expect that this framework can be exported beyond the examples considered here to other quantum chemical phenomena where the functional role of quantum resources remains unclear.

We summarize the central quantities introduced in this paper, together with their key properties in Table I. The remainder of the paper is structured as follows: Sec. II introduces the theoretical framework for resource theories with a resource-destroying map. In Sec. II A we define the resource impact functional, establish core properties such as convexity and behaviour under pre- and post-processing, and discuss their implications for when quantum effects are operationally relevant. Sec. II B introduces a dynamical version of the framework and derives variation bounds on how fast the resource impact functional can change, and Sec. II C uses these bounds to obtain minimal time constraints on achieving a prescribed resource-induced modification of a target yield, as well as feasibility bounds on yield improvements for a fixed time budget. In Sec. II D we show how Lindblad dynamics can be dissected into free and resourceful components, with only the latter contributing to a resource-induced advantage. Since not all resource theories admit a resource-destroying map, Sec. III explains how several of the concepts from Sec. II can be generalized to this more general setting. Finally, Sec. IV illustrates how the resource impact functional and instantaneous rate can be calculated analytically for the donor-acceptor model in the single excitation manifold.

## II. THEORETICAL CONCEPTS

Let  $\mathcal{H}$  be a finite-dimensional complex Hilbert space,  $\mathcal{B}(\mathcal{H})$  the set of bounded linear operators on  $\mathcal{H}$  and  $\mathcal{D}(\mathcal{H}) \subset \mathcal{B}(\mathcal{H})$  the set of density operators on  $\mathcal{H}$ . Here, we restrict to finite-dimensional Hilbert spaces, both for simplicity and because this setting closely reflects most computational frameworks in quantum chemistry.

To investigate under which circumstances chemical processes can benefit from quantum resources, we first focus on resource theories equipped with a resource-destroying map, such as those for coherence or asymmetry [47, 55, 56] (see Appendix A for a brief recap of resource theories including resource-destroying maps). In this setting, the resource-destroying map  $\mathcal{G} : \mathcal{D}(\mathcal{H}) \rightarrow \mathcal{D}(\mathcal{H})$  provides a precise notion of the corresponding ‘‘classical’’ behaviour obtained when the resource is removed, and thereby singles out a canonical free counterpart of any state or process. This will serve as the start-

Quantity	Properties
Resource impact functional $\mathcal{C}_M(\Lambda)$	<ul style="list-style-type: none"> <li>• Convexity, continuity, seminorm (Theorem 3);</li> <li>• Data-processing inequalities (Theorem 4);</li> <li>• Geometric and operational interpretations (Corollary 5, 6, Sec. II A 4);</li> <li>• For linear <math>\mathcal{G}</math>: operator-norm form (Thm. 1), free/resourceful decomposition (Theorem 10, Corollary 11).</li> </ul>
Unpaired benchmark: $\Pi_M(\Lambda)$	<ul style="list-style-type: none"> <li>• Breaks the pairing <math>\rho \mapsto \mathcal{G}(\rho)</math>;</li> <li>• Bounded from above by <math>\mathcal{C}_M(\Lambda)</math> (Corollary 2)</li> </ul>
Instantaneous rate $\Gamma_M(t)$	<ul style="list-style-type: none"> <li>• Variation bound and vanishing criteria (Theorem 7, Lemma 8)</li> </ul> <p style="text-align: center;">↓</p> <ul style="list-style-type: none"> <li>• Time &amp; feasibility bounds (Corollary 9)</li> </ul>
Generalized functionals: $\mathfrak{C}_M(\Lambda), \mathfrak{T}_M(t)$	Generalization of $\mathcal{C}_M(\Lambda), \Gamma_M(t)$ to QRTs without resource-destroying maps

TABLE I. Overview of the quantities introduced in this work and their key properties.

ing point for our later generalization to resource theories without a resource-destroying map, discussed in Sec. III.

### A. Resource impact functional

Let  $\{M_i\}$  be a POVM on  $\mathcal{H}$ . For a fixed POVM element  $M$ , we define the corresponding yield by

$$Y(\rho) := \text{Tr}[M\rho], \quad \rho \in \mathcal{D}(\mathcal{H}). \quad (1)$$

In most of what follows it is not essential that  $M$  be part of a POVM and it suffices that  $M$  is a bounded self-adjoint operator on  $\mathcal{H}$ . For generality, we will therefore take  $M \in \mathcal{B}_{\text{sa}}(\mathcal{H})$  and impose the POVM constraints (i.e.,  $0 \leq M \leq \mathbb{1}$ , and  $\sum_i M_i = \mathbb{1}$  for a full measurement) only when explicitly required.

Consider a resource theory equipped with a resource-destroying map  $\mathcal{G}$  (see Appendix A 2). In general,  $\mathcal{G}$  need not be linear. In fact, for non-convex resource theories (such as quantum discord [55]) any resource-destroying map that is idempotent and fixes all free states cannot be linear, since the image of the convex set of density operators  $\mathcal{D}(\mathcal{H})$  under a linear map is convex, whereas the free set of a non-convex resource theory is not. Because an adjoint  $\mathcal{G}^\dagger$  is defined only for linear maps, one cannot, in general, transfer statements to the Heisenberg picture via  $\mathcal{G}^\dagger$  when  $\mathcal{G}$  is non-linear. However, the Heisenberg picture will turn out to be useful in the following. Accordingly, we first develop results that do not rely on an adjoint (allowing potentially non-linear  $\mathcal{G}$ ), and then present refinements for the case in which  $\mathcal{G}$  is linear. Additional simplifications arise when  $\mathcal{G}$  is self-adjoint, i.e.,  $\mathcal{G} = \mathcal{G}^\dagger$  with respect to the Hilbert-Schmidt inner product. Most examples of linear resource-destroying maps in the literature, including dephasing maps and group twirls, are self-adjoint. For an example of a resource theory with a linear resource-destroying map that is not self-adjoint, see Appendix A 2.

Given a fixed quantum channel  $\Lambda$  and an input state  $\rho \in \mathcal{D}(\mathcal{H})$ , we define the yield difference relative to the resource-free baseline as

$$\Delta Y(\rho) := \text{Tr}[M(\Lambda(\rho) - \Lambda(\mathcal{G}(\rho)))] . \quad (2)$$

If  $\mathcal{G} : \mathcal{B}(\mathcal{H}) \rightarrow \mathcal{B}(\mathcal{H})$  is linear, then by moving to the Heisenberg picture we can write

$$\Delta Y(\rho) = \text{Tr}[(\text{id} - \mathcal{G}^\dagger)(\Lambda^\dagger(M))\rho] \quad (\mathcal{G} \text{ linear}), \quad (3)$$

where  $\text{id} : \mathcal{B}(\mathcal{H}) \rightarrow \mathcal{B}(\mathcal{H})$  is the identity map. If in addition  $\mathcal{G}$  is self-adjoint,  $\mathcal{G}^\dagger = \mathcal{G}$ , and the linear functional  $\Delta Y(\rho)$  can be written as the expectation value of the observable  $X := (\text{id} - \mathcal{G})(\Lambda^\dagger(M))$ .

#### 1. Definition

The yield change  $\Delta Y$  defined above is state-specific. To quantify how strongly a quantum channel describing some physical process can, in principle, exploit the presence of a quantum resource, we introduce the *resource impact functional* with respect to a POVM element  $M$  as

$$\mathcal{C}_M(\Lambda) := \sup_{\rho \in \mathcal{D}(\mathcal{H})} |\text{Tr}[M(\Lambda(\rho) - \Lambda(\mathcal{G}(\rho)))]| \geq 0. \quad (4)$$

In other words,  $\mathcal{C}_M(\Lambda)$  is the maximal change, over all density operators, in the figure of merit encoded by  $M$  that can be induced by a single application of  $\Lambda$  when comparing a state to its free counterpart. For a fixed choice of  $M$ , the state-dependent yield change  $\Delta Y(\rho)$  can be decomposed into its maximal enhancement  $\mathcal{C}_M^+(\Lambda) := \sup_{\rho} \Delta Y \geq 0$  and maximal suppression  $\mathcal{C}_M^-(\Lambda) := \sup_{\rho} (-\Delta Y) = -\inf_{\rho} \Delta Y$ , such that

$$-\mathcal{C}_M^-(\Lambda) \leq \Delta Y \leq \mathcal{C}_M^+(\Lambda) \quad (5)$$

and  $\mathcal{C}_M(\Lambda) = \max\{\mathcal{C}_M^-(\Lambda), \mathcal{C}_M^+(\Lambda)\}$ .

In resource theories where the resource-destroying map  $\mathcal{G}$  is not unique, the quantity  $\mathcal{C}_M(\Lambda)$  implicitly depends on the choice of  $\mathcal{G}$ . In the following we fix one such  $\mathcal{G}$  and omit it from the notation, i.e.  $\mathcal{C}_M(\Lambda) \equiv \mathcal{C}_{M,\mathcal{G}}(\Lambda)$ ; all statements are to be understood with respect to this fixed choice.

Since for finite-dimensional  $\mathcal{H}$  the state space  $\mathcal{D}(\mathcal{H})$  is compact and the functional in Eq. (4) is continuous, so the supremum is in fact a maximum. We now derive a

first specialization of  $\mathcal{C}_M(\Lambda)$ , which relies on the linearity of  $\mathcal{G}$ .

**Theorem 1.** *Let  $M \in \mathcal{B}_{\text{sa}}(\mathcal{H})$ ,  $\dim(\mathcal{H}) < \infty$ ,  $\Lambda$  be a quantum channel, and let  $\mathcal{G} : \mathcal{B}(\mathcal{H}) \rightarrow \mathcal{B}(\mathcal{H})$  be a linear resource-destroying map. Define  $\mathcal{C}_M(\Lambda)$  as in Eq. (4). Then:*

(i) *The supremum in Eq. (4) can be restricted to pure states,*

$$\mathcal{C}_M(\Lambda) = \sup_{\substack{|\Psi\rangle \in \mathbb{P}(\mathcal{H}) \\ \|\Psi\|=1}} |\text{Tr}[(\text{id} - \mathcal{G}^\dagger)(\Lambda^\dagger(M)) |\Psi\rangle\langle\Psi|]|, \quad (6)$$

where  $\mathbb{P}(\mathcal{H})$  denotes the complex projective Hilbert space.

(ii) *If  $\mathcal{G}$  is Hermiticity preserving, then*

$$\mathcal{C}_M(\Lambda) = \|(\text{id} - \mathcal{G}^\dagger)(\Lambda^\dagger(M))\|_\infty. \quad (7)$$

(iii) *If, in addition,  $\mathcal{G}$  is idempotent (i.e.,  $\mathcal{G} \circ \mathcal{G} = \mathcal{G}$ ), then a necessary and sufficient condition for  $\mathcal{C}_M(\Lambda) = 0$  is*

$$\Lambda^\dagger(M) \in \text{im}(\mathcal{G}^\dagger), \quad (8)$$

where  $\text{im}(\mathcal{G}^\dagger)$  denotes the image of  $\mathcal{G}^\dagger$ .

We provide the proof of Theorem 1 in Appendix C.

In the non-linear case, the adjoint-based criterion (iii) does not apply. A simple sufficient, but generally stronger than necessary, condition ensuring  $\mathcal{C}_M(\Lambda) = 0$  is a kind of “resource blindness” of the quantum channel  $\Lambda$ , namely  $\Lambda(\rho) = \Lambda(\mathcal{G}(\rho))$  for all  $\rho \in \mathcal{D}(\mathcal{H})$ . In this situation the resource under consideration affords no yield advantage for the observable  $M$  and is, in this sense, not operationally functional for the task defined by  $(\Lambda, M)$ . For linear  $\mathcal{G}$ , the minimal necessary and sufficient condition is given by (iii), which is strictly weaker than full resource blindness of  $\Lambda$ . Moreover, (iii) together with (i) implies that  $\mathcal{C}_M(\Lambda)$  vanishes for linear  $\mathcal{G}$  whenever  $\Lambda$  is  $\mathcal{G}$ -covariant and  $M$  is  $\mathcal{G}$ -invariant, as expected as in that case the dynamics and the readout are insensitive to the resource-destroying operation.

For non-linear  $\mathcal{G}$ , the objective  $f(\rho) = |\Delta Y(\rho)|$  is in general non-convex in  $\rho$  because of the non-linear dependence  $\rho \mapsto \mathcal{G}(\rho)$ . As a consequence, the supremum in Eq. (4) need not be attained at an extremal point (i.e., pure state) of  $\mathcal{D}(\mathcal{H})$  and there can be settings in which a mixed input state outperforms every pure state input. This should be contrasted with the case of linear  $\mathcal{G}$ , where  $\Delta Y(\rho)$  is affine in  $\rho$  and hence  $f(\rho)$  is convex. Thus, mixing (e.g., due to non-zero temperature or environmental noise) cannot increase  $f(\rho)$  beyond its value for the best component state. In the future, it will be interesting to characterize the maximizers in Eq. (4) for given pairs  $(\Lambda, \mathcal{G})$ , in order to identify which properties of a quantum state have operational impact on the target yield and how they interact with the dynamics described by  $\Lambda$ .

At this point, it is important to explain how the resource impact functional  $\mathcal{C}_M(\Lambda)$  differs from related notions in the literature [47, 53–55, 62–72]. A widely studied, and resource theory specific, example is the coherence-generating power [54, 64–66, 68, 69], which quantifies how much coherence a channel can create from free (incoherent) states, as evaluated by a chosen coherence monotone. By contrast, when applied to the resource theory of coherence,  $\mathcal{C}_M(\Lambda)$  does not measure the increase of coherence itself. Instead, it captures how strongly the quantum channel  $\Lambda$  can exploit a resource to change a task-specific readout described by  $M$ , i.e., the anticipated target yield. This shift from resource creation to task-level impact is essential for analysing the operational role of quantum resources in physical processes described by  $\Lambda$ . Furthermore, the yield change  $\Delta Y(\rho)$  in Eq. (2) enables a state-resolved analysis when required. Finally, the definition of  $\mathcal{C}_M(\Lambda)$  in Eq. (4) only assumes the existence of a resource-destroying map and is otherwise universally applicable to any resource theory with such a map. Extensions to resource theories without a resource-destroying map will be discussed in Sec. III.

Furthermore, suppose the system is prepared in a (possibly mixed) state  $\rho$  and undergoes the transformation  $\Lambda(\rho)$ . If  $\Lambda$  is not a free operation in the chosen resource theory, then the achievable change in the target yield  $Y$  can exceed what is possible under free operations, i.e., it can be larger than the maximal yield change obtainable when  $\Lambda$  is restricted to the free set of quantum channels. The task specific response functional  $\mathcal{C}_M(\Lambda)$  therefore measures the maximum modification that the single-step process  $\Lambda$  can draw from the resource with respect to  $M$ , while  $\mathcal{C}_M(\Lambda) = 0$  means that the quantum resource is effectively irrelevant for the process described by  $\Lambda$  and the observable  $M$ . In the case where  $\mathcal{G}$  is linear, Theorem 1 provides a precise condition for when this happens.

To further emphasise the distinct operational meaning of  $\mathcal{C}_M(\Lambda)$ , consider a resource theory with a set of free states  $\mathcal{F}$  and define

$$\Pi_M(\Lambda) := \sup_{\rho \in \mathcal{D}(\mathcal{H})} |\text{Tr}[M \Lambda(\rho)]| - \sup_{\sigma \in \mathcal{F}} |\text{Tr}[M \Lambda(\sigma)]| \geq 0, \quad (9)$$

which is the difference between the optimal performance achievable with arbitrary input states and the optimal performance achievable when the input is restricted to free states. The quantity  $\Pi_M(\Lambda)$  thus provides a meaningful measure of the operational advantage enabled by resourceful states, and functionals which consider the optimum over all states versus an optimum over free states are common in the literature [50, 51, 53, 73]. We discuss in Appendix D how  $\Pi_M(\Lambda)$  can be interpreted as the maximal advantage of resourceful states in an appropriate binary decision (discrimination-type) task, in the sense of Ref. [73].

However, unlike  $\mathcal{C}_M(\Lambda)$ , the definition in Eq. (9) does not compare a state  $\rho$  with a specific free baseline obtained from it (such as  $\mathcal{G}(\rho)$  in the presence of a resource-destroying map). Instead, the two optimisations are car-

ried out independently over all density operators  $\rho \in \mathcal{D}(\mathcal{H})$  and over free states  $\sigma \in \mathcal{F}$ . As a result, the explicit pairing between each state and its resource-free counterpart, which is crucial for the interpretation of  $\mathcal{C}_M(\Lambda)$ , is lost.

**Corollary 2.** *Let  $M \in \mathcal{B}_{sa}(\mathcal{H})$ ,  $\Lambda$  a linear CPTP map, and  $\mathcal{F}$  denote the set of free states of a given resource theory. Then,*

$$\Pi_M(\Lambda) \leq \mathcal{C}_M(\Lambda) \quad (10)$$

where  $\mathcal{C}_M(\Lambda)$  and  $\Pi_M(\Lambda)$  are defined in Eqs. (4) and (9), respectively.

The proof of Corollary 2 is provided in Appendix E.

We can interpret Corollary 2 as follows: In the definition of  $\Pi_M(\Lambda)$  in Eq. (9), the second term selects the free input state that maximises the yield for the given task specified by  $(\Lambda, M)$ . Using this globally optimal free strategy as a benchmark makes the free theory look as strong as possible and can therefore only decrease the observed advantage of resourceful inputs. In contrast,  $\mathcal{C}_M(\Lambda)$  compares each state  $\rho$  with its own “free counterpart”  $\mathcal{G}(\rho)$ , so the resourceful input and the baseline are not optimised independently. Since  $\mathcal{G}(\rho)$  is just one particular free state, the contrast per state appearing in  $\mathcal{C}_M(\Lambda)$  can only be larger than or equal to the advantage measured against the globally optimal free input. This explains why  $\Pi_M(\Lambda)$  is always a lower bound to  $\mathcal{C}_M(\Lambda)$ .

## 2. Key properties

We now analyse the properties of the resource impact functional  $\mathcal{C}_M(\Lambda)$  introduced in the previous section. The next two theorems make no linearity assumption on  $\mathcal{G}$ .

**Theorem 3.** *Let  $\mathcal{H}$  be a finite-dimensional Hilbert space,  $M \in \mathcal{B}_{sa}(\mathcal{H})$ ,  $\mathcal{G} : \mathcal{B}(\mathcal{H}) \rightarrow \mathcal{B}(\mathcal{H})$  a (possibly non-linear) resource-destroying map, and  $\mathcal{C}_M(\Lambda)$  as defined in Eq. (4).*

(i) (Convexity) For any  $p_k \geq 0$ ,  $\sum_k p_k = 1$ ,

$$\mathcal{C}_M\left(\sum_k p_k \Lambda_k\right) \leq \sum_k p_k \mathcal{C}_M(\Lambda_k). \quad (11)$$

(ii) (Lipschitz continuity) For any two linear CPTP maps  $\Lambda_1, \Lambda_2$ , the resource impact functional  $\mathcal{C}_M(\Lambda)$  is Lipschitz continuous,

$$|\mathcal{C}_M(\Lambda_1) - \mathcal{C}_M(\Lambda_2)| \leq K \|\Lambda_1 - \Lambda_2\|_\diamond, \quad (12)$$

with Lipschitz constant  $K := 2\|M\|_\infty$ . If  $\mathcal{G}$  is a linear unital CPTP map, Eq. (12) holds with  $K$  replaced by  $K' = \|M\|_\infty < K$ .

(iii) (Seminorm) Let  $M_1, M_2 \in \mathcal{B}_{sa}(\mathcal{H})$  and  $a, b \in \mathbb{R}$ . Then,

$$\mathcal{C}_{aM_1+bM_2}(\Lambda) \leq |a|\mathcal{C}_{M_1}(\Lambda) + |b|\mathcal{C}_{M_2}(\Lambda). \quad (13)$$

The proof of Theorem 3 is shown in Appendix F.

Convexity of  $\mathcal{C}_M(\Lambda)$  implies that mixing channels, i.e., classical randomness in the dynamics, cannot increase the potential advantage provided by a resource. In addition, when optimizing  $\mathcal{C}_M(\Lambda)$  over a convex set of admissible quantum channels, the maximum is attained at an extremal element. Furthermore, Lipschitz continuity is important as it ensures that  $\mathcal{C}_M(\Lambda)$  is insensitive with respect to small implementation errors of the quantum channel  $\Lambda$ . Furthermore, the map  $M \mapsto \mathcal{C}_M(\Lambda)$  is absolutely homogeneous and subadditive as a consequence of (iii) and, thus, a seminorm on the real vector space of Hermitian operators.

The next theorem collects several data-processing inequalities that hold for an arbitrary resource-destroying map  $\mathcal{G}$ . We then discuss their implications afterwards and explain the geometric picture underlying  $\mathcal{C}_M(\Lambda)$  and its connection to the post-processing bound in Sec. II A 3.

**Theorem 4.** *Let  $\mathcal{H}$  be a finite-dimensional Hilbert space,  $M \in \mathcal{B}_{sa}(\mathcal{H})$ ,  $\mathcal{G} : \mathcal{B}(\mathcal{H}) \rightarrow \mathcal{B}(\mathcal{H})$  a (possibly non-linear) resource-destroying map, and  $\mathcal{C}_M(\Lambda)$  as defined in Eq. (4).*

(i) (Post-processing inequality) Let  $\Lambda_{1/2} : \mathcal{B}(\mathcal{H}) \rightarrow \mathcal{B}(\mathcal{H})$  be two linear CPTP maps. The resource impact functional  $\mathcal{C}_M(\Lambda)$  satisfies a Heisenberg pull-back identity

$$\mathcal{C}_M(\Lambda_2 \circ \Lambda_1) = \mathcal{C}_{\Lambda_2^\dagger(M)}(\Lambda_1). \quad (14)$$

Moreover, the following post-processing bounds hold:

$$\begin{aligned} \mathcal{C}_M(\Lambda_2 \circ \Lambda_1) &\leq \mathcal{C}_M(\Lambda_1) + \mathcal{C}_{\Delta M_{\Lambda_2}}(\Lambda_1) \\ &\leq \mathcal{C}_M(\Lambda_1) + \|\Delta M_{\Lambda_2}\|_\infty R_{\mathcal{G}}, \end{aligned} \quad (15)$$

where  $\Delta M_{\Lambda_2} := \Lambda_2^\dagger(M) - M$  and the “resource radius”

$$R_{\mathcal{G}} := \max_{\rho \in \mathcal{D}(\mathcal{H})} \|\rho - \mathcal{G}(\rho)\|_1. \quad (16)$$

describes how far a state can be from its resource-destroyed counterpart in trace distance.

(ii) (Pre-processing with a  $\mathcal{G}$ -covariant channel) Let  $\Lambda_1$  be a linear CPTP map with  $\mathcal{G} \circ \Lambda_1 = \Lambda_1 \circ \mathcal{G}$ . Then,

$$\mathcal{C}_M(\Lambda_2 \circ \Lambda_1) \leq \mathcal{C}_M(\Lambda_2). \quad (17)$$

(iii) (Classical coarse-graining) Let  $\{M_i\}_i$  be a POVM, and  $\widetilde{M}_j = \sum_i V_{ji} M_i$  for a column stochastic matrix  $V$ . Then, for any quantum channel  $\Lambda$  and measurement outcome  $j$ ,

$$\mathcal{C}_{\widetilde{M}_j}(\Lambda) \leq \sum_i V_{ji} \mathcal{C}_{M_i}(\Lambda). \quad (18)$$

Theorem 4 is proven in Appendix G.

Parts (i)-(iii) in Theorem 4 show how the resource impact functional  $\mathcal{C}_M(\Lambda)$  changes under pre-processing or post-processing with a second quantum channel. Eq. (14) says that post-processing by a quantum channel  $\Lambda_2$  acts as a readout deformation  $M \mapsto \Lambda_2^\dagger(M)$ . Then, the first inequality in Eq. (15) allows us to decompose the maximal yield change as described by  $\mathcal{C}_M(\Lambda)$  into a part which corresponds to initial  $M$  and a second term associated with the readout deformation induced by  $\Lambda_2$ . The second term vanishes when  $\Lambda_2^\dagger(M) = M$ , i.e., for  $\|\Delta M_{\Lambda_2}\|_\infty = 0$ , recovering the standard post-processing monotonicity. Furthermore, the second inequality in Eq. (15) shows that small readout deformations as quantified by  $\|\Delta M_{\Lambda_2}\|_\infty$  cannot lead to large changes in  $\mathcal{C}_M(\Lambda)$ .

Property (ii) in Theorem 4 states that free pre-processing with a  $\mathcal{G}$ -covariant quantum channel cannot increase the maximally possible yield change. Importantly, while every  $\mathcal{G}$ -covariant map is a free operation for the given resource theory, not every free operation is  $\mathcal{G}$ -covariant. Consequently, one should not expect a general monotonicity statement under all free operations and (ii) isolates the subset of free operations under which such a data-processing inequality holds.

Classical coarse-graining plays an important role if we would like to apply  $\mathcal{C}_M(\Lambda)$  to non-idealised experimental settings, where coarse-graining is naturally incorporated in the readout model [74–76]. For this, recall that  $M$  is an element of a POVM  $\{M_i\}_i$ . Measuring  $\{M_i\}_i$  and then classically coarse-graining the outcomes by a classical channel described by a column-stochastic matrix  $V$  (i.e.,  $V_{ji} \geq 0$  for all  $i, j$  and  $\sum_j V_{ji} = 1$  for each  $i$ ) is equivalent to measuring the POVM  $\{\tilde{M}_j\}_j$  with

$$\tilde{M}_j = \sum_i V_{ji} M_i, \quad (19)$$

where  $V_{ji}$  is the conditional probability to map the “ideal” outcome  $i$  to the recorded outcome  $j$  [77, 78], and similar constructions hold for continuous outcome measurements [79–81].

### 3. Geometric picture

Next, we show that the resource impact functional admits a natural geometric interpretation: it is the support function of a convex set and, thus, the post-processing inequality in Eq. (15) becomes the well-known subadditivity of support functions. For this, we first define the set

$$\mathcal{M}_{\mathcal{G},\Lambda} := \{\Lambda(\rho) - \Lambda(\mathcal{G}(\rho)) \mid \rho \in \mathcal{D}(\mathcal{H})\} \subset \mathcal{B}_{\text{sa}}(\mathcal{H}) \quad (20)$$

and introduce the convex hull of the union of  $\mathcal{M}_{\mathcal{G},\Lambda}$  with  $-\mathcal{M}_{\mathcal{G},\Lambda}$  as

$$\tilde{\mathcal{M}}_{\mathcal{G},\Lambda} := \text{conv}(\mathcal{M}_{\mathcal{G},\Lambda} \cup (-\mathcal{M}_{\mathcal{G},\Lambda})). \quad (21)$$

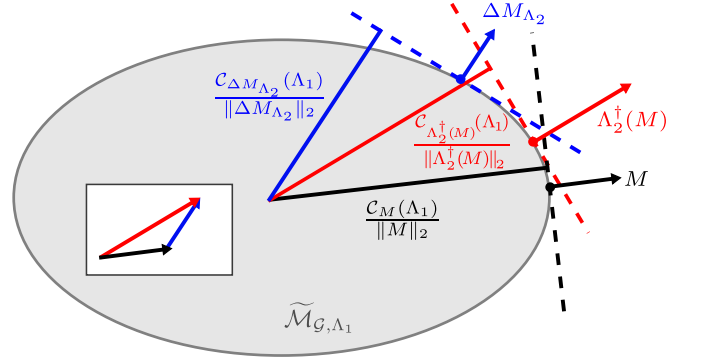


FIG. 1. Schematic illustration of the geometric picture behind the post-processing bound in Eq. (15) and Corollary 5. (See main text for details.)

**Corollary 5.** *Let  $M \in \mathcal{B}_{\text{sa}}(\mathcal{H})$ . Then the resource impact functional  $\mathcal{C}_M(\Lambda)$  is equal to the support function of the convex set  $\tilde{\mathcal{M}}_{\mathcal{G},\Lambda}$  evaluated at  $M$ :*

$$\mathcal{C}_M(\Lambda) = \sup_{O \in \tilde{\mathcal{M}}_{\mathcal{G},\Lambda}} \langle M, O \rangle_{\text{HS}} =: h_{\tilde{\mathcal{M}}_{\mathcal{G},\Lambda}}(M). \quad (22)$$

The proof of Corollary 5 is provided in Appendix H.

We now describe the geometric picture of the post-processing inequality in Eq. (15), as illustrated in Fig. 1. For a non-zero  $M$ , introduce the unit vector  $m := M/\|M\|_2$  and define the supporting hyperplane

$$H_{\tilde{\mathcal{M}}_{\mathcal{G},\Lambda}}(M) := \left\{ O \in \mathcal{B}_{\text{sa}}(\mathcal{H}) \mid \langle M, O \rangle_{\text{HS}} = h_{\tilde{\mathcal{M}}_{\mathcal{G},\Lambda}}(M) \right\}. \quad (23)$$

Since  $\tilde{\mathcal{M}}_{\mathcal{G},\Lambda}$  is compact and convex, the supremum defining  $h_{\tilde{\mathcal{M}}_{\mathcal{G},\Lambda}}(M)$  is attained, so  $H_{\tilde{\mathcal{M}}_{\mathcal{G},\Lambda}}(M)$  is indeed a supporting hyperplane.

Then, it follows as a direct consequence of Corollary 5 that

$$\begin{aligned} \mathcal{C}_M(\Lambda) &= \|M\|_2 h_{\tilde{\mathcal{M}}_{\mathcal{G},\Lambda}}(m) \\ &= \|M\|_2 \text{dist}(0, H_{\tilde{\mathcal{M}}_{\mathcal{G},\Lambda}}(M)), \end{aligned} \quad (24)$$

where  $\text{dist}(\cdot, \cdot)$  denotes the distance induced by the Hilbert-Schmidt inner product. In other words,  $\mathcal{C}_M(\Lambda)$  is proportional to the distance from the origin 0 to the supporting hyperplane  $H_{\tilde{\mathcal{M}}_{\mathcal{G},\Lambda}}(M)$ .

In Fig. 1, we depict the supporting hyperplanes (dashed lines) corresponding to  $\mathcal{C}_M(\Lambda_1)$  (black),  $\mathcal{C}_{\Delta M_{\Lambda_2}}(\Lambda_1)$  (blue), and  $\mathcal{C}_{\Lambda_2^\dagger(M)}(\Lambda_1)$  (red) appearing in Eq. (15). Their distances from the origin equal  $\mathcal{C}_M(\Lambda_1)/\|M\|_2$ ,  $\mathcal{C}_{\Delta M_{\Lambda_2}}(\Lambda_1)/\|\Delta M_{\Lambda_2}\|_2$ , and  $\mathcal{C}_{\Lambda_2^\dagger(M)}(\Lambda_1)/\|\Lambda_2^\dagger(M)\|_2$ , respectively. Thus, the subadditivity of support functions [82] then reads

$$h_{\tilde{\mathcal{M}}_{\mathcal{G},\Lambda_1}}(\Lambda_2^\dagger(M)) \leq h_{\tilde{\mathcal{M}}_{\mathcal{G},\Lambda_1}}(M) + h_{\tilde{\mathcal{M}}_{\mathcal{G},\Lambda_1}}(\Delta M_{\Lambda_2}). \quad (25)$$

This is precisely the geometric content of the post-processing inequality (15).

In addition, Corollary 5 also admits a dual formulation in terms of polar sets, which provides further insights into the meaning of  $\mathcal{C}_M(\Lambda)$  as we explain below. In general, given a subset  $\mathcal{X} \subset \mathcal{B}_{\text{sa}}(\mathcal{H})$  that contains the origin, its polar is defined as [83]

$$\mathcal{X}^\circ := \{M \in \mathcal{B}_{\text{sa}}(\mathcal{H}) \mid \langle M, O \rangle_{\text{HS}} \leq 1 \ \forall O \in \mathcal{X}\}, \quad (26)$$

i.e., it is the intersection of the closed half-spaces  $\{M : \langle M, O \rangle_{\text{HS}} \leq 1\}$  generated by  $O \in \mathcal{X}$ . Since we work in finite-dimensional settings, the polar is closed and convex, even if  $\mathcal{X}$  is not [83].

**Corollary 6** (Polar characterization of  $\mathcal{C}_M(\Lambda)$ ). *Let  $M \in \mathcal{B}_{\text{sa}}(\mathcal{H})$ . Then*

$$\mathcal{C}_M(\Lambda) = h_{\widetilde{\mathcal{M}}_{\mathcal{G},\Lambda}^\circ}(M) = \inf \left\{ t \geq 0 \mid M \in t \widetilde{\mathcal{M}}_{\mathcal{G},\Lambda}^\circ \right\}. \quad (27)$$

*Equivalently, the polar set is the unit ball of the functional  $M \mapsto \mathcal{C}_M(\Lambda)$ :*

$$\widetilde{\mathcal{M}}_{\mathcal{G},\Lambda}^\circ = \{M \in \mathcal{B}_{\text{sa}}(\mathcal{H}) \mid \mathcal{C}_M(\Lambda) \leq 1\}. \quad (28)$$

The short proof of Corollary 6 follows from the definition of the polar set in Eq. (26) and is provided in Appendix I. Thus, Corollary 6 yields a complementary, dual interpretation of the resource impact functional:  $\mathcal{C}_M(\Lambda)$  is the smallest factor by which one must rescale the observable  $M$  so that it belongs to the polar set  $\widetilde{\mathcal{M}}_{\mathcal{G},\Lambda}^\circ$ , i.e., to the class of normalized observables whose response to all resource-induced output deviations is uniformly bounded. In other words,  $M \in \widetilde{\mathcal{M}}_{\mathcal{G},\Lambda}^\circ$  if and only if

$$\left| \text{Tr}[M(\Lambda(\rho) - \Lambda(\mathcal{G}(\rho)))] \right| \leq 1 \quad \forall \rho \in \mathcal{D}(\mathcal{H}). \quad (29)$$

Accordingly, elements of  $\widetilde{\mathcal{M}}_{\mathcal{G},\Lambda}^\circ$  may be viewed as bounded sensitivity probes, while  $\mathcal{C}_M(\Lambda)$  quantifies the largest magnitude of the yield change induced by the deviations  $\Lambda(\rho) - \Lambda(\mathcal{G}(\rho))$ .

Because the definition of  $\mathcal{C}_M(\Lambda)$  involves an absolute value,  $\mathcal{C}_M(\Lambda)$  also admits a description in terms of the absolute polar

$$\mathcal{M}_{\mathcal{G},\Lambda}^{\circ a} := \{M \in \mathcal{B}_{\text{sa}}(\mathcal{H}) \mid |\langle M, O \rangle_{\text{HS}}| \leq 1 \ \forall O \in \mathcal{M}_{\mathcal{G},\Lambda}\}. \quad (30)$$

Geometrically,  $\mathcal{M}_{\mathcal{G},\Lambda}^{\circ a}$  is the intersection of the slabs  $\{M : |\langle M, O \rangle_{\text{HS}}| \leq 1\}$  induced by  $O \in \mathcal{M}_{\mathcal{G},\Lambda}$ . This is further reflected by the symmetrization in Eq. (21), which implies that the polar of  $\widetilde{\mathcal{M}}_{\mathcal{G},\Lambda}$  equals the absolute polar,  $\widetilde{\mathcal{M}}_{\mathcal{G},\Lambda}^\circ = \mathcal{M}_{\mathcal{G},\Lambda}^{\circ a}$  and, thus, Eq. (27) holds also with  $\widetilde{\mathcal{M}}_{\mathcal{G},\Lambda}^\circ$  replaced by  $\mathcal{M}_{\mathcal{G},\Lambda}^{\circ a}$ .

Finally, since  $\widetilde{\mathcal{M}}_{\mathcal{G},\Lambda}$  is closed, convex, and contains the origin, the bipolar theorem [83] implies that it can be recovered from its polar,  $(\widetilde{\mathcal{M}}_{\mathcal{G},\Lambda}^\circ)^\circ = \widetilde{\mathcal{M}}_{\mathcal{G},\Lambda}$ . Thus, while  $\widetilde{\mathcal{M}}_{\mathcal{G},\Lambda}$  and  $\widetilde{\mathcal{M}}_{\mathcal{G},\Lambda}^\circ$  are equivalent descriptions (via polarity), the polar viewpoint can be more convenient for questions posed in observable space, such as certifying that an experimentally accessible class of measurements is insensitive to the resource-induced deviations, or optimizing  $\mathcal{C}_M(\Lambda)$  over a constrained family of observables.

#### 4. Operational interpretation

In this section, we collect several properties of the resource impact functional  $\mathcal{C}_M(\Lambda)$  introduced in Secs. II A and II A 2 into a unified operational interpretation.

Consider a two-outcome POVM  $\{M, \mathbb{1} - M\}$  with  $0 \leq M \leq \mathbb{1}$  and the following binary hypothesis testing task. Hypothesis  $H_0$  is that the input state before applying  $\Lambda$  (and then measuring  $M$ ) was the resource-free state  $\mathcal{G}(\rho)$ , while hypothesis  $H_1$  is that the input state was the potentially resourceful  $\rho$ , with prior probabilities  $p_0 = p_1 = 1/2$ . Moreover, we label the outcome associated with  $M$  by  $X = 1$  and the complementary outcome by  $X = 0$ . Then, for a given pair  $(\rho, \mathcal{G}(\rho))$ ,

$$P(X = 1 | H_0) = p_0(\rho) := \text{Tr}[M\Lambda(\mathcal{G}(\rho))], \quad (31)$$

$$P(X = 1 | H_1) = p_1(\rho) := \text{Tr}[M\Lambda(\rho)], \quad (32)$$

such that

$$p_1(\rho) - p_0(\rho) = \Delta Y(\rho) \quad (33)$$

with  $\Delta Y(\rho)$  as in Eq. (2). Since  $M$  is a POVM element in this section,  $\mathcal{C}_M(\Lambda) \in [0, 1]$ . This contrasts with the more general case where  $M$  is an arbitrary observable, for which  $\mathcal{C}_M(\Lambda)$  can exceed 1.

For fixed  $\rho$ , and given the measurement  $\{M, \mathbb{1} - M\}$ , the optimal single-shot decision rule (for equal priors) is to decide  $H_1$  on the outcome that is more likely under  $H_1$  than under  $H_0$  and  $H_0$  otherwise. The corresponding success probability follows as

$$p_{\text{succ}}^{(1)}(\rho) = \frac{1}{2} + \frac{1}{2} |\Delta Y(\rho)|. \quad (34)$$

Thus, the maximal bias above random guessing in distinguishing whether the input state was  $\rho$  or its free counterpart  $\mathcal{G}(\rho)$  is  $|\Delta Y(\rho)|/2$ . Optimizing over all input states,

$$p_{\text{succ,max}}^{(1)} = \sup_{\rho \in \mathcal{D}(\mathcal{H})} p_{\text{succ}}^{(1)}(\rho) = \frac{1}{2} + \frac{1}{2} \mathcal{C}_M(\Lambda). \quad (35)$$

Equivalently,  $\mathcal{C}_M(\Lambda)$  equals twice the maximal improvement over random guessing in distinguishing a resourceful input from its paired free counterpart solely from the statistics of measuring  $M$  after applying the channel  $\Lambda$ .

This leads to a simple dichotomy. First,  $\mathcal{C}_M(\Lambda) = 0$  if and only if  $p_{\text{succ}}^{(1)}(\rho) = 1/2$  for all  $\rho \in \mathcal{D}(\mathcal{H})$ , i.e., independent of the input state,  $\Lambda$  followed by  $M$  cannot distinguish  $\rho$  from  $\mathcal{G}(\rho)$ . Second,  $\mathcal{C}_M(\Lambda) > 0$  whenever there exists a  $\rho$  such that  $p_{\text{succ}}^{(1)}(\rho) > 1/2$ , i.e., at least one state for which the resource makes a statistically detectable difference in the readout associated with  $M$ . In this sense, the resource is then operationally relevant for the task defined by  $(\Lambda, M)$ , in line with the discussion in Sec. II A. To summarize,  $\mathcal{C}_M(\Lambda)$  answers the binary question of whether a resource under the dynamics can affect the chosen measurement at all, and at the same time quantifies how strongly it can do so.

For  $\mathcal{G}$  linear, Theorem 1 shows that

$$\mathcal{C}_M(\Lambda) = \|B_{M,\Lambda}\|_\infty, \quad B_{M,\Lambda} := (\text{id} - \mathcal{G}^\dagger)(\Lambda^\dagger(M)). \quad (36)$$

The states that are optimal for the single-shot hypothesis test are precisely the eigenstates of  $B_{M,\Lambda}$  associated with an extremal eigenvalue (of largest magnitude). Accordingly, for a given triple  $(\Lambda, M, \mathcal{G})$ , reconstructing (or approximating)  $B_{M,\Lambda}$  identifies which state preparations are maximally sensitive to the resource for that specific process and readout. This operational viewpoint is equivalent to the geometric picture in Sec. II A 3: fixing  $M$  selects a direction in operator space, and the optimal eigenstates correspond to preparations whose deviation  $O = \Lambda(\rho) - \Lambda(\mathcal{G}(\rho))$  lies on the supporting face of  $\widetilde{\mathcal{M}}_{\mathcal{G},\Lambda}$  in that direction.

We can lift this discussion to a multi-shot setting, which shows that  $\mathcal{C}_M(\Lambda)$  not only determines whether a resource can affect a task at all, but also sets a natural scale for the statistical rate at which repeated experiments can reveal that effect. To this end, consider  $n$  independent and identically distributed (i.i.d.) repetitions of the above single-shot experiment with the same input state  $\rho$ . This allows us to upper bound the total error probability  $P_{\text{err}}^{(n)}(\rho)$ , which is the average probability of making an error over the two hypotheses  $H_0$  and  $H_1$  when occurring with equal probability in terms of the yield change  $|\Delta Y(\rho)|$ , as shown in Appendix J.

To connect  $P_{\text{err}}^{(n)}(\rho)$  to the resource impact functional  $\mathcal{C}_M(\Lambda)$ , we consider a state  $\rho^*$  that (approximately) maximizes  $|\Delta Y(\rho)|$ . In fact, for any  $\varepsilon > 0$  there exists a  $\rho^*$  with

$$|\Delta Y(\rho^*)| \geq \mathcal{C}_M(\Lambda) - \varepsilon. \quad (37)$$

For this state, the total error probability is then bounded by (recall Eq. (J6) in Appendix J)

$$P_{\text{err}}^{(n)}(\rho^*) \leq \exp\left(-\frac{n}{2}(\mathcal{C}_M(\Lambda) - \varepsilon)^2\right). \quad (38)$$

Thus, whenever  $\mathcal{C}_M(\Lambda) > 0$ , there exist preparations  $\rho^*$  for which the error probability decays exponentially fast in  $n$ , with an exponent that can be made arbitrarily close to  $\mathcal{C}_M(\Lambda)^2/2$ . In contrast, if  $\mathcal{C}_M(\Lambda) = 0$ , then  $\Delta Y(\rho) = 0$  for all  $\rho$ , so that  $p_0(\rho) = p_1(\rho)$  and the outcome distributions under  $H_0$  and  $H_1$  coincide. In that case no decision rule can outperform random guessing, and hence  $P_{\text{err}}^{(n)}(\rho) = 1/2$  for all  $n$  and all  $\rho$ .

## B. Instantaneous rate

In the following, we introduce a dynamical version of the resource impact functional to investigate whether a given resource can provide a fixed target yield improvement in given time interval.

Then, the (static) resource impact functional at a given time  $t$  is defined analogous to Eq. (4) with  $\Lambda$  replaced by

$\Lambda_t$ . This provides a time-dependent curve  $t \mapsto \mathcal{C}_M(\Lambda_t)$  but not a rate at which the resource can change the target yield associated with  $M$ . For  $\Lambda_t$  with a possibly time-dependent generator  $\mathcal{L}_t$  satisfying a time-local master equation,  $d\Lambda_t/dt = \mathcal{L}_t \circ \Lambda_t$  [84, 85] and, thus, its adjoint satisfies  $d\Lambda_t^\dagger/dt = \Lambda_t^\dagger \circ \mathcal{L}_t^\dagger$  (see Appendix B for a brief recap of time-local master equations). Then, the time derivative of the yield change  $\Delta Y(\rho; t)$  in Eq. (2) is given by

$$\frac{d\Delta Y(\rho; t)}{dt} = \text{Tr}[M\mathcal{L}_t(\Lambda_t(\rho - \mathcal{G}(\rho)))] \quad (39)$$

This allows us to define an instantaneous rate as

$$\Gamma_M(t) := \sup_{\rho \in \mathcal{D}(\mathcal{H})} |\text{Tr}[M\mathcal{L}_t(\Lambda_t(\rho - \mathcal{G}(\rho)))]| \quad (40)$$

which describes the largest possible change per unit time at a given instant of time of the resource induced yield change associated with  $M$ . Furthermore, in case  $\mathcal{G}$  is linear and CPTP, we have

$$\Gamma_M(t) = \|(\text{id} - \mathcal{G}^\dagger)(\Lambda_t^\dagger(\mathcal{L}_t^\dagger(M)))\|_\infty \quad (\mathcal{G} \text{ linear CPTP}) \quad (41)$$

Note that  $\Gamma_M(t)$  is *not* the same as the time derivative of  $\mathcal{C}_M(\Lambda_t)$  since the absolute value and the operator norm are in general non-smooth and, thus,  $\mathcal{C}_M(\Lambda_t)$  may not be everywhere differentiable. In addition it may not equal  $\Gamma_M(t)$  when its time derivative exists. Still, we can derive a variation bound for  $\mathcal{C}_M(\Lambda_t)$ :

**Theorem 7** (Variation bound and Dini derivatives). *Let  $\mathcal{H}$  be a finite-dimensional Hilbert space,  $M \in \mathcal{B}_{\text{sa}}(\mathcal{H})$ , and  $\mathcal{G} : \mathcal{B}(\mathcal{H}) \rightarrow \mathcal{B}(\mathcal{H})$  a (possibly non-linear) resource-destroying map, and  $\mathcal{C}_M(\Lambda_t)$  and  $\Gamma_M(t)$  are defined as in Eqs. (4) and (40). Let  $\mathcal{I} \subset \mathbb{R}$  be an interval and  $\{\Lambda_t\}_{t \in \mathcal{I}}$  a family of CPTP maps on  $\mathcal{B}(\mathcal{H})$  such that*

(i) *there exists a family of bounded linear maps  $\{\mathcal{L}_t\}_{t \in \mathcal{I}}$  with  $t \mapsto \mathcal{L}_t$  strongly measurable and  $t \mapsto \|\mathcal{L}_t\|_{1 \rightarrow 1}$  locally integrable on  $\mathcal{I}$ , and*

(ii)  *$\{\Lambda_t\}$  solves the time-local master equation*

$$\Lambda_t = \Lambda_{t_0} + \int_{t_0}^t \mathcal{L}_s \circ \Lambda_s ds \quad \forall t, t_0 \in \mathcal{I}. \quad (42)$$

Then for all  $t_1 \leq t_2$  in  $\mathcal{I}$ ,

$$|\mathcal{C}_M(\Lambda_{t_2}) - \mathcal{C}_M(\Lambda_{t_1})| \leq \int_{t_1}^{t_2} ds \Gamma_M(s). \quad (43)$$

Furthermore,  $t \mapsto \mathcal{C}_M(\Lambda_t)$  is absolutely continuous on compact subintervals of  $\mathcal{I}$ , and its right Dini derivatives satisfy

$$D^+ \mathcal{C}_M(\Lambda_t) \leq \Gamma_M(t), \quad D_+ \mathcal{C}_M(\Lambda_t) \geq -\Gamma_M(t) \quad (44)$$

for Lebesgue almost every  $t \in \mathcal{I}$ . The analogous left-sided bounds hold as well. If  $t \mapsto \Gamma_M(t)$  is continuous, then (44) holds for all  $t \in \mathcal{I}$ .

We prove Theorem 7 in Appendix K.

Thus, at any time  $t$  where  $\Gamma_M(t)$  is finite and continuous, Theorem 7 implies that all four one-sided Dini derivatives of  $t \mapsto \mathcal{C}_M(\Lambda_t)$  are finite and all lie in the interval  $[-\Gamma_M(t), \Gamma_M(t)]$ . If at some  $t_0$  the upper right and upper left Dini derivatives differ,  $D^+\mathcal{C}_M(\Lambda_{t_0}) \neq D^-\mathcal{C}_M(\Lambda_{t_0})$ , then  $\mathcal{C}_M(\Lambda_t)$  is not differentiable at  $t_0$ , since an ordinary derivative (if it existed) would have to coincide with all four one-sided Dini derivatives. Moreover, if  $t_0$  is a local maximum of  $\mathcal{C}_M(\Lambda_t)$ , then the one-sided Dini derivatives obey

$$D^+\mathcal{C}_M(\Lambda_{t_0}) \leq 0 \leq D^-\mathcal{C}_M(\Lambda_{t_0}), \quad (45)$$

and similarly for  $D_+\mathcal{C}_M(\Lambda_{t_0}), D_-\mathcal{C}_M(\Lambda_{t_0})$ , even if  $\mathcal{C}_M(\Lambda_t)$  is not differentiable at  $t_0$ . In this sense, the Dini derivatives capture the behaviour of the maximal advantage described by  $\mathcal{C}_M(\Lambda_t)$  around local extrema, independent of differentiability.

Furthermore, a vanishing  $\Gamma_M(t)$  over a given time interval  $\mathcal{I} \in [t_1, t_2]$  implies that  $\mathcal{C}_M(\Lambda_t)$  stays constant within  $\mathcal{I}$ . The condition under which  $\Gamma_M(t) = 0$  follows immediately from the definition of  $\Gamma_M(t)$  in Eq. (40) and is stated in the following Lemma:

**Lemma 8.** *Let  $M \in \mathcal{B}_{\text{sa}}(\mathcal{H})$ , let  $\mathcal{G}$  be a resource-destroying map, and let  $\Gamma_M(t)$  be defined as in Eq. (40). Then, for any  $t$ ,*

$$\Gamma_M(t) = 0 \quad \Leftrightarrow \quad \Lambda_t^\dagger(\mathcal{L}_t^\dagger(M)) \in \mathcal{V}_{\mathcal{G}}^\perp, \quad (46)$$

where

$$\mathcal{V}_{\mathcal{G}}^\perp := \{O \in \mathcal{B}_{\text{sa}}(\mathcal{H}) \mid \langle O, X \rangle_{\text{HS}} = 0 \quad \forall X \in \mathcal{V}_{\mathcal{G}}\} \quad (47)$$

with

$$\mathcal{V}_{\mathcal{G}} := \text{span}_{\mathbb{R}}(\{\rho - \mathcal{G}(\rho) \mid \rho \in \mathcal{D}(\mathcal{H})\}) \subset \mathcal{B}_{\text{sa}}(\mathcal{H}). \quad (48)$$

We provide the proof of Lemma 8 in Appendix L. Consequently, in case Eq. (46) is satisfied for all  $t \in [t_1, t_2]$ , the variation bound in Eq. (43) enforces  $|\mathcal{C}_M(\Lambda_{t_2}) - \mathcal{C}_M(\Lambda_{t_1})| = 0$ .

In summary, Eq. (43) shows that the change of  $\mathcal{C}_M(\Lambda_t)$  between times  $t_1$  and  $t_2$  is bounded by the time integral of the instantaneous rate  $\Gamma_M(t)$ . In other words, the maximal resource induced advantage encoded in  $\mathcal{C}_M(\Lambda_t)$  cannot increase or decrease faster than allowed by  $\Gamma_M(t)$ . We will show in the next section that this leads to a *resource-aware quantum speed limit* on how fast the maximal resource based advantage for the task  $M$  can vary. In contrast to standard quantum speed limits [86–89], which bound changes in terms of distances in state space, our bound is explicitly task and resource dependent as it is written directly in terms of the target yield associated with  $M$ , and free contributions are filtered out through the resource-destroying map  $\mathcal{G}$ .

### C. Time and feasibility bounds

In the following, we show that Theorem 7 yields explicit lower bounds on the time required to achieve a prescribed increase in the task specific  $\mathcal{C}_M(\Lambda_t)$ , i.e., the maximum resource induced change of the yield associated with  $M$ . Vice versa we can obtain a feasibility bound on the change in  $\mathcal{C}_M(\Lambda_t)$  for a *fixed* time budget  $T_{\text{max}}$ . We summarize these two aspects in the following corollary:

**Corollary 9** (Time and feasibility bounds). *Let the assumptions of Theorem 7 hold, and let*

$$\Delta\mathcal{C}_M(\Lambda_{t_2}, \Lambda_{t_1}) := \mathcal{C}_M(\Lambda_{t_2}) - \mathcal{C}_M(\Lambda_{t_1}) \quad (49)$$

for  $t_1 \leq t_2$  in  $\mathcal{I}$ . Define the resource radius  $R_{\mathcal{G}}$  as in Eq. (16) and

$$c_{M,\mathcal{G}} := \|M\|_{\infty} R_{\mathcal{G}} \leq 2\|M\|_{\infty}. \quad (50)$$

Then, for every interval  $[t_1, t_2] \subset \mathcal{I}$ ,

$$|\Delta\mathcal{C}_M(\Lambda_{t_2}, \Lambda_{t_1})| \leq c_{M,\mathcal{G}} \Delta\tau \sup_{s \in [t_1, t_2]} \|\mathcal{L}_s\|_{1 \rightarrow 1}, \quad (51)$$

where  $\Delta\tau := t_2 - t_1$ . Moreover, for a uniform bound  $\|\mathcal{L}_s\|_{1 \rightarrow 1} \leq L_{\text{max}}$  for all  $s \in \mathcal{I}$ , any evolution that achieves a change  $\Delta\mathcal{C}_M(\Lambda_{t_2}, \Lambda_{t_1})$  must satisfy the minimal time constraint

$$\Delta\tau \geq \frac{|\Delta\mathcal{C}_M(\Lambda_{t_2}, \Lambda_{t_1})|}{c_{M,\mathcal{G}} L_{\text{max}}}. \quad (52)$$

Conversely, given a fixed maximal time budget  $T_{\text{max}} < \infty$  and a uniform generator bound  $\|\mathcal{L}_s\|_{1 \rightarrow 1} \leq L_{\text{max}}$  on  $[t_1, t_1 + T_{\text{max}}]$ , the achievable change in the advantage is bounded by

$$|\Delta\mathcal{C}_M(\Lambda_{t_2}, \Lambda_{t_1})| \leq T_{\text{max}} c_{M,\mathcal{G}} L_{\text{max}}, \quad (53)$$

where  $0 \leq t_2 - t_1 \leq T_{\text{max}}$ .

The proof of Corollary 9 is provided in Appendix M.

Suppose we want to achieve a fixed target change  $\Delta\mathcal{C}_M^* \geq 0$  of  $\mathcal{C}_M(\Lambda_t)$ . We define the corresponding minimal time as

$$\Delta\tau^*(\Delta\mathcal{C}_M^*) := \inf \{t_2 - t_1 \geq 0 \mid t_1, t_2 \in \mathcal{I}, |\Delta\mathcal{C}_M(\Lambda_{t_2}, \Lambda_{t_1})| \geq \Delta\mathcal{C}_M^*\}. \quad (54)$$

In words,  $\Delta\tau^*(\Delta\mathcal{C}_M^*)$  is the shortest time interval over which the given dynamics can produce a change in  $\mathcal{C}_M$  of at least  $\Delta\mathcal{C}_M^*$ . The uniform bound in Eq. (51) then implies a *resource-aware quantum speed limit* in the sense that for any time interval  $[t_1, t_2]$ ,

$$\frac{|\Delta\mathcal{C}_M(\Lambda_{t_2}, \Lambda_{t_1})|}{\Delta\tau} \leq c_{M,\mathcal{G}} \sup_{s \in [t_1, t_2]} \|\mathcal{L}_s\|_{1 \rightarrow 1}, \quad (55)$$

where  $\Delta\tau := t_2 - t_1$ . Thus, the average rate of change of  $\mathcal{C}_M$  is bounded from above by a quantity that depends

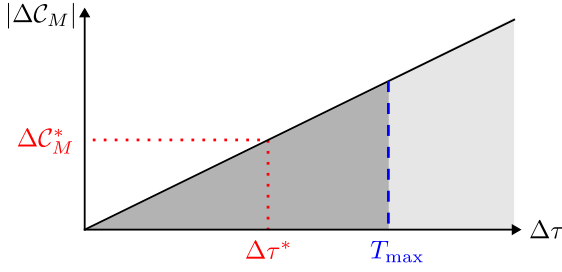


FIG. 2. Schematic illustration of the uniform time and feasibility bounds in Corollary 9. The horizontal axis shows the evolution time  $\Delta\tau$  and the vertical axis the change  $|\Delta\mathcal{C}_M|$ . For a uniform generator bound  $\|\mathcal{L}_s\|_{1\rightarrow 1} \leq L_{\max}$ , the light and dark gray regions below the line  $|\Delta\mathcal{C}_M| = c_{M,\mathcal{G}}L_{\max}\Delta\tau$  contain all admissible pairs. A time budget  $T_{\max}$  limits the achievable change to  $|\Delta\mathcal{C}_M| \leq T_{\max}c_{M,\mathcal{G}}L_{\max}$  (dark gray), while a target change  $\Delta\mathcal{C}_M^*$  defines a minimal time  $\Delta\tau^*$  via Eq. (54).

only on the task specified by the tuple  $(M, \mathcal{G})$  and on the family  $\{\mathcal{L}_t\}_t$  of Lindblad generators. Equivalently, for a fixed target  $\mathcal{C}_M^*$  and a uniform generator bound  $\|\mathcal{L}_s\|_{1\rightarrow 1} \leq L_{\max}$ , the minimal time satisfies

$$\Delta\tau^*(\Delta\mathcal{C}_M^*) \geq \frac{\Delta\mathcal{C}_M^*}{c_{M,\mathcal{G}}L_{\max}}. \quad (56)$$

Conversely, for a given maximal time budget  $T_{\max}$  and the same generator bound, Corollary 9 implies

$$|\Delta\mathcal{C}_M(\Lambda_{t_2}, \Lambda_{t_1})| \leq T_{\max}c_{M,\mathcal{G}}L_{\max} \quad (57)$$

for  $0 \leq t_2 - t_1 \leq T_{\max}$ , such that  $T_{\max}$  and  $\Delta\tau^*$  play dual roles:  $T_{\max}$  constrains *how much*  $\mathcal{C}_M$  can change, while  $\Delta\tau^*$  constrains *how fast* a prescribed change in  $\mathcal{C}_M$  can be reached.

At the same time, because Eq. (51) is model independent and uses the worst case supremum  $\sup_{s \in [t_1, t_2]} \|\mathcal{L}_s\|_{1\rightarrow 1}$ , the resulting bound can be loose when this supremum is a crude approximation to the actual time dependence of  $\Gamma_M(s)$ . Tighter, model-dependent bounds can be obtained by working directly with the integral  $\int_{t_1}^{t_2} \Gamma_M(s) ds$  (see Sec. IV for an analytical example).

We illustrate the simple concept underlying the uniform time and feasibility bounds in Fig. 2. The horizontal axis shows the time interval  $\Delta\tau = t_2 - t_1$  and the vertical axis the achievable change  $|\Delta\mathcal{C}_M(\Lambda_{t_2}, \Lambda_{t_1})|$ . The solid line represents the uniform bound for a generator satisfying  $\|\mathcal{L}_s\|_{1\rightarrow 1} \leq L_{\max}$  as in Eq. (57). The light-gray region below this line indicates the admissible pairs  $(\Delta\tau, |\Delta\mathcal{C}_M|)$ . A finite time budget  $T_{\max}$  imposes the additional vertical cut-off at  $\Delta\tau = T_{\max}$ , such that that the dark-gray rectangle highlights the maximal achievable change  $|\Delta\mathcal{C}_M| \leq T_{\max}c_{M,\mathcal{G}}L_{\max}$ . Conversely, for a fixed target change  $\Delta\mathcal{C}_M^*$  (recall Eq. (54)), the intersection with the bound line defines the minimal required time  $\Delta\tau^*$ , illustrating the resource-aware speed limit.

A common form of the Lindblad generator  $\mathcal{L}_t$  is the GKLS form (see Eq. (B10)). In that case, we can use

$$\Gamma_M(t) \leq R_{\mathcal{G}} \|\mathcal{L}_t^\dagger(M)\|_\infty \quad (58)$$

to obtain an explicit bound on  $\Delta\tau^*$  in terms of the Hamiltonian  $\tilde{H}(t) = H_S(t) + H_L(t)$ , which consists of the system's Hamiltonian  $H_S$  and a Lamb shift contribution  $H_L$ , and the Lindblad jump operators  $L_k(t)$ . Moreover, the Heisenberg adjoint of  $\mathcal{L}_t$  reads

$$\begin{aligned} \mathcal{L}_t^\dagger(M) &= i[\tilde{H}(t), M] + \sum_k [L_k^\dagger(t)ML_k(t) \\ &\quad - \frac{1}{2}\{L_k^\dagger(t)L_k(t), M\}] \end{aligned} \quad (59)$$

such that

$$\Gamma_M(t) \leq 2R_{\mathcal{G}}\|M\|_\infty \left( \|\tilde{H}(t)\|_\infty + \sum_k \|L_k(t)\|_\infty^2 \right). \quad (60)$$

Together with the variation bound Eq. (43) this implies that increasing  $\Delta\mathcal{C}_M(\Lambda_{t_2}, \Lambda_{t_1})$  (or, equivalently, lowering the lower bound on  $\Delta\tau$ ) requires either allocating more time or increasing the Hamiltonian or dissipator strengths.

#### D. Dissecting dynamics into free and resourceful components

In this section, we eventually show that for linear, idempotent resource-destroying maps  $\mathcal{G}$ , any channel (and its generator) admits a canonical decomposition into a  $\mathcal{G}$ -commuting “free” part and a “resource” part. The following theorem explains how we determine the free and resource parts and shows that only the resource part can affect  $\mathcal{C}_M(\Lambda_t)$ .

**Theorem 10** (Decomposition with respect to a resource-destroying map). *Let  $\mathcal{H}$  be a finite-dimensional Hilbert space, and let  $\mathcal{G} : \mathcal{B}(\mathcal{H}) \rightarrow \mathcal{B}(\mathcal{H})$  be a linear idempotent map. Let  $\{\Lambda_t\}_{t \in [0, T]}$  be a family of CPTP maps with  $\Lambda_0 = \text{id}$ , and let  $\mathcal{L}_t$  denote the corresponding time-local Lindblad generator,  $\frac{d}{dt}\Lambda_t = \mathcal{L}_t \circ \Lambda_t$ .*

(i) *For each  $t$  there are canonical decompositions*

$$\Lambda_t = \Lambda_{t,\text{free}} + \Lambda_{t,\text{res}}, \quad (61)$$

$$\mathcal{L}_t = \mathcal{L}_{t,\text{free}} + \mathcal{L}_{t,\text{res}}, \quad (62)$$

*defined by*

$$\Lambda_{t,\text{free}} := \mathcal{G} \circ \Lambda_t \circ \mathcal{G}, \quad \Lambda_{t,\text{res}} := \Lambda_t - \Lambda_{t,\text{free}}, \quad (63)$$

$$\mathcal{L}_{t,\text{free}} := \mathcal{G} \circ \mathcal{L}_t \circ \mathcal{G}, \quad \mathcal{L}_{t,\text{res}} := \mathcal{L}_t - \mathcal{L}_{t,\text{free}}. \quad (64)$$

*These decompositions are uniquely determined by  $\mathcal{G}$  and satisfy*

$$\Lambda_{t,\text{free}} = \mathcal{G} \circ \Lambda_{t,\text{free}} = \Lambda_{t,\text{free}} \circ \mathcal{G}, \quad (65)$$

$$\mathcal{G} \circ \Lambda_{t,\text{res}} \circ \mathcal{G} = 0, \quad (66)$$

and analogously

$$\mathcal{L}_{t,\text{free}} = \mathcal{G} \circ \mathcal{L}_{t,\text{free}} = \mathcal{L}_{t,\text{free}} \circ \mathcal{G}, \quad \mathcal{G} \circ \mathcal{L}_{t,\text{res}} \circ \mathcal{G} = 0. \quad (67)$$

(ii) For any observable  $M \in \mathcal{B}_{\text{sa}}(\mathcal{H})$ , the resource induced advantage depends only on the resource part of the channel, in the sense that

$$\mathcal{C}_M(\Lambda_t) = \sup_{\rho \in \mathcal{D}(\mathcal{H})} |\text{Tr}[M \Lambda_t(\rho - \mathcal{G}(\rho))]| = \mathcal{C}_M(\Lambda_{t,\text{res}}). \quad (68)$$

(iii) If  $\mathcal{G}$  is CPTP, then the free part  $\Lambda_{t,\text{free}}$  is CPTP for every  $t$ .

We provide the proof of Theorem 10 in Appendix N.

Here it is important to notice that  $\Lambda_{t,\text{free}}$  (and similarly  $\mathcal{L}_{t,\text{free}}$ ), as defined in Eq. (63), is in general *not* the same as the largest part of  $\Lambda_t$  that commutes with  $\mathcal{G}$ . To see this, recall the decomposition of any linear map  $T : \mathcal{B}(\mathcal{H}) \rightarrow \mathcal{B}(\mathcal{H})$  from Eq. (N3). Writing  $\mathcal{G}^\perp := \text{id} - \mathcal{G}$ , we have

$$T = \mathcal{G} \circ T \circ \mathcal{G} + \mathcal{G}^\perp \circ T \circ \mathcal{G}^\perp + \mathcal{G}^\perp \circ T \circ \mathcal{G} + \mathcal{G} \circ T \circ \mathcal{G}^\perp. \quad (69)$$

The ‘‘block-diagonal’’ part

$$\tilde{T} := \mathcal{G} \circ T \circ \mathcal{G} + \mathcal{G}^\perp \circ T \circ \mathcal{G}^\perp \quad (70)$$

preserves both  $\text{im}(\mathcal{G})$  and  $\text{ker}(\mathcal{G})$  and commutes with  $\mathcal{G}$ ,  $[\tilde{T}, \mathcal{G}] = 0$ . In contrast, the cross terms  $\mathcal{G}^\perp \circ T \circ \mathcal{G}$  and  $\mathcal{G} \circ T \circ \mathcal{G}^\perp$  need not commute with  $\mathcal{G}$  for a generic  $T$ . Thus  $\tilde{T}$  can be viewed as the projection of  $T$  onto the subspace of maps that commute with  $\mathcal{G}$  (block-diagonal in the decomposition  $\mathcal{B}(\mathcal{H}) = \text{im}(\mathcal{G}) \oplus \text{ker}(\mathcal{G})$ ), whereas in Theorem 10 we defined the ‘‘free’’ part of  $\Lambda_t$  and  $\mathcal{L}_t$  as the projection onto the image of  $\mathcal{G}$  only:

$$\Lambda_{t,\text{free}} = \mathcal{G} \circ \Lambda_t \circ \mathcal{G}, \quad \mathcal{L}_{t,\text{free}} = \mathcal{G} \circ \mathcal{L}_t \circ \mathcal{G}. \quad (71)$$

This choice is motivated by operational considerations:  $\mathcal{G} \circ T \circ \mathcal{G}$  is, by construction, the unique component of  $T$  that acts non-trivially only on the ‘‘free’’ sector  $\text{im}(\mathcal{G})$ . The residual part  $T_{\text{res}} := T - \mathcal{G} \circ T \circ \mathcal{G}$  then collects all contributions that involve the resourceful directions  $\text{ker}(\mathcal{G})$ . In particular, Theorem 10 part (ii) shows that  $\Lambda_{t,\text{res}}$  contains precisely those ‘‘resourceful’’ contributions of  $\Lambda_t$  that can generate a non-zero response functional  $\mathcal{C}_M(\Lambda_t)$ . This is reflected in Eqs. (65) and (66), and yields a clean splitting between free and resourceful parts of the dynamics.

For  $\mathcal{G}$  linear, the algebraic decompositions in Eqs. (N1) and (62) are always well defined. If  $\mathcal{G}$  is non-linear, however,  $\text{im}(\mathcal{G})$  and  $\text{ker}(\mathcal{G})$  are no longer linear subspaces in general, so the direct-sum decomposition (N1) is not available. Nevertheless, for both linear and non-linear idempotent  $\mathcal{G}$  one can still define the residual map

$$\tilde{\Lambda}_{\text{res}} := \Lambda - \Lambda \circ \mathcal{G}, \quad (72)$$

and a direct calculation using  $\mathcal{G}^2 = \mathcal{G}$  shows that

$$\mathcal{C}_M(\Lambda) = \mathcal{C}_M(\tilde{\Lambda}_{\text{res}}). \quad (73)$$

When  $\mathcal{G}$  is linear, Theorem 10 part (ii) additionally gives  $\mathcal{C}_M(\Lambda) = \mathcal{C}_M(\Lambda_{\text{res}})$ , such that

$$\mathcal{C}_M(\Lambda) = \mathcal{C}_M(\tilde{\Lambda}_{\text{res}}) = \mathcal{C}_M(\Lambda_{\text{res}}), \quad (74)$$

even though in general  $\tilde{\Lambda}_{\text{res}} \neq \Lambda_{\text{res}}$ . Equality of the maps  $\tilde{\Lambda}_{\text{res}}, \Lambda_{\text{res}}$  holds if and only if

$$\Lambda \circ \mathcal{G} = \mathcal{G} \circ \Lambda \circ \mathcal{G} = \Lambda_{\text{free}}. \quad (75)$$

A sufficient condition for this is  $\mathcal{G}$ -covariance of  $\Lambda$ , i.e.  $\Lambda \circ \mathcal{G} = \mathcal{G} \circ \Lambda$ , in which case  $\mathcal{G} \circ \Lambda \circ \mathcal{G} = \Lambda \circ \mathcal{G}$ .

The two cross terms in (N3) have natural interpretations in the resource theoretic setting. The block  $\mathcal{G}^\perp \circ \Lambda \circ \mathcal{G}$  describes the part of  $\Lambda$  that sends free inputs (in  $\text{im}(\mathcal{G})$ ) into resourceful sectors (i.e., elements of  $\text{ker}(\mathcal{G})$ ), while  $\mathcal{G} \circ \Lambda \circ \mathcal{G}^\perp$  describes the converse direction. In the terminology of Ref. [55], a channel  $\Lambda$  is *resource non-generating* if and only if

$$\mathcal{G} \circ \Lambda \circ \mathcal{G} = \Lambda \circ \mathcal{G}, \quad (76)$$

which is equivalent to

$$\mathcal{G}^\perp \circ \Lambda \circ \mathcal{G} = 0. \quad (77)$$

Similarly,  $\Lambda$  is *resource non-activating* if and only if

$$\mathcal{G} \circ \Lambda \circ \mathcal{G} = \mathcal{G} \circ \Lambda, \quad (78)$$

which is equivalent to

$$\mathcal{G} \circ \Lambda \circ \mathcal{G}^\perp = 0. \quad (79)$$

As shown in Ref. [55],  $\Lambda$  is both resource non-generating and resource non-activating if and only if it is  $\mathcal{G}$ -covariant,  $\Lambda \circ \mathcal{G} = \mathcal{G} \circ \Lambda$ .

Finally, even when  $\mathcal{G}$  is CPTP, the free component  $\Lambda_{t,\text{free}} = \mathcal{G} \circ \Lambda_t \circ \mathcal{G}$  is CPTP, but the residual map  $\Lambda_{t,\text{res}} = \Lambda_t - \Lambda_{t,\text{free}}$  need not be CPTP. Likewise, the projected generators  $\mathcal{L}_{t,\text{free}}$  and  $\mathcal{L}_{t,\text{res}}$  are algebraic objects and are not guaranteed to be physical Lindblad generators in their own right. In Corollary 11 we make precise what we mean by  $\mathcal{L}_{t,\text{free}}$  being *compatible* with  $\Lambda_{t,\text{free}}$  and give a simple criterion. For this, recall that in the time-independent case a linear map  $\mathcal{L}$  on  $\mathcal{B}(\mathcal{H})$  is a physical Lindblad generator if and only if it generates a quantum dynamical semigroup  $\Lambda_t = e^{t\mathcal{L}}$ , or equivalently a GKLS master equation [90]. In the time-dependent case,  $\mathcal{L}_t$  is typically called physical if it generates a CPTP family via a time-local master equation, or equivalently if the corresponding dynamical map is completely positive divisible [91, 92] (see also Appendix B for more information).

**Corollary 11.** *Let  $\Lambda_{t,\text{free}}$  and  $\mathcal{L}_{t,\text{free}}$  be defined as in Theorem 10, and let  $\mathcal{G}^\perp := \text{id} - \mathcal{G}$ . Then the following are equivalent:*

(i)  $\Lambda_{t,\text{free}}$  solves the time-local master equation

$$\frac{d}{dt}\Lambda_{t,\text{free}} = \mathcal{L}_{t,\text{free}} \circ \Lambda_{t,\text{free}} \quad \forall t \in [0, T] \quad (80)$$

with  $\Lambda_{0,\text{free}} = \mathcal{G}$ .

(ii) The following compatibility condition holds:

$$\mathcal{G} \circ \mathcal{L}_t \circ \mathcal{G}^\perp \circ \Lambda_t \circ \mathcal{G} = 0 \quad \forall t \in [0, T]. \quad (81)$$

In particular, each of the stronger conditions  $\mathcal{G} \circ \mathcal{L}_t \circ \mathcal{G}^\perp = 0$  or  $\mathcal{G}^\perp \circ \Lambda_t \circ \mathcal{G} = 0$  for all  $t \in [0, T]$  is sufficient to guarantee (80).

The short proof of Corollary 11 is shown in Appendix O.

Clearly,  $\Lambda_t$  being  $\mathcal{G}$ -covariant,  $\Lambda_t \circ \mathcal{G} = \mathcal{G} \circ \Lambda_t$  for all  $t$ , is a stronger condition than the compatibility condition in Corollary 11 and is therefore sufficient to guarantee that  $\Lambda_{t,\text{free}}$  and  $\mathcal{L}_{t,\text{free}}$  are compatible in the sense of Eq. (80). In particular,  $\mathcal{G}$ -covariance implies that  $\Lambda_t$  is both resource non-generating and non-activating [55], such that  $\mathcal{G}^\perp \circ \Lambda_t \circ \mathcal{G} = 0$  for all  $t$ . As discussed above, this is already enough to ensure that Eq. (81) is satisfied and, hence, that  $\mathcal{L}_{t,\text{free}}$  solves the time-local master equation for  $\Lambda_{t,\text{free}}$ . More generally, for any family  $\{\Lambda_t\}_{t \in [0, T]}$  such that each  $\Lambda_t$  is resource non-generating (i.e.  $\mathcal{G}^\perp \circ \Lambda_t \circ \mathcal{G} = 0$ ), the projected generator  $\mathcal{L}_{t,\text{free}}$  generates the projected dynamics  $\Lambda_{t,\text{free}}$  via Eq. (80).

We now illustrate the splitting of the dynamics into free and resourceful components introduced in Theorem 10 for some well-known Lindblad generators and investigate in each case whether  $\Lambda_{t,\text{free}}$  solves the corresponding projected time-local master equation. We present one example where the “free” components of the Lindblad generator and the quantum channel are compatible, and one where they are not.

As a concrete setting we consider a single qubit with Hilbert space  $\mathcal{H} \cong \mathbb{C}^2$  and choose as resource-destroying map the dephasing map in the computational basis,

$$\mathcal{G}(\rho) = \sum_{i=0,1} |i\rangle\langle i| \rho |i\rangle\langle i|, \quad (82)$$

which is CPTP. In Liouville space  $\mathcal{H} \otimes \mathcal{H}$  this dephasing map has the matrix representation

$$\mathcal{G} = \frac{1}{2}(\sigma_z \otimes \sigma_z + \mathbb{1}_{\mathcal{H} \otimes \mathcal{H}}), \quad (83)$$

where we use row-stacking (see Eq. (B6) in Appendix B) to represent superoperators acting on vectorized density operators  $|\rho\rangle\rangle$ . For notational simplicity we use the same symbols  $\mathcal{G}$ ,  $\Lambda_t$  and  $\mathcal{L}_t$  for both the maps and their matrix representations.

An example of a time-local generator  $\mathcal{L}_t \in \mathcal{B}(\mathcal{H} \otimes \mathcal{H})$  for which  $\mathcal{L}_{t,\text{free}}$  is compatible with  $\Lambda_{t,\text{free}}$  is

$$\mathcal{L}_t = \sum_{i \in \{x, y, z\}} \gamma_i(t) (\sigma_i \otimes \sigma_i^T - \mathbb{1}_{\mathcal{H} \otimes \mathcal{H}}), \quad (84)$$

with  $\gamma_i(t) \geq 0$  for all  $t$  and  $\sigma_i$  the Pauli matrices in the computational basis. The Lindblad superoperator (84) describes a qubit subject to three independent decoherence channels [92]. Since  $\mathcal{G}$  is defined in the same basis,  $\mathcal{L}_t$  preserves the decomposition into diagonal and off-diagonal operators, and one finds

$$\begin{aligned} \mathcal{L}_{t,\text{free}} = & (\gamma_x(t) + \gamma_y(t)) \left[ \sigma_- \otimes \sigma_- + \sigma_+ \otimes \sigma_+ \right. \\ & \left. - \frac{1}{2}(\sigma_z \otimes \sigma_z + \mathbb{1}_{\mathcal{H} \otimes \mathcal{H}}) \right]. \end{aligned} \quad (85)$$

In particular,  $\mathcal{G} \circ \mathcal{L}_t \circ \mathcal{G}^\perp = 0$ , so by Corollary 11 the projected generator  $\mathcal{L}_{t,\text{free}}$  indeed generates the projected dynamics  $\Lambda_{t,\text{free}}$ .

In contrast, not every projected channel  $\Lambda_{t,\text{free}}$  is compatible with its projected generator. A simple example is provided by purely Hamiltonian evolution

$$\mathcal{L}(\rho) = -i[H, \rho], \quad H = \frac{\Omega}{2}\sigma_x. \quad (86)$$

For the dephasing map  $\mathcal{G}$  in Eq. (83), any diagonal state  $\rho$  satisfies that  $[H, \rho]$  is purely off-diagonal, such that

$$\mathcal{L}_{\text{free}} = \mathcal{G} \circ \mathcal{L} \circ \mathcal{G} = 0. \quad (87)$$

At the same time, the projected dynamics  $\Lambda_{t,\text{free}} = \mathcal{G} \circ \Lambda_t \circ \mathcal{G}$  is non-trivial and can be written in Liouville form as

$$\begin{aligned} \Lambda_{t,\text{free}} = & \frac{1}{2} \cos^2\left(\frac{\Omega t}{2}\right) (\sigma_z \otimes \sigma_z + \mathbb{1} \otimes \mathbb{1}) \\ & + \sin^2\left(\frac{\Omega t}{2}\right) (\sigma_- \otimes \sigma_- + \sigma_+ \otimes \sigma_+). \end{aligned} \quad (88)$$

Since  $\mathcal{L}_{\text{free}} = 0$  but  $\Lambda_{t,\text{free}}$  is time-dependent for all  $t \neq 2\pi m/\Omega$ ,  $m \in \mathbb{Z}$ , the projected channel does not satisfy the projected differential equation  $\frac{d}{dt}\Lambda_{t,\text{free}} = \mathcal{L}_{\text{free}} \circ \Lambda_{t,\text{free}}$  except at those isolated times. This illustrates that the “free” components of generator and channel need not be compatible in general.

### III. RESOURCE THEORIES WITHOUT RESOURCE DESTROYING MAP

Although having a free-state set that forms an affine subset of the state space is a necessary condition for the existence of a linear resource-destroying map, it is not sufficient as there exist affine resource theories that do not admit any such map. In the absence of a resource-destroying map (linear or not), we can no longer use it to define the “classical” baseline that we relied on in Sec. II to quantify how much advantage a channel can extract from a resource. In what follows, we show how the concepts from Sec. II can be extended to resource theories without a resource-destroying map. This extension, however, comes with a subtle change in perspective and in the interpretation of the analogue of the resource impact functional  $\mathcal{C}_M(\Lambda)$ , which we discuss below.

We consider a resource theory with a set of free states  $\mathcal{F}$ , a set of free operations  $\mathcal{O}$  (see Appendix A 1), and a divergence  $D(\cdot\|\cdot)$  such that

$$D(\Phi(\rho)\|\Phi(\sigma)) \leq D(\rho\|\sigma) \quad \forall \rho, \sigma \in \mathcal{D}(\mathcal{H}), \forall \Phi \in \mathcal{O}, \quad (89)$$

i.e.,  $D$  is contractive under all free operations. Moreover, we assume that  $\mathcal{F}$  is compact and that  $D(\rho\|\sigma)$  is lower semi-continuous in  $\sigma$  such that, for each  $\rho \in \mathcal{D}(\mathcal{H})$ , the minimiser of  $D(\rho\|\sigma)$  over  $\sigma \in \mathcal{F}$  exists. We denote the set of minimisers by

$$\mathcal{P}(\rho) := \arg \min_{\sigma \in \mathcal{F}} D(\rho\|\sigma) \subset \mathcal{F}. \quad (90)$$

In analogy to the definition of  $\mathcal{C}_M(\Lambda)$  in Eq. (4), we then define the resource impact functional ( $\mathcal{H}$  finite-dimensional)

$$\mathfrak{C}_M(\Lambda) := \max_{\rho \in \mathcal{D}(\mathcal{H})} \max_{\pi(\rho) \in \mathcal{P}(\rho)} |\text{Tr}[M(\Lambda(\rho) - \Lambda(\pi(\rho)))]|. \quad (91)$$

Here  $\pi(\rho)$  is chosen among the free states that are closest to  $\rho$  with respect to  $D(\cdot\|\cdot)$ , and the extra maximisation over  $\pi(\rho) \in \mathcal{P}(\rho)$  resolves the possible non-uniqueness of the closest free state. By construction, we adopt an ‘‘optimistic’’ convention [93]: for each  $\rho$  we select, among all closest free baselines, the one that yields the largest task advantage. If  $\mathcal{P}(\rho)$  consists of a single state for all  $\rho$  (for instance under suitable strict convexity assumptions on  $D(\cdot\|\cdot)$ ), the inner minimisation is trivial and  $\mathfrak{C}_M(\Lambda)$  reduces to a direct analogue of  $\mathcal{C}_M(\Lambda)$  with the resource-destroying map  $\mathcal{G}$  replaced by  $\rho \mapsto \pi(\rho)$ .

In analogy to  $\mathcal{C}_M(\Lambda)$  in Eq. (4), the functional  $\mathfrak{C}_M(\Lambda)$  still pairs each density operator  $\rho$  with a corresponding free counterpart. However, its interpretation is slightly different: while the resource-destroying map  $\mathcal{G}$  in Sec. II provides an operationally defined free counterpart  $\mathcal{G}(\rho)$  obtained by physically ‘‘removing’’ the resource,  $\pi(\rho)$  selects a free baseline *geometrically*, as a minimiser of a chosen quantum information divergence  $D(\cdot\|\cdot)$ . Consequently, different choices of  $D(\cdot\|\cdot)$  lead to different notions of what it means for a state to be a ‘‘closest’’ free counterpart of  $\rho$ . For example, choosing  $\sigma$  to minimise the trace distance  $\|\rho - \sigma\|_1/2$  picks the free state that is hardest to distinguish from  $\rho$  in a single-shot minimum-error discrimination task, as quantified by the Helstrom bound [94–96]. In contrast, choosing  $\sigma$  to minimise the quantum relative entropy  $S(\rho\|\sigma) = \text{Tr}[\rho(\ln(\rho) - \ln(\sigma))]$  yields a free state that is asymptotically hardest to distinguish from  $\rho$  in a many-copy hypothesis testing scenario [97, 98].

Based on the definition of  $\mathfrak{C}_M(\Lambda)$  in Eq. (91), we can introduce an analogue of the instantaneous rate  $\Gamma_M(t)$  in Eq. (40) for the distance-projected setting by

$$\mathfrak{T}_M(t) := \max_{\rho \in \mathcal{D}(\mathcal{H})} \max_{\pi(\rho) \in \mathcal{P}(\rho)} |\text{Tr}[M \mathcal{L}_t(\Lambda_t(\rho - \pi(\rho)))]|. \quad (92)$$

Replacing  $\rho - \mathcal{G}(\rho)$  by  $\rho - \pi(\rho)$  throughout the proof of Theorem 7, and taking the maximum over the choice

of closest free state  $\pi(\rho) \in \mathcal{P}(\rho)$ , yields variation and time bounds for  $\mathfrak{C}_M(\Lambda_t)$  that are completely analogous to Theorem 7 and Corollary 9. Since these modifications are purely notational, we omit the details here, and continue with the discussion of three chemically motivated examples.

#### IV. DONOR-ACCEPTOR MODEL

In this section, we illustrate how to compute the resource impact functional  $\mathcal{C}_M(\Lambda)$  and the instantaneous advantage rate  $\Gamma_M(t)$  for a simple donor-acceptor dimer. This system can be viewed as the minimal non-trivial model of excitonic energy transfer, where an electronic excitation initially localized on the donor,  $|D\rangle := |1_e\rangle \otimes |2_g\rangle$ , can coherently hop to the acceptor,  $|A\rangle := |1_g\rangle \otimes |2_e\rangle$ , which is subject to dephasing and spontaneous emission, where  $|1_g\rangle$  ( $|1_e\rangle$ ) correspond to the ground (excited) state of the donor site, and similarly  $|2_g\rangle$  ( $|2_e\rangle$ ) refer to the ground (excited) state of the acceptor site. In photosynthetic complexes and model exciton transport networks, the population transferred to an acceptor (or trap) is often interpreted as a transport efficiency or reaction yield [99–102].

We work in the single-excitation subspace with Hilbert space

$$\mathcal{H} = \text{span}_{\mathbb{C}}\{|g\rangle, |D\rangle, |A\rangle\} \cong \mathbb{C}^3, \quad (93)$$

where  $|g\rangle := |1_g\rangle \otimes |2_g\rangle$  denotes the electronic ground state and  $|D\rangle$  and  $|A\rangle$  are the donor and acceptor exciton states, respectively.

We consider the resource theory of coherence in the site basis  $\{|D\rangle, |A\rangle\}$ . Free states are those that are diagonal in this basis, such that the corresponding set of free states is given by

$$\mathcal{F} = \{\rho \mid \rho = p_D |D\rangle\langle D| + p_A |A\rangle\langle A|, p_D, p_A \geq 0, p_D + p_A \leq 1\}, \quad (94)$$

while the resource consists of donor-acceptor coherences  $\rho_{DA} = \langle D|\rho|A\rangle \neq 0$ . As resource-destroying map we take complete dephasing in the site basis,

$$\mathcal{G}(\rho) = \sum_{i \in \{g, D, A\}} |i\rangle\langle i| \rho |i\rangle\langle i|, \quad (95)$$

and we use  $\mathcal{C}_M(\Lambda)$  and  $\Gamma_M(t)$  as defined in Eqs. (4) and (40). For the Lindblad dynamics considered below, no coherence between  $|g\rangle$  and the single-excitation manifold is generated and, hence, only the  $\{|D\rangle, |A\rangle\}$  block contributes.

As a representative task we choose  $M = |A\rangle\langle A|$ , such that  $\text{Tr}[M\Lambda(\rho)]$  is the acceptor population at the end of the process, i.e., the exciton transfer yield. In this language,  $\mathcal{C}_M(\Lambda)$  quantifies the maximal increase in acceptor yield that any initial site coherence can provide, compared to its dephased counterpart  $\mathcal{G}(\rho)$ .

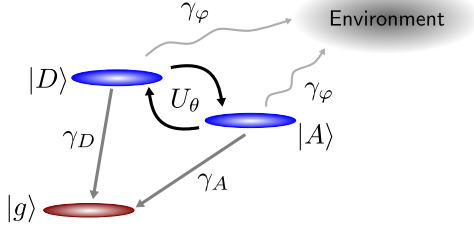


FIG. 3. Illustration of the three-site donor-acceptor model and the three processes described by the quantum channel in Eq. (99) (see text for more details).

### A. Static coherence advantage from donor-acceptor mixing

We first consider the purely coherent part of the dynamics, described by the excitonic Hamiltonian

$$H_{\text{ex}} = \frac{\Delta}{2} (|D\rangle\langle D| - |A\rangle\langle A|) + J (|D\rangle\langle A| + |A\rangle\langle D|), \quad (96)$$

with detuning  $\Delta$  and electronic coupling  $J$ . Its eigenstates are  $|+\rangle = \cos\theta|D\rangle + \sin\theta|A\rangle$  and  $|-\rangle = -\sin\theta|D\rangle + \cos\theta|A\rangle$ , where  $\theta = \frac{1}{2} \arctan(2J/\Delta)$  is the donor-acceptor mixing angle.

The associated unitary channel  $\Lambda_\theta(\rho) = U_\theta \rho U_\theta^\dagger$  with

$$U_\theta = |g\rangle\langle g| + \cos\theta(|D\rangle\langle D| + |A\rangle\langle A|) + \sin\theta(|A\rangle\langle D| - |D\rangle\langle A|) \quad (97)$$

generates coherence in the site basis and is therefore not a free operation in the resource theory of coherence. A straightforward calculation shows that

$$\mathcal{C}_{|A\rangle\langle A|}(\Lambda_\theta) = \left\| (\text{id} - \mathcal{G}) \Lambda_\theta^\dagger(M) \right\|_\infty = \frac{1}{2} |\sin(2\theta)|, \quad (98)$$

which is maximised at  $\theta = \pi/4$ , corresponding to resonant, maximally delocalised excitonic eigenstates, as expected, and  $\mathcal{C}_M(\Lambda_\theta)$  quantifies its maximal magnitude for a non-zero advantage in the exciton transfer task.

### B. Dissipative dynamics, $\Gamma_M(t)$ , and variation bounds

To make the model more realistic, we include dephasing in the excited-state manifold and spontaneous emission to the electronic ground state. At the level of a single effective ‘‘gate time’’  $\Delta t$ , we model these processes by a phase damping channel  $\Lambda_{\text{PD}}$  with parameter  $\eta$  and an amplitude damping channel  $\Lambda_{\text{AD}}$  with decay probabilities  $p_D, p_A$  from  $|D\rangle$  and  $|A\rangle$  to  $|g\rangle$ , respectively (explicit Kraus operators are given in Appendix P). Combined with the coherent donor-acceptor mixing  $\Lambda_\theta(\rho) = U_\theta \rho U_\theta^\dagger$ ,

the full one-step process is described by the CPTP map

$$\Lambda = \Lambda_{\text{AD}} \circ \Lambda_{\text{PD}} \circ \Lambda_\theta. \quad (99)$$

For a general POVM element

$$M = \mu_g |g\rangle\langle g| + \mu_D |D\rangle\langle D| + \mu_A |A\rangle\langle A| + (\nu |D\rangle\langle A| + \text{h.c.}), \quad (100)$$

with  $0 \leq M \leq \mathbb{1}$ ,  $\mu_i \in \mathbb{R}$  ( $i \in \{g, D, A\}$ ), and  $\nu \in \mathbb{C}$ , one finds that (see Appendix P)

$$\mathcal{C}_M(\Lambda) = \left| \cos(2\theta) \eta \nu \sqrt{(1-p_D)(1-p_A)} + \frac{1}{2} \sin(2\theta) \left[ \mu_A(1-p_A) - \mu_D(1-p_D) + \mu_g(p_A - p_D) \right] \right|. \quad (101)$$

In particular, for the readout  $M = |A\rangle\langle A|$  this reduces to

$$\mathcal{C}_{|A\rangle\langle A|}(\Lambda) = \frac{1}{2} (1-p_A) |\sin(2\theta)|, \quad (102)$$

i.e., a damped version of Eq. (98), as expected from amplitude damping on the acceptor.

To analyse the time dependence of coherence-induced advantage, we additionally employ a continuous-time Markovian description and propagate observables in the Heisenberg picture under the adjoint Lindblad generator  $\mathcal{L}^\dagger$ . Specifically, we consider the semigroup  $\Lambda_t^\dagger = \exp(t\mathcal{L}^\dagger)$  satisfying

$$\frac{d}{dt} \Lambda_t^\dagger(M) = \mathcal{L}^\dagger(\Lambda_t^\dagger(M)), \quad (103)$$

with

$$\mathcal{L}^\dagger(M) = i[H_{\text{ex}}, M] + \sum_{k=1}^4 \left( L_k^\dagger M L_k - \frac{1}{2} \{L_k^\dagger L_k, M\} \right), \quad (104)$$

and jump operators

$$\begin{aligned} L_1 &= \sqrt{\gamma_\varphi} |D\rangle\langle D|, & L_2 &= \sqrt{\gamma_\varphi} |A\rangle\langle A|, \\ L_3 &= \sqrt{\gamma_D} |g\rangle\langle D|, & L_4 &= \sqrt{\gamma_A} |g\rangle\langle A|. \end{aligned} \quad (105)$$

The finite-time parameters are related to the rates by  $\eta(\Delta t) = e^{-\gamma_\varphi \Delta t}$  and  $p_j(\Delta t) = 1 - e^{-\gamma_j \Delta t}$  for  $j \in \{D, A\}$ . We stress that the CPTP map in Eq. (99) and the semigroup  $\Lambda_{\Delta t} = e^{\Delta t \mathcal{L}}$  are, in general, not identical for finite  $\Delta t$  (since the coherent and dissipative generators do not commute when  $J \neq 0$ ). Instead, Eq. (99) can be viewed as a convenient splitting approximation that agrees with  $e^{\Delta t \mathcal{L}}$  to first order in  $\Delta t$  and becomes exact in the limit of sufficiently small time steps.

The adjoint dynamics preserves the block form of  $M$  in Eq. (100), such that we can parametrise

$$\begin{aligned} \Lambda_t^\dagger(M) &= x_g(t) |g\rangle\langle g| + x_D(t) |D\rangle\langle D| + x_A(t) |A\rangle\langle A| \\ &\quad + (y(t) |D\rangle\langle A| + \text{h.c.}), \end{aligned} \quad (106)$$

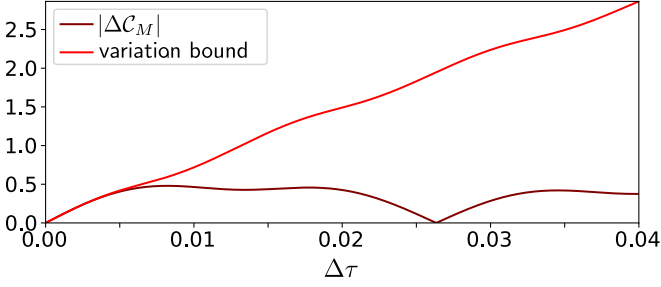


FIG. 4. Illustration of the coherence-induced task advantage and its variation bound in the donor–acceptor model. We plot the exact task advantage  $|\Delta\mathcal{C}_M|$  (dark red) and the integrated variation bound  $\int_0^t \Gamma_M(s) ds$  (light red) from Theorem 7 for  $M = |A\rangle\langle A|$ , starting at  $t_1 = 0$ , for parameters  $\Delta = 130$ ,  $J = 100$ , and  $\gamma = 5$  (in arbitrary but consistent units).

with  $x_g(t), x_D(t), x_A(t) \in \mathbb{R}$  and  $y(t) \in \mathbb{C}$ . For the dephasing map  $\mathcal{G}$  in Eq. (95) this implies (see Appendix P for more details)

$$\mathcal{C}_M(\Lambda_t) = |y(t)|, \quad \Gamma_M(t) = \left| \frac{dy(t)}{dt} \right|. \quad (107)$$

The coupled linear equations governing  $x_D(t), x_A(t), y(t)$  are collected in Eq. (P7) in Appendix P, where we also derive explicit solutions in several physically relevant regimes, which are discussed next.

#### Zero dephasing and symmetric lifetimes

As an illustrative example, consider first the case of zero dephasing ( $\gamma_\varphi = 0$ ) and symmetric lifetimes ( $\gamma_D = \gamma_A = \gamma$ ). Derivation and explicit expressions of  $\mathcal{C}_M(\Lambda)$ ,  $\Gamma_M(\Lambda)$  and the corresponding variation bound (recall Theorem 7) for general  $M$  in Eq. (100) can be found in Appendix P 1. Here, we illustrate in Fig. 4 the behaviour of  $|\Delta\mathcal{C}_M(\Lambda_{t_2}, \Lambda_{t_1})|$  (dark red) as well as the integrated variation bound (red) for  $M = |A\rangle\langle A|$ . For short time intervals the bound  $\int_0^t \Gamma_{|A\rangle\langle A|}(s) ds$  closely follows  $|\mathcal{C}_{|A\rangle\langle A|}(\Lambda_t)|$ , and in this regime, the bound provides a tight estimate of how rapidly the coherence-induced advantage for acceptor yield can grow. At longer times, however, the oscillatory Rabi dynamics of the dimer leads to modulations in the exact  $\mathcal{C}_{|A\rangle\langle A|}(\Lambda_t)$ , whereas the variation bound is monotonically increasing. The locations of the maxima of  $|\Delta\mathcal{C}_{|A\rangle\langle A|}|$  indicate the optimal times at which a given amount of coherence yields the largest enhancement of the acceptor population.

#### Zero detuning and finite dephasing

For zero detuning,  $\Delta = 0$ , but finite dephasing  $\gamma_\varphi > 0$ , the dynamics of the coherence  $y(t)$  crosses over from underdamped Rabi-like oscillations to overdamped exponential relaxation as  $\gamma_\varphi$  increases. In Appendix P 2 we

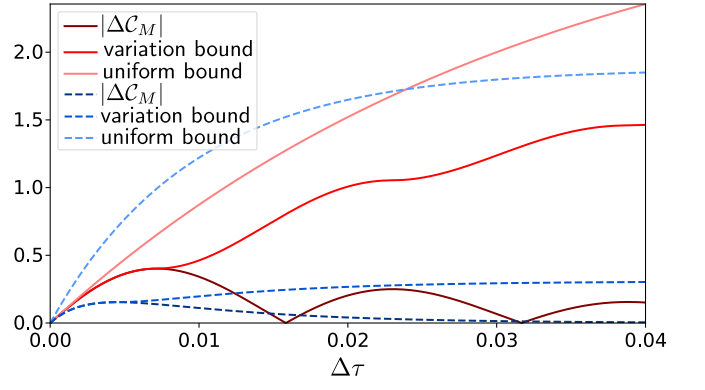


FIG. 5. Change in the coherence-induced resource impact functional in the donor-acceptor model for zero detuning and  $J = 100$ ,  $\gamma = 5$ . We plot the exact change  $|\Delta\mathcal{C}_M|$  for  $M = |A\rangle\langle A|$  (dark red solid: underdamped with  $\gamma_\varphi = 50$ ; dark blue dashed: overdamped with  $\gamma_\varphi = 500$ ), the corresponding variation bounds  $\int_0^t \Gamma_M(s) ds$  (medium red solid/medium blue dashed), and the analytic uniform bounds from Eq. (P64) (light red solid/light blue dashed). We choose  $t_1 = 0$  such that  $\Delta\tau = t_2$ .

solve the corresponding equations of motion analytically and obtain explicit expressions for  $\mathcal{C}_M(t)$ ,  $\Gamma_M(t)$ , and the induced variation bounds (43) for a generic POVM element  $M$  in Eq. (100) in the three regimes: underdamped ( $\gamma_\varphi < 4|J|$ ), critical ( $\gamma_\varphi = 4|J|$ ), and overdamped ( $\gamma_\varphi > 4|J|$ ).

Fig. 5 illustrates the time-dependent change  $|\Delta\mathcal{C}_M|$  in the resource impact functional for the special case  $M = |A\rangle\langle A|$ , both in the underdamped regime (dark red solid curve) and in the overdamped regime (dark blue dashed curve). As representative parameters we choose  $J = 100$  and  $\gamma = 5$  (as in Fig. 4), together with  $\gamma_\varphi = 50$  in the underdamped case and  $\gamma_\varphi = 500$  in the overdamped case. We set  $t_1 = 0$  such that  $|\Delta\mathcal{C}_M| = |\mathcal{C}_M(\Lambda_{t_2}) - \mathcal{C}_M(\Lambda_0)|$  reduces to  $|\mathcal{C}_M(\Lambda_{t_2})|$ , and  $\Delta\tau = t_2 - t_1 = t_2$ .

In Appendix P 2 we further show that, for  $M = |A\rangle\langle A|$ , the maximal achievable change in the resource impact functional over any interval  $[t_1, t_2]$  is bounded from above by simple functions of the system parameters  $J$ ,  $\gamma_\varphi$ , and  $\gamma$ . These lead to the analytic uniform bounds given in Eq. (P64), which provide closed form upper bounds on  $|\Delta\mathcal{C}_M|$  obtained by bounding the integral in Eq. (43). In Fig. 5 these uniform bounds are shown by the light red solid (underdamped) and light blue dashed (overdamped) curves. For comparison, the numerically integrated variation bounds  $\int_0^t \Gamma_M(s) ds$  are shown as medium red solid and medium blue dashed curves.

In the underdamped case, the analytic uniform bound remains relatively tight at short times and captures the correct order of magnitude of the oscillatory growth of  $|\Delta\mathcal{C}_M|$ . In the overdamped case, however, the uniform bound is considerably looser as the coarse estimates used to control the hyperbolic functions in  $\Gamma_M(t)$  (see Eqs. (P50), (P51) and (P53)) lead to an upper envelope

that overestimates the actual variation bound.

Finally, as discussed in Appendix P 2, the uniform bounds on  $|\Delta\mathcal{C}_M|$  imply feasibility bounds in Eq. (P66), which further constrain which target values of  $|\Delta\mathcal{C}_M|$  are reachable within the model within a finite time window. In particular, for fixed  $J$  and  $\gamma$ , increasing the dephasing rate  $\gamma_\varphi$  not only suppresses the maximal coherence-induced advantage but also shrinks the time interval over which a given  $|\Delta\mathcal{C}_M|$  can be realised (see also Fig. 5). From the exciton transport perspective, site basis coherence can enhance the donor-to-acceptor transfer yield in this minimal dimer, but only within strict quantitative limits set by the coupling strength and the environmental rates. The quantity  $\mathcal{C}_M(\Lambda_t)$  identifies the maximal coherence-assisted improvement of the transfer efficiency at time  $t$ , while  $\Gamma_M(t)$  and the associated time and feasibility bounds constrain how rapidly such an advantage can build up or decay.

## V. CONCLUSIONS AND OUTLOOK

Motivated by the goal of quantifying when quantum resources have an operational impact in chemical processes, we have introduced the resource impact functional  $\mathcal{C}_M(\Lambda)$  (recall Eq. (4)). For a fixed quantum channel  $\Lambda$  and observable  $M$ ,  $\mathcal{C}_M(\Lambda)$  quantifies the maximal change in the expectation value of  $M$  that can be induced by replacing an input state  $\rho$  with its resource-free counterpart  $\mathcal{G}(\rho)$  in a single application of  $\Lambda$ . This construction is based on a quantum-classical baseline provided by a resource-destroying map  $\mathcal{G}$ , which pairs each state  $\rho$  with the free state  $\mathcal{G}(\rho)$  obtained by removing the chosen resource. We established various key properties of  $\mathcal{C}_M(\Lambda)$ , including convexity, continuity, and pre- and post-processing inequalities, and discussed their practical relevance. A particular emphasis was placed on comparing  $\mathcal{C}_M(\Lambda)$  with alternative, “unpaired” constructions that optimise independently over all resourceful and all free inputs (e.g., see Eq. (9)). Together with the geometric and operational interpretations in Secs. II A 3 and II A 4, this clarifies the scope of  $\mathcal{C}_M(\Lambda)$ : for a given process  $(\Lambda, M)$ , it quantifies the largest resource-induced change in the target signal relative to the paired free baseline  $\mathcal{G}(\rho)$ . In this way,  $\mathcal{C}_M(\Lambda)$  characterises how the resource content of the input can affect the dynamics and, consequently, the chosen figure of merit. Since not all resource theories admit a resource-destroying map, we also explained in Sec. III how the definition of  $\mathcal{C}_M(\Lambda)$  can be generalised in such cases, and how this slightly shifts its operational interpretation.

The identification of resource measures with maximal advantages in suitable discrimination tasks is by now standard in quantum resource theory (see, e.g., Refs. [51, 53, 54]). In our setting,  $\mathcal{C}_M(\Lambda)$  is precisely twice the maximal single-shot bias above random guessing in distinguishing, using the fixed process  $(\Lambda, M)$ , whether the input was  $\rho$  or its resource-free counterpart

$\mathcal{G}(\rho)$ . This follows directly from standard results in binary hypothesis testing and quantum state discrimination. While the functional  $\mathcal{C}_M(\Lambda)$  itself appears to be new, its operational interpretation therefore fits naturally into this broader discrimination-based characterisation of quantum resources.

This perspective also opens the door to further questions, such as trade-offs between different tasks. Given two observables  $M_1$  and  $M_2$ , one may ask whether there exists a state that (approximately) maximises the yield gain for both tasks simultaneously. In general, this is not expected: for linear  $\mathcal{G}$ , the operators  $B_{M,\Lambda}$  entering  $\mathcal{C}_M(\Lambda) = \|B_{M,\Lambda}\|_\infty$  (Theorem 1, Sec. II A 4) need not have a common eigenbasis, so the states that optimise  $\mathcal{C}_{M_1}(\Lambda)$  and  $\mathcal{C}_{M_2}(\Lambda)$  may be incompatible. The tools developed here provide a natural language to analyse such incompatibilities of optimal resources across tasks. This is particularly relevant in chemical settings, where different figures of merit, e.g., competing reaction yields, selectivities, or signal contrasts, may be sensitive to different resource characteristics, and any functional role of quantum resources is likely to involve compromises or synergies between more than a single task or resource type.

To bound how quickly a resource can modify a yield, we introduced the instantaneous rate  $\Gamma_M(t)$  and showed that integral bounds in terms of  $\Gamma_M(t)$  constrain how fast the resource impact functional can change along a given dynamics (Sec. II B), independent of microscopic details. In particular, uniform bounds on  $\Gamma_M(t)$  lead to lower bounds on the time required to achieve a prescribed change in  $\mathcal{C}_M(\Lambda_t)$ , providing “activation time” guarantees that play the role of resource-aware analogues of quantum speed limits (Sec. II C). It will be interesting in future work to explore these bounds in more complex models, and to investigate whether they can be saturated or tightened for specific classes of dynamics.

Moreover, we introduced a mathematically well-defined and physically motivated decomposition of time-local master equations into free and resourceful components and showed that only the resourceful component  $\Lambda_{\text{res}}$  of a channel  $\Lambda$  contributes to the resource impact functional, i.e.,  $\mathcal{C}_M(\Lambda) = \mathcal{C}_M(\Lambda_{\text{res}})$  (see Sec. II D). This is significant because it singles out, within an arbitrary open system evolution, those parts of the dynamics that are responsible for exploiting the resource in the sense of changing the measurement statistics for  $M$ . This may be particularly valuable in more complicated scenarios where it is not obvious a priori which terms in the generator are responsible for an enhanced yield or a non-zero  $\mathcal{C}_M(\Lambda)$ .

The donor-acceptor example in Sec. IV provides a closed form evaluation of the resource impact functional  $\mathcal{C}_M(\Lambda_t)$  and the instantaneous rate  $\Gamma_M(t)$  within a standard GKSL (Lindblad) description of exciton dynamics. In this setting,  $\mathcal{C}_M(\Lambda_t)$  yields a state-independent upper bound on the maximal coherence-induced deviation of a specified readout at time  $t$  from its dephased baseline,

thereby identifying the time windows in which coherence can be operationally relevant for the task at hand. Excitation energy transfer models are a particularly instructive because experimentally relevant parameters often lie between the fully coherent and fully incoherent limits: in many molecular aggregates and excitonic network models, the electronic coupling and the effective system-bath interaction are comparable, and bath relaxation can occur on timescales comparable to the transfer dynamics [34, 103–111]. At the same time, this implies that these intermediate coupling and finite bath memory regimes require going beyond the Lindblad description using methods not relying on the Born-Markov approximation, which will be an important direction for future work.

Finally, non-Markovian dynamics and multi-time processes are crucial for realistic chemical applications, where a sequence of control operations, such pulse sequences in ultrafast spectroscopy, interacts with a quantum system. To capture such multi-time behaviour, one may extend the present framework from single-step channels to process tensors [112–120]. As a concrete example, one could construct the process tensor of a model reaction using a numerically exact time-dependent method such as time-dependent density matrix renormalisation group (TD-DMRG), where the process tensor admits a compact matrix product operator representation [115, 118, 119]. This would allow one to generalise the resource impact functional to a functional of the process tensor, thereby quantifying how much a given quantum resource can influence not just a single application of  $\Lambda$  but an entire class of control sequences acting on the system. In parallel, the same process tensor could be reconstructed (approximately) from experimental data, thus, extending ideas of quantum process tomography applied to ultrafast spectroscopy signals [121–125]. A comparison between the TD-DMRG derived and experimentally reconstructed process tensors would then provide a way of benchmarking model Hamiltonians and open system descriptions of vibrationally coupled electron transfer, such as those studied in Ref. [21]. In particular, one could (i) quantify how strongly quantum resources, e.g., coherence and memory effects, contribute to the experimentally observed dynamics, (ii) identify which model ingredients are essential to reproduce the resource impact seen in experiment, and (iii) assess the limitations of approximate Markovian or coarse grained descriptions from the perspective of their ability to capture resource-induced effects.

## ACKNOWLEDGMENTS

This research was funded by the National Science Foundation under Grant No. CHE-2537080.

## Appendix A: Recap of quantum resource theories

In the following, we briefly summarize various concepts from quantum resource theory (QRT) which are used in the main text. There are many good references for QRTs, and we refer in particular to Refs. [47, 48] for more information.

### 1. Free states and free operations

Suppose only a subset of quantum states can be prepared at negligible cost, referred to as the *free states*. Then, the general idea of a QRT is to partition physically allowed transformations into two classes: those that are implementable essentially for free, called *free operations*, and all other, costly transformations. Free operations are required to be compatible with the free states in the sense that they never generate a resource from a free input. One can specify a QRT starting either from a physically motivated set of free states and then identifying the operations that preserve it, or from a constrained class of operations and then defining the corresponding free states. In particular, the set of free operations may be chosen to be smaller than the maximum set of admissible free operations, referred to as *resource non-generating operations*, that leaves the set of free states invariant. The appropriate starting point depends on the context, and in all cases the sets of free states and free operations must be mutually consistent.

Let  $\mathcal{H}$  be a finite-dimensional complex Hilbert space of dimension  $d = \dim(\mathcal{H})$ , and denote by  $\mathcal{D}(\mathcal{H})$  the set of density operators. Since in finite dimensions, positivity of an operator implies its Hermiticity,  $\rho \in \mathcal{D}(\mathcal{H})$  if and only if  $\text{Tr}[\rho] = 1$  and  $\rho \geq 0$ . Thus,

$$\mathcal{D}(\mathcal{H}) := \{\rho \in \mathcal{B}(\mathcal{H}) | \rho \geq 0, \text{Tr}[\rho] = 1\}, \quad (\text{A1})$$

where  $\mathcal{B}(\mathcal{H})$  denotes the set of bounded linear operators on  $\mathcal{H}$ .

For systems  $A$  and  $B$  with Hilbert spaces  $\mathcal{H}_A$  and  $\mathcal{H}_B$ , we write  $\mathcal{D}_A \equiv \mathcal{D}(\mathcal{H}_A)$  and  $\mathcal{D}_B \equiv \mathcal{D}(\mathcal{H}_B)$ . A set of free states is a subset  $\mathcal{F}_A \subseteq \mathcal{D}_A$  (and similarly  $\mathcal{F}_B \subseteq \mathcal{D}_B$ ). Free operations are modelled as completely positive trace-preserving (CPTP) linear maps between operator algebras. Let

$$\text{CPTP}_{A \rightarrow B} := \{\Lambda : \mathcal{B}(\mathcal{H}_A) \rightarrow \mathcal{B}(\mathcal{H}_B) \text{ linear, CPTP}\}. \quad (\text{A2})$$

A collection  $\mathcal{O}_{A \rightarrow B} \subseteq \text{CPTP}_{A \rightarrow B}$  is a valid class of free operations (relative to the sets of free states  $\mathcal{F}_A, \mathcal{F}_B$ ) if it satisfies:

- (i) inclusion of the identity map:  $\text{id}_A \in \mathcal{O}_{A \rightarrow A}$ ,
- (ii) closure under composition: if  $\Lambda_1 \in \mathcal{O}_{A \rightarrow C}$  and  $\Lambda_2 \in \mathcal{O}_{C \rightarrow B}$ , then  $\Lambda_2 \circ \Lambda_1 \in \mathcal{O}_{A \rightarrow B}$ ,
- (iii) preservation of the set of free states:  $\Lambda(\rho) \in \mathcal{F}_B$  for all  $\rho \in \mathcal{F}_A$  and all  $\Lambda \in \mathcal{O}_{A \rightarrow B}$ .

A QRT is then specified by the pair  $(\mathcal{F}, \mathcal{O})$  of free states and free operations. In addition, most resource theories also impose that the trace map  $\text{Tr} : \mathcal{B}(\mathcal{H}) \rightarrow \mathbb{C}$  is contained in the set of free operations. Furthermore, the set of resource non-generating operations is defined as

$$\mathcal{O}_{A \rightarrow B}^{(\max)} := \{\Lambda \in \text{CPTP}_{A \rightarrow B} \mid \forall \rho \in \mathcal{F}_A : \Lambda(\rho) \in \mathcal{F}_B\} \quad (\text{A3})$$

and we may choose  $\mathcal{O}_{A \rightarrow B} \subseteq \mathcal{O}_{A \rightarrow B}^{(\max)}$ . Conversely, the minimal set  $\mathcal{F}_A^{(\min)}$  of free states compatible with a fixed class  $\mathcal{O}_{A \rightarrow B}$  is given by

$$\mathcal{F}_A^{(\min)} := \{\rho \in \mathcal{D}_A \mid \forall \sigma \in \mathcal{D}_A \exists \Lambda \in \mathcal{O}_{A \rightarrow A} : \rho = \Lambda(\sigma)\} . \quad (\text{A4})$$

In addition to the above minimal properties, many  $(\mathcal{F}, \mathcal{O})$  admit additional structures. Following Ref. [47], a QRT  $(\mathcal{F}, \mathcal{O})$  is called *convex* if, for any systems  $A, B$ , the set of free operations  $\mathcal{O}(A \rightarrow B)$  is convex, i.e.,  $p\Phi + (1-p)\Lambda \in \mathcal{O}(A \rightarrow B)$  for all  $\Phi, \Lambda \in \mathcal{O}(A \rightarrow B)$  and  $p \in [0, 1]$ . In the formulation where free states are defined as free preparations  $\mathcal{F}(\mathcal{H}) = \mathcal{O}(\mathbb{C} \rightarrow \mathcal{H})$  from a trivial system  $\mathbb{C}$ , convexity of  $\mathcal{O}$  implies that each  $\mathcal{F}(\mathcal{H})$  is convex, while the converse need not hold. Moreover, a resource theory  $(\mathcal{F}, \mathcal{O})$  is called *affine* if, for any systems  $A, B$ , every CPTP map that can be expressed as an affine combination of free operations is itself free, i.e., if  $\Phi = \sum_i \alpha_i \Phi_i$  with  $\Phi_i \in \mathcal{O}(A \rightarrow B)$  and  $\sum_i \alpha_i = 1$ , and if  $\Phi$  is CPTP, then  $\Phi \in \mathcal{O}(A \rightarrow B)$ . This condition implies that the free-state set is closed under affine combinations that yield a valid density operator, but this property alone does not imply that the QRT is affine. Many widely studied QRTs, including entanglement, coherence, asymmetry, and athermality, are convex, whereas entanglement theory provides a canonical example of a convex but non-affine QRT.

## 2. Resource destroying maps

Many resource theories come with resource destroying maps, which play a major role in the main text as they allow us to define a clear classical baseline with respect to which we can compare the effect of a given resource on the yield for a process described by a quantum channel  $\Lambda$ .

Let  $(\mathcal{F}, \mathcal{O})$  describe a QRT with  $\mathcal{F} = \mathcal{F}(\mathcal{H})$ . Then, a map  $\mathcal{G} : \mathcal{B}(\mathcal{H}) \rightarrow \mathcal{B}(\mathcal{H})$  is called resource destroying if

- (i)  $\mathcal{G}(\rho) = \rho$  for all  $\rho \in \mathcal{F}$ , and
- (ii)  $\mathcal{G}(\rho) \in \mathcal{F}$  for all  $\rho \in \mathcal{D}(\mathcal{H})$ .

While  $\mathcal{G}$  may be linear for convex resource theories, it must be non-linear for non-convex ones [55]. Consequently, in non-convex QRTs  $\mathcal{G}$  cannot be a quantum channel. Necessary and sufficient conditions for the existence and uniqueness of a *linear* resource-destroying map have been derived in Ref. [56]. In particular, for a linear  $\mathcal{G}$  to exist, the set of free states  $\mathcal{F}$  has to be affine,

while the converse does not hold and not every affine resource theory has a linear resource-destroying map [56]. Furthermore, condition (ii) implies that  $\mathcal{G}$  is idempotent, i.e.,  $\mathcal{G} \circ \mathcal{G} = \mathcal{G}$ .

Two canonical examples of resource destroying maps are the unitary group twirl for asymmetry and the dephasing map for coherence. For asymmetry, the resource destroying map is given by the corresponding group twirling operation. For a compact group  $G$  with unitary representation  $\Pi : G \rightarrow \text{U}(\mathcal{H})$  on a Hilbert space  $\mathcal{H}$  and uniform Haar measure  $d\mu(g)$ ,

$$\mathcal{G}_{\text{asy}}(\cdot) = \int d\mu(g) U(g)(\cdot)U^\dagger(g). \quad (\text{A5})$$

For finite groups, the above integral is replaced by a discrete sum according to

$$\mathcal{G}_{\text{asy}}(\cdot) = \frac{1}{|G|} \sum_{g \in G} U(g)(\cdot)U^\dagger(g). \quad (\text{A6})$$

For coherence, we fix an orthonormal basis  $\mathcal{B} = \{|i\rangle\}_{i=1}^d$  of  $\mathcal{H}$  and take the free set  $\mathcal{F}(\mathcal{H})$  to be the diagonal density operators in that basis. The associated resource destroying map is the dephasing channel, which acts on  $\rho \in \mathcal{D}(\mathcal{H})$  as

$$\mathcal{G}_{\text{coh}}(\rho) = \sum_{i=1}^d \rho_{ii} |i\rangle\langle i|, \quad \rho_{ii} = \langle i|\rho|i\rangle \forall i \in [d]. \quad (\text{A7})$$

The map  $\mathcal{G}_{\text{coh}}$  is CPTP, unital, idempotent, and Hermitian with respect to the Hilbert–Schmidt inner product.

While the two resource-destroying maps  $\mathcal{G}_{\text{asym}}$  and  $\mathcal{G}_{\text{coh}}$  are both self-adjoint, not every resource-destroying map satisfies this property. An example of a resource theory with a linear resource-destroying map that is not self-adjoint is the singleton free set  $\mathcal{F} = \{\sigma\}$ , for which the replacement channel

$$\mathcal{G}(\rho) \equiv \Lambda_\sigma(\rho) := \text{Tr}[\rho]\sigma \quad (\text{A8})$$

is a valid (and unique) resource-destroying map. Its Hilbert-Schmidt adjoint is  $\Lambda_\sigma^\dagger(A) = \text{Tr}[A\sigma] \mathbb{1}$ , such that  $\Lambda_\sigma$  is self-adjoint if and only if  $\sigma = \mathbb{1}/d$  with  $d = \dim(\mathcal{H})$ .

## Appendix B: Recap of time-local master equations

In this section, we briefly recall time-local master equations and indicate when they exist. A (reduced) quantum dynamical evolution is described by a family of linear maps  $\{\Lambda_t\}_{t \geq 0}$  acting on density operators with  $\Lambda_0 = \text{id}$  and  $\rho(t) = \Lambda_t(\rho(0))$ . The evolution is called time local if the density operator  $\rho(t)$  of the system satisfies

$$\frac{d\rho(t)}{dt} = \mathcal{L}_t(\rho(t)), \quad (\text{B1})$$

with a (possibly time-dependent) time-local generator  $\mathcal{L}_t$ . Two standard Markovian regimes are then distinguished [84, 85, 92, 126–128]:

- (i) a time-independent Lindblad generator  $\mathcal{L}_t \equiv \mathcal{L}$ , yielding a quantum dynamical semigroup

$$\Lambda_{t,0} = e^{t\mathcal{L}}; \quad (\text{B2})$$

- (ii) a general time-local generator  $\mathcal{L}_t$  of Gorini-Kossakowski-Lindblad-Sudarshan (GKLS) form at each time  $t$ , commonly referred to as time-inhomogeneous Markovian dynamics.

A convenient microscopic setting starts from a closed system-environment Hamiltonian

$$H = H_S + H_E + \kappa H_I \in \mathcal{B}(\mathcal{H}_S \otimes \mathcal{H}_E), \quad (\text{B3})$$

where  $H_S$  and  $H_E$  are the system and environment Hamiltonians acting only non-trivially on the system and environment Hilbert spaces  $\mathcal{H}_S, \mathcal{H}_E$ , respectively,  $H_I$  describes their interaction, and  $\kappa$  is a coupling parameter. In the weak-coupling (Born-Markov) regime together with a secular (rotating wave) approximation, one obtains the time-independent GKLS master equation for the reduced state  $\rho(t)$  (setting  $\hbar = 1$ ):

$$\frac{d\rho(t)}{dt} = -i[\tilde{H}, \rho] + \sum_k \gamma_k \left( L_k \rho L_k^\dagger - \frac{1}{2} \{L_k^\dagger L_k, \rho\} \right), \quad (\text{B4})$$

where  $\tilde{H} := H_S + H_L$  includes the Lamb-shift Hamiltonian  $H_L$  which, in the weak-coupling limit, commutes with  $H_S$  and encodes the environment-induced renormalization of the system's energy levels. Moreover,  $\gamma_k \geq 0$  are the so-called decoherence rates, and the Lindblad operators  $L_k$  are determined by  $H_I$  and the bath correlation functions. Furthermore, Eq. (B4) is commonly expressed in the form

$$\frac{d\rho(t)}{dt} = -i[\tilde{H}, \rho(t)] + \mathcal{D}(\rho(t)) = \mathcal{L}(\rho(t)), \quad (\text{B5})$$

where  $\mathcal{D}(\cdot)$  is the dissipator and  $\mathcal{L}(\cdot)$  the time-independent Lindblad generator. Moreover,  $\mathcal{L}$  is the Liouvillian superoperator acting on the vectorized density operator  $|\rho\rangle\rangle$ , where we use the convention (row-stacking)

$$\text{vec}(A\rho B) = (A \otimes B^T) |\rho\rangle\rangle. \quad (\text{B6})$$

Then, the Lindblad generator in Liouvillian space,  $\mathcal{H}_S \otimes \mathcal{H}_S$ , reads

$$\mathcal{L} = -i \left( \tilde{H} \otimes \mathbb{1} - \mathbb{1} \otimes \tilde{H}^T \right) + \sum_k \gamma_k \left[ L_k \otimes L_k^* - \frac{1}{2} \left( L_k^\dagger L_k \otimes \mathbb{1} + \mathbb{1} \otimes \left( L_k^\dagger L_k \right)^T \right) \right]. \quad (\text{B7})$$

This operator representation allows one to directly read off the Heisenberg adjoint  $\mathcal{L}^\dagger(\cdot)$  with respect to the Hilbert-Schmidt inner product as used in the main text.

In general, the reduced time evolution of a system is described by a family of *dynamical maps*. Under the assumption that the joint system-environment density operator  $\rho_{SE} \in \mathcal{D}(\mathcal{H}_S \otimes \mathcal{H}_E)$  at time  $t = 0$  is a product

state, i.e.,  $\rho_{SE}(0) = \rho(0) \otimes \rho_E(0)$ , the dynamical map  $\Lambda_t$  can be defined by tracing out the environmental degrees of freedom of  $\rho_{SE}(t)$  under unitary time evolution leading to

$$\rho(t) = \Lambda_t(\rho(0)), \quad (\text{B8})$$

and  $\Lambda_t$  is trace preserving and completely positive and, thus, a valid quantum channel. A dynamical process on a time interval  $[0, T]$  is thus described by a one-parameter family  $\{\Lambda_t\}_{t \in [0, T]}$  of dynamical maps  $\Lambda_t$ . It can be shown that differentiability of  $t \mapsto \Lambda_t$  and existence of the inverse map  $\Lambda_t^{-1}$  for all  $t \in [0, T]$  ensure the existence of a time-local master equation with generator [84]

$$\mathcal{L}_t = \left( \frac{d}{dt} \Lambda_t \right) \circ \Lambda_t^{-1}, \quad (\text{B9})$$

i.e.,

$$\begin{aligned} \frac{d\rho(t)}{dt} &= \mathcal{L}_t(\rho(t)) \\ &= -i[\tilde{H}(t), \rho(t)] + \sum_k \gamma_k(t) \left( L_k(t) \rho L_k^\dagger(t) - \frac{1}{2} \{L_k^\dagger(t) L_k(t), \rho(t)\} \right), \end{aligned} \quad (\text{B10})$$

where in contrast to Eq. (B4),  $\tilde{H}, \gamma_k, L_k$  are in general time-dependent. Unlike the time-independent GKLS case (B4), the general time-local master equation (B10) does not necessarily correspond to a dynamical semigroup anymore since  $\mathcal{L}_t$  is time-dependent. Moreover, the decoherence rates  $\gamma_k(t)$  may be non-positive for intermediate times.

A commonly used stronger notion of quantum Markovianity is *complete-positivity (CP) divisibility*. A process  $\{\Lambda_t\}_{t \in [0, T]}$  is called CP divisible if for all  $t \geq s$  there exists a CPTP map  $V_{t,s}$  such that

$$\Lambda_t = V_{t,s} \circ \Lambda_s. \quad (\text{B11})$$

If  $\Lambda_s$  is invertible as a linear map, then  $V_{t,s}$  is uniquely determined and can be written as  $V_{t,s} = \Lambda_t \circ \Lambda_s^{-1}$ . Moreover, invertibility alone does not guarantee that  $V_{t,s}$  is completely positive, since  $\Lambda_s^{-1}$  need not be completely positive. For sufficiently regular finite-dimensional dynamics, CP divisibility is equivalent to the time-local generator  $\mathcal{L}_t$  being of GKLS form at each time  $t$ , i.e., to the non-negativity of the decoherence rates  $\gamma_k(t)$  for all  $t$  [92].

### Appendix C: Proof of Theorem 1

*Proof.* For  $\mathcal{G}$  linear,  $\Delta Y = |\text{Tr}[\tilde{X}\rho]|$  with  $\tilde{X} := (\text{id} - \mathcal{G}^\dagger)(\Lambda^\dagger(M))$  is convex in  $\rho$  (but not necessarily affine, as otherwise the proof of (i) would be trivial). Since

$$|z| = \sup_{\theta \in [0, 2\pi)} \Re(e^{-i\theta} z) \quad (\text{C1})$$

for any complex number  $z \in \mathbb{C}$ , we have (recall that  $\mathcal{H}$  finite-dimensional)

$$\begin{aligned} \mathcal{C}_M(\Lambda) &= \max_{\rho \in \mathcal{D}(\mathcal{H})} \left| \text{Tr} \left[ \tilde{X} \rho \right] \right| \\ &= \sup_{\theta \in [0, 2\pi)} \max_{\rho \in \mathcal{D}(\mathcal{H})} \Re \left( \text{Tr} \left[ e^{-i\theta} \tilde{X} \rho \right] \right) \\ &= \sup_{\theta \in [0, 2\pi)} \max_{\rho \in \mathcal{D}(\mathcal{H})} \text{Tr} \left[ \tilde{X}_\theta \rho \right], \end{aligned} \quad (\text{C2})$$

where  $\tilde{X}_\theta := \Re(\exp(-i\theta)\tilde{X})$  is Hermitian and we used the linearity of the trace. Since for any fixed angle  $\theta \in [0, 2\pi)$  the expectation  $\text{Tr}[\tilde{X}_\theta \rho]$  is linear, it follows that

$$\begin{aligned} \mathcal{C}_M(\Lambda) &= \sup_{\theta \in [0, 2\pi)} \max_{\substack{|\Psi\rangle \in \mathbb{P}(\mathcal{H}) \\ \|\Psi\|=1}} \langle \Psi | \tilde{X}_\theta | \Psi \rangle \\ &= \max_{\substack{|\Psi\rangle \in \mathbb{P}(\mathcal{H}) \\ \|\Psi\|=1}} \left| \langle \Psi | \tilde{X} | \Psi \rangle \right|, \end{aligned} \quad (\text{C3})$$

where we used in the last line that  $\theta$  can always be chosen to align with the phase of  $|\Psi\rangle$ .

Next, we prove (ii). Since  $\mathcal{G}$  is Hermiticity preserving and  $M \in \mathcal{B}_{\text{sa}}(\mathcal{H})$ , the operator  $\tilde{X}$  is Hermitian (for  $\mathcal{G}$  CPTP this can also be shown explicitly by using the Kraus representation of  $\mathcal{G}$ ). We denote the maximal and minimal eigenvalues of  $\tilde{X}$  by  $\lambda_{\max}(\tilde{X})$  and  $\lambda_{\min}(\tilde{X})$ , respectively. Then,

$$\mathcal{C}_M(\Lambda) = \max \left\{ \left| \lambda_{\max}(\tilde{X}) \right|, \left| \lambda_{\min}(\tilde{X}) \right| \right\} = \|\tilde{X}\|_\infty, \quad (\text{C4})$$

where we used that for  $\tilde{X}$  Hermitian, the operator ( $\infty$ -Schatten) norm equals the spectral norm [129].

It remains to show (iii). Since  $\mathcal{G}$  is idempotent, which holds for any resource-destroying map,  $\mathcal{B}(\mathcal{H})$  can be decomposed into a direct sum

$$\mathcal{B}(\mathcal{H}) = \text{im}(\mathcal{G}^\dagger) \oplus \text{ker}(\mathcal{G}^\dagger), \quad (\text{C5})$$

where  $\text{im}(\mathcal{G}^\dagger)$  and  $\text{ker}(\mathcal{G}^\dagger)$  denote the image (range) and kernel of  $\mathcal{G}^\dagger$ , respectively. Thus, for  $\Lambda^\dagger(M) \in \text{im}(\mathcal{G}^\dagger)$ ,  $\mathcal{C}_M(\Lambda) = 0$  as  $\text{id} - \mathcal{G}^\dagger$  is the projector onto the kernel of  $\mathcal{G}^\dagger$ .  $\square$

#### Appendix D: $\Pi_M(\Lambda)$ as a binary discrimination task

In this section, we show how  $\Pi_M(\Lambda)$  as defined in Eq. (10) can be identified with an additive advantage of a particular binary state discrimination task, as identified via the respective success probability. For a detailed discussion of state discrimination tasks and an associated operational advantage provided by resource states, see Refs. [51, 73].

As explained in the first paragraph of Sec. II A, the yield  $Y(\rho)$  (1) is naturally defined with respect to a POVM element  $M$ , i.e.,  $0 \leq M \leq \mathbb{1}$ , such that  $Y(\rho) \in$

$[0, 1]$  corresponds to a success probability. In most theorems in the main text we skipped the constraint  $0 \leq M \leq \mathbb{1}$  and considered a general self-adjoint  $M \in \mathcal{B}_{\text{sa}}(\mathcal{H})$  whenever the mathematical derivation of the results did not require  $0 \leq M \leq \mathbb{1}$ . However, the distinction between  $M$  being a POVM element and a general self-adjoint operator becomes important when we would like to relate  $\Pi_M(\Lambda)$  to the advantage as phrased in terms of state discrimination success probabilities in Ref. [73].

We consider the two cases separately and discuss  $M$  being a POVM element first. While the goal of channel discrimination protocols as described in Ref. [73] is to determine which quantum channel  $\Lambda_i$  of an ensemble  $\{p_i, \Lambda_i\}$  with probabilities  $p_i$  had been applied to a quantum state, we work with a single quantum channel  $\Lambda$  in the definition of  $\Pi_M(\Lambda)$ . Thus, the channel discrimination becomes an a priori trivial task. Nevertheless, it is still instructive to relate  $\Pi_M(\Lambda)$  to the advantage described in Ref. [73]. For this, we identify  $p_{\text{succ}}(\rho, \Lambda, M) \equiv Y(\rho)$  such that for  $0 \leq M \leq \mathbb{1}$ :

$$\Pi_M(\Lambda) \equiv \sup_{\rho \in \mathcal{D}(\mathcal{H})} p_{\text{succ}}(\rho, \Lambda, M) - \sup_{\sigma \in \mathcal{F}} p_{\text{succ}}(\sigma, \Lambda, M), \quad (\text{D1})$$

i.e., instead of the ratio between  $p_{\text{succ}}(\rho, \Lambda, M)$  for a fixed input state  $\rho$  and the optimal success probability for states in the set  $\mathcal{F}$  of free states (see Ref. [73] for details),  $\Pi_M(\Lambda)$  quantifies the maximal possible yield change in agreement with  $\mathcal{C}_M(\Lambda)$  using an “additive” notion of advantage rather than a “multiplicative” one.

In case  $M$  is not a POVM element but a general observable, we first have to modify  $\Pi_M(\Lambda)$  accordingly before we can identify its constituents with two success probabilities for an input state  $\rho$  and a free state  $\sigma$  as in Eq. (D1). For this, we build a binary POVM  $\{\tilde{M}, \mathbb{1} - \tilde{M}\}$  from  $M$  as follows: first, denote the maximal and minimal eigenvalues of  $M$  by  $\lambda_{\max}^{(M)}$  and  $\lambda_{\min}^{(M)}$ , respectively. Then, we construct a linear function of  $M$  according to (assume  $M \neq \alpha \mathbb{1}, \alpha \in \mathbb{R}$ )

$$\tilde{M} = \frac{M - \lambda_{\min}^{(M)} \mathbb{1}}{\lambda_{\max}^{(M)} - \lambda_{\min}^{(M)}}, \quad (\text{D2})$$

which is well-defined for finite-dimensional Hilbert spaces  $\mathcal{H}$  as this ensures that  $M$  is bounded with  $\lambda_{\min}^{(M)}, \lambda_{\max}^{(M)} \in (-\infty, \infty)$ . In addition, we excluded the degenerate case  $\lambda_{\min}^{(M)} = \lambda_{\max}^{(M)}$ , which implies  $M \neq \alpha \mathbb{1}, \alpha \in \mathbb{R}$  as in that case  $\Pi_M(\Lambda) = 0$ . Note that  $\tilde{M}$  is only one particular way to construct a POVM element from an observable  $M$ . Next, we abbreviate  $\Delta\lambda^{(M)} := \lambda_{\max}^{(M)} - \lambda_{\min}^{(M)}$ . Then,  $\Pi_M(\Lambda)$  can be written as

$$\begin{aligned} \Pi_M(\Lambda) &= \Delta\lambda^{(M)} \left[ \sup_{\rho \in \mathcal{D}(\mathcal{H})} \left| p_{\text{succ}}(\rho, \Lambda, \tilde{M}) + \frac{\lambda_{\min}^{(M)}}{\Delta\lambda^{(M)}} \right| \right. \\ &\quad \left. - \sup_{\sigma \in \mathcal{F}} \left| p_{\text{succ}}(\sigma, \Lambda, \tilde{M}) + \frac{\lambda_{\min}^{(M)}}{\Delta\lambda^{(M)}} \right| \right]. \end{aligned} \quad (\text{D3})$$

In particular, if  $M \geq 0$  then  $\text{Tr}[M\Lambda(\rho)] \geq 0$  for all states  $\rho$ , so the absolute values in the definition of  $\Pi_M(\Lambda)$  are redundant. In this case the constant shift  $\lambda_{\min}^{(M)}/\Delta\lambda^{(M)}$  cancels between the two suprema, and we obtain

$$\begin{aligned} \Pi_M(\Lambda) = \Delta\lambda^{(M)} \left[ \sup_{\rho \in \mathcal{D}(\mathcal{H})} p_{\text{succ}}(\rho, \Lambda, \widetilde{M}) \right. \\ \left. - \sup_{\sigma \in \mathcal{F}} p_{\text{succ}}(\sigma, \Lambda, \widetilde{M}) \right]. \end{aligned} \quad (\text{D4})$$

Comparing with Eq. (D1), where  $M$  itself is a POVM element, we see that also for a general  $M \geq 0$  the quantity  $\Pi_M(\Lambda)$  can be expressed entirely in terms of success probabilities  $p_{\text{succ}}(\cdot, \Lambda, \widetilde{M})$  of a suitably normalised effect  $\widetilde{M}$ , and thus fits into the operational advantage framework of channel discrimination tasks in Ref. [73], up to the overall scaling factor  $\Delta\lambda^{(M)}$ .

### Appendix E: Proof of Corollary 2

*Proof.* For any density operator  $\rho \in \mathcal{D}(\mathcal{H})$ , we have

$$|\text{Tr}[M\Lambda(\rho)]| \leq |\text{Tr}[M\Lambda(\mathcal{G}(\rho))]| + |\text{Tr}[M\Lambda(\rho - \mathcal{G}(\rho))]|. \quad (\text{E1})$$

Taking on both sides the supremum over all  $\rho \in \mathcal{D}(\mathcal{H})$  and using that  $\mathcal{G}(\rho) \in \mathcal{F}$  for all  $\rho \in \mathcal{D}(\mathcal{H})$  yields Eq. (10).  $\square$

### Appendix F: Proof of Theorem 3

*Proof.* We abbreviate  $\Delta_{\Lambda_k} := \Lambda_k(\rho) - \Lambda_k(\mathcal{G}(\rho))$ . Then, convexity of  $\mathcal{C}_M(\Lambda)$  in  $\Lambda$  follows from

$$\begin{aligned} \mathcal{C}_M \left( \sum_k p_k \Lambda_k \right) &= \max_{\rho \in \mathcal{D}(\mathcal{H})} \left| \text{Tr} \left[ M \sum_k p_k \Delta_{\Lambda_k}(\rho) \right] \right| \\ &\leq \max_{\rho \in \mathcal{D}(\mathcal{H})} \sum_k p_k |\text{Tr}[M\Delta_{\Lambda_k}(\rho)]| \\ &\leq \sum_k p_k \mathcal{C}_M(\Lambda_k). \end{aligned} \quad (\text{F1})$$

Let  $\Delta\mathcal{C}_M^{(\Lambda_1, \Lambda_2)} := |\mathcal{C}_M(\Lambda_1) - \mathcal{C}_M(\Lambda_2)|$ . To show Lipschitz continuity, we first observe that

$$\begin{aligned} \Delta\mathcal{C}_M^{(\Lambda_1, \Lambda_2)} &\leq \max_{\rho \in \mathcal{D}(\mathcal{H})} \left| |\text{Tr}[M\Delta_{\Lambda_1}(\rho)]| - |\text{Tr}[M\Delta_{\Lambda_2}(\rho)]| \right| \\ &\leq \max_{\rho \in \mathcal{D}(\mathcal{H})} |\text{Tr}[M(\Delta_{\Lambda_1}(\rho) - \Delta_{\Lambda_2}(\rho))]| \\ &\leq \max_{\rho \in \mathcal{D}(\mathcal{H})} \left\{ |\text{Tr}[M(\Lambda_1 - \Lambda_2)(\rho)]| \right. \\ &\quad \left. + |\text{Tr}[M(\Lambda_1 - \Lambda_2)(\mathcal{G}(\rho))]| \right\} \\ &\leq \|M\|_{\infty} \max_{\rho \in \mathcal{D}(\mathcal{H})} [\|(\Lambda_1 - \Lambda_2)(\rho)\|_1 \\ &\quad + \|(\Lambda_1 - \Lambda_2)(\mathcal{G}(\rho))\|_1], \end{aligned} \quad (\text{F2})$$

where we used the (reverse) triangle inequality and Hölder's inequality for Schatten norms with  $p = 1, q = \infty$ . The diamond norm  $\|\cdot\|_{\diamond}$  on superoperators (and, thus, quantum channels) is defined in Refs. [130–133]. Since for any quantum channel  $\Lambda$

$$\|\Lambda\|_{\diamond} := \sup_{k \geq 1} \|\Lambda \otimes \text{id}_k\|_1, \quad (\text{F3})$$

and  $\mathcal{G}$  maps density operators to density operators, we can choose  $k = 1$  to obtain

$$\begin{aligned} \Delta\mathcal{C}_M^{(\Lambda_1, \Lambda_2)} &\leq \|M\|_{\infty} \|\Lambda_1 - \Lambda_2\|_{\diamond} (\|\rho\|_1 + \|\mathcal{G}(\rho)\|_1) \\ &= K \|\Lambda_1 - \Lambda_2\|_{\diamond} \end{aligned} \quad (\text{F4})$$

with Lipschitz constant  $K := 2\|M\|_{\infty}$ . In case  $\mathcal{G}$  is linear, we can use Eq. (7) to show that

$$\Delta\mathcal{C}_M^{(\Lambda_1, \Lambda_2)} \leq \|\text{id} - \mathcal{G}\|_{\infty \rightarrow \infty} \|M\|_{\infty} \|\Lambda_1 - \Lambda_2\|_{\diamond}, \quad (\text{F5})$$

where the superoperator norm  $\|\mathcal{G}\|_{\infty \rightarrow \infty}$  is defined as

$$\|\mathcal{G}\|_{\infty \rightarrow \infty} := \sup_{\mathcal{B}(\mathcal{H}) \ni M \neq 0} \frac{\|\mathcal{G}(M)\|_{\infty}}{\|M\|_{\infty}}. \quad (\text{F6})$$

If  $\mathcal{G}$  is an idempotent, unital CPTP map, it is a pinching quantum channel [96, 134] such that for any  $O \in \mathcal{B}(\mathcal{H})$

$$\mathcal{G}(O) = \sum_i P_i O P_i, \quad (\text{F7})$$

where  $\{P_i\}_i$  is a set of orthogonal projectors. Then,  $\mathcal{G}^{\dagger} = \mathcal{G}$  because for any two  $A, B \in \mathcal{B}(\mathcal{H})$ ,

$$\text{Tr}[\mathcal{G}(B)] = \text{Tr}[\mathcal{G}^{\dagger}(A)B] = \text{Tr}[\mathcal{G}(A)B]. \quad (\text{F8})$$

Moreover,  $\|O - \mathcal{G}(O)\|_{\infty} \leq \|O\|_{\infty}$  [135] such that  $\|\text{id} - \mathcal{G}\|_{\infty \rightarrow \infty} \leq 1$ .

Property (iii) immediately follows from

$$\begin{aligned} \mathcal{C}_{aM_1 + bM_2}(\Lambda) &\leq \sup_{\rho \in \mathcal{D}(\mathcal{H})} (|a\text{Tr}[M_1\Delta_{\Lambda}(\rho)]| + |b\text{Tr}[M_2\Delta_{\Lambda}(\rho)]|) \\ &\leq |a| \sup_{\rho \in \mathcal{D}(\mathcal{H})} |\text{Tr}[M_1\Delta_{\Lambda}(\rho)]| \\ &\quad + |b| \sup_{\rho \in \mathcal{D}(\mathcal{H})} |\text{Tr}[M_2\Delta_{\Lambda}(\rho)]| \\ &= |a|\mathcal{C}_{M_1}(\Lambda) + |b|\mathcal{C}_{M_2}(\Lambda). \end{aligned} \quad (\text{F9})$$

$\square$

### Appendix G: Proof of Theorem 4

*Proof.* Eq. (14) is a direct consequence of the linearity of  $\Lambda_2$  and the definition of the adjoint of a quantum channel,

$$\begin{aligned} \mathcal{C}_M(\Lambda_2 \circ \Lambda_1) &= \max_{\rho \in \mathcal{D}(\mathcal{H})} \left| \text{Tr} \left[ \Lambda_2^{\dagger}(M) (\Lambda_1(\rho) - \Lambda_1(\mathcal{G}(\rho))) \right] \right| \\ &= \mathcal{C}_{\Lambda_2^{\dagger}(M)}(\Lambda_1). \end{aligned} \quad (\text{G1})$$

Let  $\Delta_{\Lambda_1}(\rho) := \Lambda_1(\rho) - \Lambda_1(\mathcal{G}(\rho))$ . Then, adding  $\pm M\Delta_{\Lambda_1}(\rho)$  inside the trace yields

$$\begin{aligned} \mathcal{C}_{\Lambda_2^\dagger(M)}(\Lambda_1) &\leq \mathcal{C}_M(\Lambda_1) + \max_{\rho \in \mathcal{D}(\mathcal{H})} |\text{Tr}[\Delta M(\Delta_{\Lambda_1}(\rho))]| \\ &= \mathcal{C}_M(\Lambda_1) + \mathcal{C}_{\Delta M}(\Lambda_1). \end{aligned} \quad (\text{G2})$$

Moreover, it follows from Hölder's inequality for Schatten norms with  $p = 1, q = \infty$  that

$$\begin{aligned} \mathcal{C}_{\Delta M}(\Lambda_1) &\leq \|\Delta M\|_\infty \max_{\rho \in \mathcal{D}(\mathcal{H})} \|\Delta_{\Lambda_1}\rho\|_1 \\ &\leq \|\Delta M\|_\infty \underbrace{\max_{\rho \in \mathcal{D}(\mathcal{H})} \|\rho - \mathcal{G}(\rho)\|_1}_{=: R_{\mathcal{G}}}, \end{aligned} \quad (\text{G3})$$

where we used in the last line that the trace distance is contractive under CPTP maps [95].

We show (ii) next. Adding  $\pm \Lambda_2(\mathcal{G}(\Lambda_1(\rho)))$  inside the trace in Eq. (4) and using the triangle inequality yields

$$\begin{aligned} \mathcal{C}(\Lambda_2 \circ \Lambda_1) &\leq \sup_{\rho \in \mathcal{D}(\mathcal{H})} \{ |\text{Tr}[M\Delta_{\Lambda_2}(\Lambda_1(\rho))]| \\ &\quad + |\text{Tr}[M\Lambda_2(\mathcal{G}(\Lambda_1(\rho)) - \Lambda_1(\mathcal{G}(\rho)))]| \} \\ &\leq \sup_{\rho \in \text{im}(\Lambda_1)} |\text{Tr}[M\Delta_{\Lambda_2}(\rho)]| \\ &\quad + \sup_{\rho \in \mathcal{D}(\mathcal{H})} |\text{Tr}[M\Lambda_2(\mathcal{G}(\Lambda_1(\rho)) - \Lambda_1(\mathcal{G}(\rho)))]| \end{aligned} \quad (\text{G4})$$

The second term in the last inequality,

$$Y_{\mathcal{G}, \Lambda_1} := \sup_{\rho \in \mathcal{D}(\mathcal{H})} |\text{Tr}[M\Lambda_2(\mathcal{G}(\Lambda_1(\rho)) - \Lambda_1(\mathcal{G}(\rho)))]|, \quad (\text{G5})$$

vanishes if  $\Lambda_1$  is  $\mathcal{G}$ -covariant. Moreover, we have  $\text{im}(\Lambda_1) \subseteq \mathcal{D}(\mathcal{H})$  and it follows that

$$\mathcal{C}(\Lambda_2 \circ \Lambda_1) \leq \mathcal{C}_M(\Lambda_2) \quad (\text{G6})$$

whenever  $\mathcal{G} \circ \Lambda_1 = \Lambda_1 \circ \mathcal{G}$ .

The classical coarse-graining inequality (iii) follows from (recall  $\Delta_\Lambda(\rho) := \Lambda(\rho) - \Lambda(\mathcal{G}(\rho))$ )

$$\begin{aligned} \mathcal{C}_{\widetilde{M}_j}(\Lambda) &\leq \sup_{\rho \in \mathcal{D}(\mathcal{H})} \sum_j V_{ji} |\text{Tr}[M_i \Delta_\Lambda(\rho)]| \\ &\leq \sum_j V_{ji} \sup_{\rho \in \mathcal{D}(\mathcal{H})} |\text{Tr}[M_i \Delta_\Lambda(\rho)]| \\ &= \sum_i V_{ji} \mathcal{C}_{M_i}(\Lambda). \end{aligned} \quad (\text{G7})$$

□

## Appendix H: Proof of Corollary 5

*Proof.* For any linear real-valued function  $f : X \rightarrow \mathbb{R}$  we have

$$\begin{aligned} \sup_{x \in X} |f(x)| &= \max \left\{ \sup_{x \in X} f(x), \sup_{x \in X} -f(x) \right\} \\ &= \sup_{x \in X \cup (-X)} f(x) \\ &= \sup_{x \in \text{conv}(X \cup (-X))} f(x). \end{aligned} \quad (\text{H1})$$

Applied to  $\mathcal{C}_M(\Lambda)$  this yields

$$\mathcal{C}_M(\Lambda) = \sup_{O \in \mathcal{M}_{\mathcal{G}, \Lambda}} |\langle M, O \rangle_{\text{HS}}| = \sup_{O \in \widetilde{\mathcal{M}}_{\mathcal{G}, \Lambda}} \langle M, O \rangle_{\text{HS}}. \quad (\text{H2})$$

The last equation is nothing else than the definition of a support function  $h_K(y)$  of a convex set  $K$  [82] and, thus,  $\mathcal{C}_M(\Lambda) = h_{\widetilde{\mathcal{M}}_{\mathcal{G}, \Lambda}}(M)$ . □

## Appendix I: Proof of Corollary 6

*Proof.* The statement is a direct consequence of the following well-known theorem (see, e.g., [82])

**Theorem 12.** *Let  $\mathcal{X} \subset \mathcal{B}_{\text{sa}}(\mathcal{H})$  be non-empty and contain the origin. Then, for every  $M \in \mathcal{B}_{\text{sa}}(\mathcal{H})$ ,*

$$h_{\mathcal{X}}(M) = \inf \{ t \geq 0 \mid M \in t\mathcal{X}^\circ \}. \quad (\text{I1})$$

*In particular,  $h_{\mathcal{X}}(M) \leq 1$  holds if and only if  $M \in \mathcal{X}^\circ$ .*

Theorem 12 follows from the definition of the polar set in Eq. (26) as  $M \in t\mathcal{X}^\circ$  is equivalent to  $\langle X, O \rangle_{\text{HS}} \leq t$  for all  $O \in \mathcal{X}$ , and the smallest such  $t$  is the supremum defining  $h_{\mathcal{X}}(X)$ . Applying Theorem 12 to  $\mathcal{X} = \widetilde{\mathcal{M}}_{\mathcal{G}, \Lambda}$  in combination with Corollary 5 yields Corollary 6. □

## Appendix J: Total error probability for multi-shot hypothesis testing

In this appendix, we derive an upper bound on the total error probability

$$P_{\text{err}}^{(n)}(\rho) := \frac{1}{2} [\text{Pr}(\text{error} \mid H_0) + \text{Pr}(\text{error} \mid H_1)], \quad (\text{J1})$$

i.e., the average probability of error over the two hypotheses  $H_0$  and  $H_1$  introduced in Sec. II A 4 when they occur with equal prior probability 1/2.

For a fixed input state  $\rho$ , consider  $n$  independent and identically distributed (i.i.d.) repetitions of the single-shot hypothesis-testing experiment described in Sec. II A 4. Let  $X_k \in \{0, 1\}$  denote the outcome in run  $k$  (with  $X_k = 1$  corresponding to the outcome associated with  $M$ ), and  $x^n := (x_1, \dots, x_n) \in \{0, 1\}^n$  the observed

□

string. The product distributions of  $x^n$  under  $H_0$  and  $H_1$  are then

$$P_0(x^n) = \prod_{k=1}^n p_0^{x_k} (1-p_0)^{1-x_k}, \quad (\text{J2})$$

$$P_1(x^n) = \prod_{k=1}^n p_1^{x_k} (1-p_1)^{1-x_k}, \quad (\text{J3})$$

where  $p_i \equiv p_i(\rho)$  for brevity. Any (deterministic) decision rule is a function  $f : \{0, 1\}^n \rightarrow \{0, 1\}$ , where the output 0 stands for  $H_0$  and 1 for  $H_1$ . By the Neyman-Pearson Lemma [136], the optimal decision rule in our setting is the likelihood-ratio test, which in the i.i.d. Bernoulli case depends on  $x^n$  only through the empirical mean  $\bar{X} := \sum_{k=1}^n X_k/n$  and is therefore equivalent to a threshold test on  $\bar{X}$ .

Suppose  $p_1 \geq p_0$  (otherwise swap the labels), and consider the symmetric threshold  $\tau := (p_0 + p_1)/2$ . Define a decision rule that decides in favour of  $H_1$  if  $\bar{X} \geq \tau$  and in favour of  $H_0$  otherwise. Under  $H_0$ , we have  $\mathbb{E}_0[\bar{X}] = p_0$ , and an error occurs when  $\bar{X} \geq \tau$ , i.e., when  $\bar{X} - p_0 \geq (p_1 - p_0)/2$ . Similarly, under  $H_1$ ,  $\mathbb{E}_1[\bar{X}] = p_1$  and an error occurs when  $\bar{X} < \tau$ , i.e., when  $p_1 - \bar{X} \geq (p_1 - p_0)/2$ . Then, Hoeffding's inequality [137] implies that

$$P_0\left(\bar{X} - p_0 \geq \frac{p_1 - p_0}{2}\right) \leq \exp\left(-\frac{n}{2}(p_1 - p_0)^2\right), \quad (\text{J4})$$

$$P_1\left(p_1 - \bar{X} \geq \frac{p_1 - p_0}{2}\right) \leq \exp\left(-\frac{n}{2}(p_1 - p_0)^2\right). \quad (\text{J5})$$

Therefore, the total error probability for this explicit decision rule is bounded by

$$P_{\text{err}}^{(n)}(\rho) \leq \exp\left(-\frac{n}{2}(p_1 - p_0)^2\right) = \exp\left(-\frac{n}{2}(\Delta Y(\rho))^2\right). \quad (\text{J6})$$

Finally, the decision rule just constructed is not necessarily optimal for all finite  $n$ , but it provides a valid upper bound on the minimal achievable error probability. Hence, the optimal total error probability in discriminating  $\rho$  from  $\mathcal{G}(\rho)$  using  $n$  independent runs of  $(\Lambda, M)$  satisfies Eq. (J6).

### Appendix K: Proof of Theorem 7

*Proof.* To show the variation bound, we use that for any two functions  $f_1, f_2 : X \rightarrow \mathbb{R}$ ,

$$\left| \sup_{x \in X} |f_1(x)| - \sup_{x \in X} |f_2(x)| \right| \leq \sup_{x \in X} |f_1(x) - f_2(x)|. \quad (\text{K1})$$

By assumption,  $\{\Lambda_t\}_{t \in \mathcal{I}}$  solves the time-local master equation in integral form,

$$\Lambda_{t_2} - \Lambda_{t_1} = \int_{t_1}^{t_2} \mathcal{L}_s \circ \Lambda_s ds \quad (t_1 \leq t_2). \quad (\text{K2})$$

In particular,  $t \mapsto \mathcal{L}_t \circ \Lambda_t$  is Bochner integrable on every compact subinterval of  $\mathcal{I}$ . Next, we define

$$f_t(\rho) := \text{Tr}[M(\Lambda_t(\rho) - \Lambda_t(\mathcal{G}(\rho)))] \quad (\text{K3})$$

such that

$$\mathcal{C}_M(\Lambda_t) = \sup_{\rho \in \mathcal{D}(\mathcal{H})} |f_t(\rho)|. \quad (\text{K4})$$

Using Eq. (K1), we obtain

$$|\mathcal{C}_M(\Lambda_{t_2}) - \mathcal{C}_M(\Lambda_{t_1})| \leq \sup_{\rho \in \mathcal{D}(\mathcal{H})} |f_{t_2}(\rho) - f_{t_1}(\rho)| \quad (\text{K5})$$

Then, for each fixed  $\rho$ , Eq. (K2) implies that

$$\begin{aligned} f_{t_2}(\rho) - f_{t_1}(\rho) &= \text{Tr}[M(\Lambda_{t_2}(\rho - \mathcal{G}(\rho)) - \Lambda_{t_1}(\rho - \mathcal{G}(\rho)))] \\ &= \int_{t_1}^{t_2} ds \text{Tr}[M \mathcal{L}_s(\Lambda_s(\rho - \mathcal{G}(\rho)))] , \end{aligned} \quad (\text{K6})$$

which leads to

$$|f_{t_2}(\rho) - f_{t_1}(\rho)| \leq \int_{t_1}^{t_2} ds |\text{Tr}[M \mathcal{L}_s(\Lambda_s(\rho - \mathcal{G}(\rho)))]|. \quad (\text{K7})$$

Taking the supremum over  $\rho$  in (K7) and using monotonicity of the integral yields

$$\sup_{\rho \in \mathcal{D}(\mathcal{H})} |f_{t_2}(\rho) - f_{t_1}(\rho)| \leq \int_{t_1}^{t_2} ds \Gamma_M(s).$$

Combining this with (K5) gives the variation bound (43).

Next, we show Eq. (44). The right Dini derivatives of a continuous function  $f : \mathbb{R} \rightarrow \mathbb{R}$  are defined as [138]

$$\begin{aligned} D^+ f(t) &:= \limsup_{h \rightarrow 0^+} \frac{f(t+h) - f(t)}{h}, \\ D_+ f(t) &:= \liminf_{h \rightarrow 0^+} \frac{f(t+h) - f(t)}{h}. \end{aligned} \quad (\text{K8})$$

Here,  $f(t) = \mathcal{C}_M(\Lambda_t)$ . From (43) we have, for every  $t$  and  $h > 0$ ,

$$|\mathcal{C}_M(\Lambda_{t+h}) - \mathcal{C}_M(\Lambda_t)| \leq \int_t^{t+h} ds \Gamma_M(s), \quad (\text{K9})$$

and hence

$$\frac{\mathcal{C}_M(\Lambda_{t+h}) - \mathcal{C}_M(\Lambda_t)}{h} \leq \frac{1}{h} \int_t^{t+h} ds \Gamma_M(s), \quad (\text{K10})$$

$$\frac{\mathcal{C}_M(\Lambda_{t+h}) - \mathcal{C}_M(\Lambda_t)}{h} \geq -\frac{1}{h} \int_t^{t+h} ds \Gamma_M(s). \quad (\text{K11})$$

Since  $t \mapsto \Gamma_M(t)$  is locally integrable by assumption, the Lebesgue differentiation theorem implies that for Lebesgue almost every  $t \in \mathcal{I}$ ,

$$\lim_{h \rightarrow 0^+} \frac{1}{h} \int_t^{t+h} ds \Gamma_M(s) = \Gamma_M(t). \quad (\text{K12})$$

Taking the limes superior of (K10) as  $h \rightarrow 0^+$  then gives

$$D^+ \mathcal{C}_M(\Lambda_t) \leq \limsup_{h \rightarrow 0^+} \frac{1}{h} \int_t^{t+h} ds \Gamma_M(s) = \Gamma_M(t) \quad (\text{K13})$$

for almost every  $t$ . Similarly, from Eq. (K11) and the identity  $\liminf_{x \rightarrow 0^+} (-g(x)) = -\limsup_{x \rightarrow 0^+} g(x)$  we obtain that

$$D_+ \mathcal{C}_M(\Lambda_t) \geq -\limsup_{h \rightarrow 0^+} \frac{1}{h} \int_t^{t+h} ds \Gamma_M(s) = -\Gamma_M(t) \quad (\text{K14})$$

for almost every  $t$ . The analogous bounds for the left Dini derivatives follow by applying the same argument on intervals  $[t-h, t]$  instead of  $[t, t+h]$ .  $\square$

### Appendix L: Proof of Lemma 8

*Proof.* Suppose  $\Lambda_t^\dagger(\mathcal{L}_t^\dagger(M)) \in \mathcal{V}_{\mathcal{G}}^\perp$ . Then, by definition, we have

$$\text{Tr} \left[ \Lambda_t^\dagger(\mathcal{L}_t^\dagger(M)) X \right] = 0 \quad \forall X \in \mathcal{V}_{\mathcal{G}}, \quad (\text{L1})$$

so the above equality holds in particular for any  $\rho - \mathcal{G}(\rho)$ . This implies  $\Gamma_M(t) = 0$ . To show the reverse direction, we start with  $\Gamma_M(t) = 0$ . Then,

$$\sup_{\rho \in \mathcal{D}(\mathcal{H})} \left| \text{Tr} \left[ \Lambda_t^\dagger(\mathcal{L}_t^\dagger(M)) (\rho - \mathcal{G}(\rho)) \right] \right| = 0. \quad (\text{L2})$$

Since every term in the supremum is positive and the trace is linear, it follows that Eq. (L1) holds for any  $X \in \mathcal{V}_{\mathcal{G}}$ . Thus,  $\Lambda_t^\dagger(\mathcal{L}_t^\dagger(M)) \in \mathcal{V}_{\mathcal{G}}^\perp$ .  $\square$

### Appendix M: Proof of Corollary 9

*Proof.* We first bound the instantaneous advantage rate  $\Gamma_M(s)$ . We use Hölder's inequality for Schatten norms with  $p = 1, q = \infty$  to show that the instantaneous advantage rate  $\Gamma_M(s)$  as defined in Eq. (40) is bounded from above by

$$\begin{aligned} \Gamma_M(s) &\leq \|M\|_\infty \sup_{\rho \in \mathcal{D}(\mathcal{H})} \|\mathcal{L}_s(\Lambda_s(\rho - \mathcal{G}(\rho)))\|_1 \\ &\leq \|M\|_\infty \|\mathcal{L}_s\|_{1 \rightarrow 1} \sup_{\rho \in \mathcal{D}(\mathcal{H})} \|\rho - \mathcal{G}(\rho)\|_1 \\ &= \|M\|_\infty R_{\mathcal{G}} \|\mathcal{L}_s\|_{1 \rightarrow 1}, \end{aligned} \quad (\text{M1})$$

where we used in the second line the definition of the operator norm which implies that  $\|T(O)\|_{1 \rightarrow 1} \|O\|_1 \geq \|T(O)\|_1$  for all linear maps  $T : \mathcal{B}(\mathcal{H}) \rightarrow \mathcal{B}(\mathcal{H})$  and  $O \in \mathcal{B}(\mathcal{H})$ , and  $R_{\mathcal{G}}$  is the resource radius defined in Eq. (16). Thus, it follows that

$$\Gamma_M(s) \leq c_{M, \mathcal{G}} \|\mathcal{L}_s\|_{1 \rightarrow 1} \quad (\text{M2})$$

with  $c_{M, \mathcal{G}} = \|M\|_\infty R_{\mathcal{G}} \leq 2\|M\|_\infty$ .

Inserting (M2) into the variation bound in Eq. (43) yields

$$\begin{aligned} |\Delta \mathcal{C}_M(\Lambda_{t_2}, \Lambda_{t_1})| &\leq c_{M, \mathcal{G}} \int_{t_1}^{t_2} ds \|\mathcal{L}_s\|_{1 \rightarrow 1} \\ &\leq c_{M, \mathcal{G}} \Delta\tau \sup_{s \in [t_1, t_2]} \|\mathcal{L}_s\|_{1 \rightarrow 1}, \end{aligned} \quad (\text{M3})$$

where  $\Delta\tau := t_2 - t_1$ . Moreover, from Eq. (M3) it follows that

$$\Delta\tau \geq \frac{|\Delta \mathcal{C}_M(\Lambda_{t_2}, \Lambda_{t_1})|}{c_{M, \mathcal{G}} \sup_{s \in [t_1, t_2]} \|\mathcal{L}_s\|_{1 \rightarrow 1}}, \quad (\text{M4})$$

which is the time bound (51). In particular, if one considers the minimal time  $\Delta\tau^*$  over all intervals that achieve a prescribed change  $|\Delta \mathcal{C}_M|$ , it must satisfy the same lower bound.

Finally, for an external time budget  $T_{\max}$  with  $0 \leq \Delta\tau \leq T_{\max}$ , Eq. (M3) implies that

$$\begin{aligned} |\Delta \mathcal{C}_M(\Lambda_{t_2}, \Lambda_{t_1})| &\leq c_{M, \mathcal{G}} \Delta\tau \sup_{s \in [t_1, t_2]} \|\mathcal{L}_s\|_{1 \rightarrow 1} \\ &\leq T_{\max} c_{M, \mathcal{G}} \sup_{s \in [t_1, t_1 + T_{\max}]} \|\mathcal{L}_s\|_{1 \rightarrow 1}, \end{aligned} \quad (\text{M5})$$

which is the feasibility bound (53).  $\square$

### Appendix N: Proof of Theorem 10

*Proof.* Since  $\mathcal{G}$  is a linear and idempotent,  $\mathcal{B}(\mathcal{H})$  decomposes into a direct sum

$$\mathcal{B}(\mathcal{H}) = \text{im}(\mathcal{G}) \oplus \text{ker}(\mathcal{G}), \quad (\text{N1})$$

where  $\text{im}(\mathcal{G})$  denotes the image of  $\mathcal{G}$  and  $\text{ker}(\mathcal{G})$  its kernel. As a consequence, we can uniquely decompose any  $X \in \mathcal{B}(\mathcal{H})$  as

$$X = \underbrace{\mathcal{G}(X)}_{\in \text{im}(\mathcal{G})} + \underbrace{\mathcal{G}^\perp(X)}_{\in \text{ker}(\mathcal{G})}, \quad (\text{N2})$$

where  $\mathcal{G}^\perp := \text{id} - \mathcal{G}$  with  $(\mathcal{G}^\perp)^2 = \mathcal{G}^\perp$  and  $\text{im}(\mathcal{G}^\perp) = \text{ker}(\mathcal{G})$ , such that  $\mathcal{G}^\perp$  is the projection onto the kernel of  $\mathcal{G}$ .

Moreover, every linear map  $T : \mathcal{B}(\mathcal{H}) \rightarrow \mathcal{B}(\mathcal{H})$  can be written as

$$T = \mathcal{G} \circ T \circ \mathcal{G} + \mathcal{G}^\perp \circ T \circ \mathcal{G}^\perp + \mathcal{G}^\perp \circ T \circ \mathcal{G} + \mathcal{G} \circ T \circ \mathcal{G}^\perp. \quad (\text{N3})$$

Applied to a quantum channel  $\Lambda_t$ , this motivates the definitions

$$\Lambda_{t, \text{free}} := \mathcal{G} \circ \Lambda_t \circ \mathcal{G}, \quad \Lambda_{t, \text{res}} := \Lambda_t - \Lambda_{t, \text{free}}, \quad (\text{N4})$$

and, similarly, for the generator,

$$\mathcal{L}_{t, \text{free}} := \mathcal{G} \circ \mathcal{L}_t \circ \mathcal{G}, \quad \mathcal{L}_{t, \text{res}} := \mathcal{L}_t - \mathcal{L}_{t, \text{free}}. \quad (\text{N5})$$

By construction, we have

$$\Lambda_t = \Lambda_{t,\text{free}} + \Lambda_{t,\text{res}}, \quad \mathcal{L}_t = \mathcal{L}_{t,\text{free}} + \mathcal{L}_{t,\text{res}}, \quad (\text{N6})$$

which proves the decompositions (61) and (62). Using  $\mathcal{G}^2 = \mathcal{G}$  and  $(\mathcal{G}^\perp)^2 = \mathcal{G}^\perp$ , we obtain

$$\mathcal{G} \circ \Lambda_{t,\text{free}} = \mathcal{G} \circ \mathcal{G} \circ \Lambda_t \circ \mathcal{G} = \mathcal{G} \circ \Lambda_t \circ \mathcal{G} = \Lambda_{t,\text{free}}, \quad (\text{N7})$$

and

$$\Lambda_{t,\text{free}} \circ \mathcal{G} = \mathcal{G} \circ \Lambda_t \circ \mathcal{G} \circ \mathcal{G} = \mathcal{G} \circ \Lambda_t \circ \mathcal{G} = \Lambda_{t,\text{free}}, \quad (\text{N8})$$

so  $\Lambda_{t,\text{free}}$  satisfies (65). Moreover,

$$\mathcal{G} \circ \Lambda_{t,\text{res}} \circ \mathcal{G} = \mathcal{G} \circ \Lambda_t \circ \mathcal{G} - \mathcal{G} \circ (\mathcal{G} \circ \Lambda_t \circ \mathcal{G}) \circ \mathcal{G} = 0. \quad (\text{N9})$$

The same relations hold for  $\mathcal{L}_{t,\text{free}}$  and  $\mathcal{L}_{t,\text{res}}$  by the same argument. From  $\mathcal{G} \circ \Lambda_{t,\text{free}} = \Lambda_{t,\text{free}} = \Lambda_{t,\text{free}} \circ \mathcal{G}$  (and analogously for  $\mathcal{L}_{t,\text{free}}$ ) it also follows that  $[\mathcal{G}, \Lambda_{t,\text{free}}] = [\mathcal{G}, \mathcal{L}_{t,\text{free}}] = 0$ .

If  $\Lambda_t$  is CPTP and  $\mathcal{G}$  is CPTP, then  $\Lambda_{t,\text{free}} = \mathcal{G} \circ \Lambda_t \circ \mathcal{G}$  is a composition of CPTP maps, hence CPTP as claimed in part (iii).

It remains to show (ii). For any  $\rho \in \mathcal{D}(\mathcal{H})$ ,

$$\Lambda_{t,\text{free}}(\rho - \mathcal{G}(\rho)) = \mathcal{G}(\Lambda_t(\mathcal{G}(\rho) - \mathcal{G}^2(\rho))) = \mathcal{G}(\Lambda_t(0)) = 0, \quad (\text{N10})$$

such that

$$\begin{aligned} \Lambda_t(\rho - \mathcal{G}(\rho)) &= \Lambda_{t,\text{free}}(\rho - \mathcal{G}(\rho)) + \Lambda_{t,\text{res}}(\rho - \mathcal{G}(\rho)) \\ &= \Lambda_{t,\text{res}}(\rho - \mathcal{G}(\rho)). \end{aligned} \quad (\text{N11})$$

This implies that

$$\text{Tr}[M\Lambda_t(\rho - \mathcal{G}(\rho))] = \text{Tr}[M\Lambda_{t,\text{res}}(\rho - \mathcal{G}(\rho))] \quad \forall \rho \in \mathcal{D}(\mathcal{H}), \quad (\text{N12})$$

and taking the supremum over  $\rho$  yields

$$\mathcal{C}_M(\Lambda_t) = \mathcal{C}_M(\Lambda_{t,\text{res}}). \quad (\text{N13})$$

□

### Appendix O: Proof of Corollary 11

*Proof.* The equivalence follows from the chain rule

$$\frac{d}{dt}\Lambda_{t,\text{free}} = \mathcal{L}_{t,\text{free}} \circ \Lambda_{t,\text{free}} + (\mathcal{G} \circ \mathcal{L}_t \circ \mathcal{G}^\perp) \circ (\mathcal{G}^\perp \circ \Lambda_t \circ \mathcal{G}) \quad (\text{O1})$$

with the initial condition  $\Lambda_{0,\text{free}} = \mathcal{G}$  originating from the definition of  $\Lambda_{t,\text{free}}$  in Eq. (61). □

### Appendix P: Derivation of $\mathcal{C}_M(\Lambda)$ and $\Gamma_M(t)$ for the donor-acceptor model

In this section we provide the detailed derivation of the resource impact functional  $\mathcal{C}_M(\Lambda)$ , the instantaneous

rate  $\Gamma_M(t)$ , and the associated variation and time bounds for the donor-acceptor model.

We recall the three-step process  $\Lambda = \Lambda_{\text{AD}} \circ \Lambda_{\text{PD}} \circ \Lambda_\theta$  from Eq. (99), where  $\Lambda_\theta$  is the unitary channel generated by the excitonic Hamiltonian in Eq. (96) and describes coherent mixing between the singly excited donor and acceptor states,  $\Lambda_{\text{PD}}$  is a phase-damping channel acting on the excited-state manifold, and  $\Lambda_{\text{AD}}$  describes spontaneous emission from  $|D\rangle$  and  $|A\rangle$  to the ground state  $|g\rangle$  via amplitude damping. Each map is CPTP, and so is their concatenation.

Let  $K_i^{\text{PD}}$  and  $K_k^{\text{AD}}$  denote Kraus operators of  $\Lambda_{\text{PD}}$  and  $\Lambda_{\text{AD}}$ , with  $i \in \{0, 1\}$  and  $k \in \{0, 1, 2\}$ . A Kraus representation of  $\Lambda_{\text{AD}} \circ \Lambda_{\text{PD}}$  is then given by  $K_{ik} := K_i^{\text{AD}} K_k^{\text{PD}}$ , and one convenient choice (in the basis  $\{|g\rangle, |D\rangle, |A\rangle\}$ ) is given by

$$\begin{aligned} K_{00} &= |g\rangle\langle g| + \sqrt{\frac{(1+\eta)(1-p_D)}{2}}|D\rangle\langle D| \\ &\quad + \sqrt{\frac{(1+\eta)(1-p_A)}{2}}|A\rangle\langle A|, \\ K_{10} &= \sqrt{\frac{(1-\eta)(1-p_D)}{2}}|D\rangle\langle D| \\ &\quad - \sqrt{\frac{(1-\eta)(1-p_A)}{2}}|A\rangle\langle A|, \\ K_{01} &= \sqrt{\frac{p_D(1+\eta)}{2}}|g\rangle\langle D|, \quad K_{02} = \sqrt{\frac{p_A(1+\eta)}{2}}|g\rangle\langle A|, \\ K_{11} &= \sqrt{\frac{p_D(1-\eta)}{2}}|g\rangle\langle D|, \quad K_{12} = -\sqrt{\frac{p_A(1-\eta)}{2}}|g\rangle\langle A|. \end{aligned} \quad (\text{P1})$$

Here  $\eta$  is the phase damping parameter, and  $p_D, p_A$  are the spontaneous emission probabilities from  $|D\rangle$  and  $|A\rangle$ , respectively. One readily checks that  $\sum_j K_j^\dagger K_j = \mathbb{1}$ . A Kraus representation for the full channel  $\Lambda$  is obtained by composing these with the unitary  $U_\theta$  in Eq. (97), that is,  $\{K_j U_\theta\}_j$ .

Since  $\mathcal{G}$  in Eq. (95) is linear and Hermitian, we work in the following in the Heisenberg picture with  $\mathcal{C}_M(\Lambda)$  given by Eq. (7). The adjoint of the quantum channel  $\Lambda$  acts on  $M$  as

$$\Lambda^\dagger(M) = \Lambda_\theta^\dagger \circ \Lambda_{\text{PD}}^\dagger \circ \Lambda_{\text{AD}}^\dagger(M), \quad (\text{P2})$$

and for a POVM element  $M$  of the form in Eq. (100) this yields the expression for  $\mathcal{C}_M(\Lambda)$  shown in Eq. (98).

To compute the advantage rate  $\Gamma_M(t)$  we propagate  $\Lambda_t^\dagger(M)$  under the adjoint Lindblad generator  $\mathcal{L}^\dagger$  associated with  $\Lambda$ . In the time-independent case,  $\Lambda_t^\dagger = e^{t\mathcal{L}^\dagger}$  satisfies the Heisenberg equation

$$\frac{d}{dt}\Lambda_t^\dagger(M) = \mathcal{L}^\dagger(\Lambda_t^\dagger(M)) \quad (\text{P3})$$

$$\begin{aligned} &= i \left[ H_{\text{ex}}, \Lambda_t^\dagger(M) \right] + \sum_{k=1}^4 \left( L_k^\dagger \Lambda_t^\dagger(M) L_k \right. \\ &\quad \left. - \frac{1}{2} \left\{ L_k^\dagger L_k, \Lambda_t^\dagger(M) \right\} \right), \end{aligned} \quad (\text{P4})$$

where the jump operators are

$$\begin{aligned} L_1 &= \sqrt{\gamma_\varphi}|D\rangle\langle D|, & L_2 &= \sqrt{\gamma_\varphi}|A\rangle\langle A|, \\ L_3 &= \sqrt{\gamma_D}|g\rangle\langle D|, & L_4 &= \sqrt{\gamma_A}|g\rangle\langle A|. \end{aligned} \quad (\text{P5})$$

The dephasing rate  $\gamma_\varphi$  and the relaxation rates  $\gamma_D, \gamma_A$  are related to the finite-time parameters by  $\eta(\Delta t) = e^{-\gamma_\varphi \Delta t}$  and  $p_i(\Delta t) = 1 - e^{-\gamma_i \Delta t}$ ,  $i \in \{D, A\}$ .

For an observable  $M$  of the form in Eq. (100), the dynamics (P3) does not generate coherences between  $|g\rangle$  and  $\{|D\rangle, |A\rangle\}$ , so  $\Lambda_t^\dagger(M)$  preserves the block-diagonal form of  $M$  according to

$$\begin{aligned} \Lambda_t^\dagger(M) &= x_g(t)|g\rangle\langle g| + x_D(t)|D\rangle\langle D| + x_A(t)|A\rangle\langle A| \\ &\quad + (y(t)|D\rangle\langle A| + \text{h.c.}), \end{aligned} \quad (\text{P6})$$

with  $x_g(t), x_D(t), x_A(t) \in \mathbb{R}$  and  $y(t) \in \mathbb{C}$ . Inserting this ansatz into Eq. (P3) yields the following set of coupled linear differential equations

$$\begin{aligned} \frac{d}{dt}x_D(t) &= 2J\Im[y(t)] + \gamma_D[x_g(t) - x_D(t)], \\ \frac{d}{dt}x_A(t) &= -2J\Im[y(t)] + \gamma_A[x_g(t) - x_A(t)], \\ \frac{d}{dt}y(t) &= i[\Delta y(t) + J(x_A(t) - x_D(t))] - \xi y(t), \end{aligned} \quad (\text{P7})$$

where  $\xi := \gamma_\varphi + (\gamma_D + \gamma_A)/2$ . The initial conditions are  $x_g(0) = \mu_g$ ,  $x_D(0) = \mu_D$ ,  $x_A(0) = \mu_A$ , and  $y(0) = \nu$ , where  $\mu_g, \mu_D, \mu_A, \nu$  are the matrix elements of  $M$ .

Writing  $y(t) = u(t) + iv(t)$  and collecting the variables into

$$\mathbf{z}(t) := (u(t), v(t), x_D(t), x_A(t))^T \quad (\text{P8})$$

the system in (P7) takes the form

$$\frac{d}{dt}\mathbf{z}(t) = A\mathbf{z}(t) + \mathbf{b} \quad (\text{P9})$$

with

$$\mathbf{b} := (0, 0, \gamma_D\mu_g, \gamma_A\mu_g)^T, \quad (\text{P10})$$

$$A := \begin{pmatrix} -\xi & -\Delta & 0 & 0 \\ \Delta & -\xi & -J & J \\ 0 & 2J & -\gamma_D & 0 \\ 0 & -2J & 0 & -\gamma_A \end{pmatrix}. \quad (\text{P11})$$

The inhomogeneous term can be removed by introducing shifted variables

$$\tilde{x}_D := x_D - \mu_g, \quad \tilde{x}_A := x_A - \mu_g, \quad (\text{P12})$$

which leaves  $A$  unchanged. In terms of  $\tilde{\mathbf{z}} := (u, v, \tilde{x}_D, \tilde{x}_A)^T$ , this leads to  $d\mathbf{z}(t)/dt = A\mathbf{z}(t)$  with initial condition

$$\tilde{\mathbf{z}}(0) = (\Re(\nu), \Im(\nu), \mu_D - \mu_g, \mu_A - \mu_g)^T \quad (\text{P13})$$

and, hence,  $\tilde{\mathbf{z}}(t) = e^{At}\tilde{\mathbf{z}}(0)$ . Evaluating  $\tilde{\mathbf{z}}(t)$  analytically for general parameters  $(\gamma_\varphi, \gamma_D, \gamma_A, \Delta, J)$  is cumbersome. In the following, we therefore specialise to the cases (i)  $\gamma_\varphi = 0$  with  $\gamma_D = \gamma_A$ , and (ii)  $\Delta = 0$  with  $\gamma_D = \gamma_A$ , for which closed-form expressions and explicit time bounds can be obtained.

### 1. Zero dephasing and symmetric lifetimes

For  $\gamma_\varphi = 0$  and symmetric lifetimes  $\gamma_D = \gamma_A = \gamma$  we have  $\xi = \gamma$ , and the eigenvalues of the matrix  $A$  in Eq. (P10) are

$$\lambda_1 = \lambda_2 = -\gamma, \quad \lambda_{3,4} = -\gamma \pm i\Omega, \quad (\text{P14})$$

where  $\Omega = \sqrt{4J^2 + \Delta^2}$  is the generalised Rabi frequency. It is convenient to introduce the population difference

$$s(t) := x_A(t) - x_D(t) \quad (\text{P15})$$

and the total excited-state population

$$N(t) := x_A(t) + x_D(t). \quad (\text{P16})$$

With the initial conditions in Eq. (P13), one obtains

$$\begin{aligned} u(t) &= e^{-\gamma t} \left[ \Re(\nu) - \frac{\Delta \Im(\nu)}{\Omega} \sin(\Omega t) \right. \\ &\quad \left. + \frac{\Delta[\Delta \Re(\nu) + J(\mu_A - \mu_D)]}{\Omega^2} (\cos(\Omega t) - 1) \right], \\ v(t) &= e^{-\gamma t} \left[ \Im(\nu) \cos(\Omega t) \right. \\ &\quad \left. + \frac{\Delta \Re(\nu) + J(\mu_A - \mu_D)}{\Omega} \sin(\Omega t) \right], \\ s(t) &= e^{-\gamma t} \left[ \mu_A - \mu_D - \frac{4J\Im(\nu)}{\Omega} \sin(\Omega t) \right. \\ &\quad \left. + \frac{4J[\Delta \Re(\nu) + J(\mu_A - \mu_D)]}{\Omega^2} (\cos(\Omega t) - 1) \right], \\ N(t) &= 2\mu_g + (\mu_A + \mu_D - 2\mu_g)e^{-\gamma t}. \end{aligned} \quad (\text{P17})$$

For  $\mathcal{G}$  the dephasing map in the site basis  $\{|g\rangle, |A\rangle, |D\rangle\}$ , the task-response functional and the instantaneous rate take the simple form

$$\mathcal{C}_M(\Lambda_t) = |y(t)|, \quad \Gamma_M(t) = \left| \frac{dy(t)}{dt} \right|, \quad (\text{P18})$$

since  $(\text{id} - \mathcal{G})\Lambda_t^\dagger(M)$  is supported only on the  $|D\rangle\langle A|/|A\rangle\langle D|$  block with eigenvalues  $\pm|y(t)|$ . Thus  $\mathcal{C}_M(\Lambda_t)$  follows directly from  $u(t), v(t)$  in Eq. (P17), and  $\Gamma_M(t)$  is obtained by differentiating  $y(t) = u(t) + iv(t)$ .

For the measurement operator  $M = |A\rangle\langle A|$ , this yields the instantaneous rate

$$\Gamma_{|A\rangle\langle A|}(t) = e^{-\gamma t} |J| \sqrt{\Delta^2 \left( \frac{\gamma(\cos(\Omega t) - 1)}{\Omega^2} + \frac{\sin(\Omega t)}{\Omega} \right)^2 + \left( \cos(\Omega t) - \frac{\gamma}{\Omega} \sin(\Omega t) \right)^2}. \quad (\text{P19})$$

We now apply Theorem 7 to bound the change

$$\begin{aligned} |\Delta \mathcal{C}_{|A\rangle\langle A|}| &\equiv |\mathcal{C}_{|A\rangle\langle A|}(\Lambda_{t_2}) - \mathcal{C}_{|A\rangle\langle A|}(\Lambda_{t_1})| \\ &\leq \int_{t_1}^{t_2} ds \Gamma_{|A\rangle\langle A|}(s), \end{aligned} \quad (\text{P20})$$

where the implicit time-dependence of  $|\Delta \mathcal{C}_{|A\rangle\langle A|}|$  is omitted to simplify the notation. For generic  $\Delta$ , the integral in Eq. (P19) is best evaluated numerically and we illustrate both the actual change  $|\Delta \mathcal{C}_{|A\rangle\langle A|}|$  evaluated from Eq. (P18) and the variation bound  $\int_0^t ds \Gamma_{|A\rangle\langle A|}(t)$  for  $t_1 = 0$  and  $t_2 \geq t_1$  and a chosen set of parameters in Fig. 4 in the main text.

We continue with a discussion of the uniform time and feasibility bounds from Corollary 9. For this, we recall that Corollary 9 implies that for any  $t_1 \leq t_2$

$$|\mathcal{C}_M(\Lambda_{t_2}) - \mathcal{C}_M(\Lambda_{t_1})| \leq \Delta \tau c_{M,\mathcal{G}} \sup_{s \in [t_1, t_2]} \|\mathcal{L}_s\|_{1 \rightarrow 1}, \quad (\text{P21})$$

where  $\Delta \tau := t_2 - t_1$ , with  $c_{M,\mathcal{G}} = \|M\|_\infty R_{\mathcal{G}}$  and  $R_{\mathcal{G}}$  the resource radius defined in Eq. (16). In the donor-acceptor model considered in this section, the generator  $\mathcal{L}_s \equiv \mathcal{L}$  is time-independent, such that

$$L_{\max} := \sup_{s \in [t_1, t_2]} \|\mathcal{L}_s\|_{1 \rightarrow 1} = \|\mathcal{L}\|_{1 \rightarrow 1}, \quad (\text{P22})$$

and the bound becomes

$$|\mathcal{C}_M(\Lambda_{t_2}) - \mathcal{C}_M(\Lambda_{t_1})| \leq \Delta \tau c_{M,\mathcal{G}} \|\mathcal{L}\|_{1 \rightarrow 1}. \quad (\text{P23})$$

While  $\|\mathcal{L}\|_{1 \rightarrow 1}$  can in principle be computed exactly for fixed  $(\Delta, J, \gamma)$  via semidefinite programming, there is no simple closed-form expression in terms of these parameters. An analytic estimate of the induced trace norm  $\|\mathcal{L}\|_{1 \rightarrow 1}$  is obtained by splitting  $\mathcal{L}$  into its Hamiltonian and dissipative parts (recall  $L_1 = L_2 = 0$  for  $\gamma_\varphi = 0$ ),

$$\mathcal{L}(\rho) = -i[H_{\text{ex}}, \rho] + \underbrace{\sum_{k=3,4} \left( L_k \rho L_k^\dagger - \frac{1}{2} \{L_k^\dagger L_k, \rho\} \right)}_{=: \mathcal{D}(\rho)}, \quad (\text{P24})$$

with  $H_{\text{ex}}$  and  $L_k$  given by Eqs. (96) and (P5). Then, for any operator  $X \in \mathcal{B}_{\text{sa}}(\mathcal{H})$  we have

$$\| -i[H_{\text{ex}}, X] \|_1 \leq 2 \|H_{\text{ex}}\|_\infty \|X\|_1, \quad (\text{P25})$$

where we used Hölder's inequality for Schatten  $p$ -norms, such that  $\| -i[H_{\text{ex}}, \cdot] \|_{1 \rightarrow 1} \leq 2 \|H_{\text{ex}}\|_\infty$ . Since the eigenvalues of  $H_{\text{ex}}$  on the  $\{|D\rangle, |A\rangle\}$  subspace are  $\pm \Omega/2$  with  $\Omega = \sqrt{4J^2 + \Delta^2}$ , we obtain  $\|H_{\text{ex}}\|_\infty = \Omega/2$  and hence  $\| -i[H_{\text{ex}}, \cdot] \|_{1 \rightarrow 1} \leq \Omega$ .

To bound the second term in Eq. (P24), we observe that each jump operator  $L_k$ ,

$$\begin{aligned} \|L_k X L_k^\dagger\|_1 &\leq \|L_k\|_\infty^2 \|X\|_1, \\ \left\| \frac{1}{2} \{L_k^\dagger L_k, X\} \right\|_1 &\leq \|L_k^\dagger L_k\|_\infty \|X\|_1 = \|L_k\|_\infty^2 \|X\|_1, \end{aligned} \quad (\text{P26})$$

which implies that

$$\left\| L_k X L_k^\dagger - \frac{1}{2} \{L_k^\dagger L_k, X\} \right\|_1 \leq 2 \|L_k\|_\infty^2 \|X\|_1. \quad (\text{P27})$$

and, thus, the dissipator  $\mathcal{D}(\cdot)$  in Eq. (P24) satisfies

$$\begin{aligned} \|\mathcal{D}\|_{1 \rightarrow 1} &:= \left\| \sum_{k=3,4} L_k(\cdot) L_k^\dagger - \frac{1}{2} \{L_k^\dagger L_k, \cdot\} \right\|_{1 \rightarrow 1} \\ &\leq 2 \sum_{k=3,4} \|L_k\|_\infty^2. \end{aligned} \quad (\text{P28})$$

In the zero-dephasing, symmetric-lifetime case, we have  $L_3 = \sqrt{\gamma} |g\rangle\langle D|$  and  $L_4 = \sqrt{\gamma} |g\rangle\langle A|$ , such that  $\|L_3\|_\infty^2 = \|L_4\|_\infty^2 = \gamma$  and

$$\|\mathcal{D}\|_{1 \rightarrow 1} \leq 4\gamma. \quad (\text{P29})$$

Combining these estimates via the triangle inequality eventually yields

$$\|\mathcal{L}\|_{1 \rightarrow 1} \leq \Omega + 4\gamma = \sqrt{4J^2 + \Delta^2} + 4\gamma. \quad (\text{P30})$$

Inserting Eq. (P30) into Eq. (P23) gives the explicit uniform variation bound

$$|\mathcal{C}_M(\Lambda_{t_2}) - \mathcal{C}_M(\Lambda_{t_1})| \leq \Delta \tau c_{M,\mathcal{G}} \left( \sqrt{4J^2 + \Delta^2} + 4\gamma \right). \quad (\text{P31})$$

For the donor-acceptor yield observable  $M = |A\rangle\langle A|$ , we have  $\|M\|_\infty = 1$ , so  $c_{M,\mathcal{G}} = R_{\mathcal{G}}$ , which is a fixed constant depending only on the dephasing map  $\mathcal{G}$  in the site basis with  $R_{\mathcal{G}} < 2$ . Here it is important to note that the bound in Eq. (P31) will be in general an upper bound to the (numerically determined) true value of  $\|\mathcal{L}\|_{1 \rightarrow 1}$ , which is not directly accessible in a closed analytic form for the chosen Lindblad generator describing the dynamics of our donor-acceptor dimer.

On resonance,  $\Delta = 0$  and  $\Omega = 2|J|$  (see also Appendix P2 for a general discussion of zero detuning with non-zero dephasing), the expressions for the resource impact functional and the instantaneous rate simplify to

$$\mathcal{C}_{|A\rangle\langle A|}(\Lambda_t) = \frac{1}{2} e^{-\gamma t} |\sin(2Jt)| \quad (\text{P32})$$

and

$$\begin{aligned} \Gamma_{|A\rangle\langle A|}(t) &= e^{-\gamma t} |J| \left| \cos(2Jt) - \frac{\gamma}{2J} \sin(2Jt) \right| \\ &= e^{-\gamma t} |J| R |\cos(2Jt + \phi)|, \end{aligned} \quad (\text{P33})$$

where

$$R := \sqrt{1 + \frac{\gamma^2}{4J^2}}, \quad \phi := \arctan\left(\frac{\gamma}{2J}\right). \quad (\text{P34})$$

Using  $|\cos(\cdot)| \leq 1$ , we obtain the uniform variation bound

$$|\Delta C_{|A\rangle\langle A|}| \leq \frac{|J|}{\gamma} \sqrt{1 + \frac{\gamma^2}{4J^2}} (e^{-\gamma t_1} - e^{-\gamma t_2}). \quad (\text{P35})$$

For a fixed initial time  $t_1$ , Eq. (P35) yields a lower bound on the minimal time  $\Delta\tau^* = t_2 - t_1$  (recall Eq. (54)) required to achieve a target change  $|\Delta C_{|A\rangle\langle A|}^*|$ :

$$\Delta\tau^* \geq \frac{1}{\gamma} \ln \left( 1 - \frac{\gamma e^{\gamma t_1} |\Delta C_{|A\rangle\langle A|}^*|}{|J| \sqrt{1 + \gamma^2/(4J^2)}} \right)^{-1}. \quad (\text{P36})$$

Feasibility (i.e., the existence of a finite  $\Delta\tau > 0$ ) requires the argument of the logarithm to be at least one, which is equivalent to

$$0 \leq \frac{\gamma e^{\gamma t_1} |\Delta C_{|A\rangle\langle A|}^*|}{|J| \sqrt{1 + \gamma^2/(4J^2)}} < 1, \quad (\text{P37})$$

or

$$|\Delta C_{|A\rangle\langle A|}| < \frac{|J|}{\gamma} e^{-\gamma t_1} \sqrt{1 + \frac{\gamma^2}{4J^2}} \quad (\text{feasibility bound}). \quad (\text{P38})$$

Thus the maximal achievable change in the task capacity over any interval starting at  $t_1$  is directly bounded in terms of the coupling  $J$  and decay rate  $\gamma$ . If the desired  $|\Delta C_{|A\rangle\langle A|}|$  exceeds this bound in Eq. (P38), it cannot be achieved within this model: no amount of coherence generated by  $\Lambda_\theta$  will produce such a change in finite time for the given  $J$  and  $\gamma$ .

Finally, we return to the looser uniform bound arising bounding  $\|\mathcal{L}_s\|_{1 \rightarrow 1} \leq L_{\max}$  in Eq. (P31). Specialising to resonance,  $\Delta = 0$  and, thus,  $\Omega = 2|J|$ , the bound in Eq. (P31) becomes

$$|\Delta C_{|A\rangle\langle A|}| \leq \Delta\tau R_G (2|J| + 4\gamma). \quad (\text{P39})$$

As expected, this  $L_{\max}$ -based uniform bound is looser than the resonant bound in Eq. (P35), which exploits the explicit form of  $\Gamma_{|A\rangle\langle A|}(t)$  and its exponential decay. In particular, the right-hand side of Eq. (P35) saturates at a finite value as  $t_2 \rightarrow \infty$ , whereas Eq. (P31) grows linearly with  $\Delta\tau$ .

## 2. Zero detuning and symmetric lifetimes

We now consider the case of zero detuning,  $\Delta = 0$ , and symmetric lifetimes  $\gamma_A = \gamma_D = \gamma$ , while the pure dephasing rate  $\gamma_\varphi$  remains arbitrary. For  $\Delta = 0$ , the coupled linear differential equations in Eq. (P7) simplify to

$$\begin{aligned} \frac{d}{dt}u(t) &= -\xi u(t), & \frac{d}{dt}v(t) &= -\xi v(t) + Js(t), \\ \frac{d}{dt}s(t) &= -4Jv(t) - \gamma s(t), & \frac{d}{dt}N(t) &:= -\gamma[N(t) - 2\mu_g] \end{aligned} \quad (\text{P40})$$

with

$$\xi := \gamma_\varphi + \gamma. \quad (\text{P41})$$

The equations for  $u$  and  $N$  integrate immediately to

$$u(t) = \Re(\nu) e^{-\xi t}, \quad (\text{P42})$$

$$N(t) = (\mu_A + \mu_D - 2\mu_g) e^{-\gamma t} + 2\mu_g. \quad (\text{P43})$$

The remaining coupled equations for  $v(t)$  and  $s(t)$  can be rearranged into a single damped harmonic oscillator equation. Then, eliminating  $s(t)$  yields

$$\frac{d^2}{dt^2}v(t) + (\gamma + \xi) \frac{d}{dt}v(t) + (4J^2 + \gamma\xi)v(t) = 0, \quad (\text{P44})$$

with characteristic roots

$$\lambda_{\pm} = -\frac{1}{2} \left( \gamma + \xi \pm \sqrt{\gamma_\varphi^2 - 16J^2} \right). \quad (\text{P45})$$

In the following, we distinguish the underdamped regime  $\gamma_\varphi < 4|J|$ , the overdamped regime  $\gamma_\varphi > 4|J|$ , and the critical case  $\gamma_\varphi = 4|J|$ .

In the underdamped case,  $\gamma_\varphi < 4|J|$ , the roots are complex,  $\lambda_{\pm} = -\zeta \pm i\omega$ , with

$$\zeta := \frac{\gamma + \xi}{2}, \quad \omega := \frac{1}{2} \sqrt{16J^2 - \gamma_\varphi^2}. \quad (\text{P46})$$

Imposing the initial conditions  $v(0) = \Im(\nu)$  and  $s(0) = \mu_A - \mu_D$  leads to

$$v(t) = e^{-\zeta t} \left[ \Im(\nu) \cos(\omega t) + \frac{2J(\mu_A - \mu_D) - \gamma_\varphi \Im(\nu)}{2\omega} \sin(\omega t) \right], \quad (\text{P47})$$

$$s(t) = e^{-\zeta t} \left[ (\mu_A - \mu_D) \cos(\omega t) + \frac{\gamma_\varphi(\mu_A - \mu_D) - 8J\Im(\nu)}{2\omega} \sin(\omega t) \right]. \quad (\text{P48})$$

In the overdamped case,  $\gamma_\varphi > 4|J|$ , the roots are real and negative,  $\lambda_\pm = -\zeta \pm \kappa$ , with

$$\kappa := \frac{1}{2}\sqrt{\gamma_\varphi^2 - 16J^2} > 0, \quad (\text{P49})$$

and the solutions become

$$v(t) = e^{-\zeta t} \left[ \Im(\nu) \cosh(\kappa t) + \frac{2J(\mu_A - \mu_D) - \gamma_\varphi \Im(\nu)}{2\kappa} \sinh(\kappa t) \right], \quad (\text{P50})$$

$$s(t) = e^{-\zeta t} \left[ (\mu_A - \mu_D) \cosh(\kappa t) + \frac{\gamma_\varphi(\mu_A - \mu_D) - 8J\Im(\nu)}{2\kappa} \sinh(\kappa t) \right]. \quad (\text{P51})$$

The critical case  $\gamma_\varphi = 4|J|$  is obtained as the limit  $\omega \rightarrow 0$  (or equivalently  $\kappa \rightarrow 0$ ) and yields polynomial prefactors multiplying  $e^{-(\gamma+2|J|)t}$ . In all three regimes the task advantage norm and instantaneous advantage rate follow as

$$\mathcal{C}_M(\Lambda_t) = \sqrt{u^2(t) + v^2(t)}, \quad (\text{P52})$$

$$\Gamma_M(t) = \sqrt{\xi^2 u^2(t) + [Js(t) - \xi v(t)]^2}, \quad (\text{P53})$$

in agreement with Eq. (P18).

To obtain analytic variation and time bounds, we first use

$$\Gamma_M(t) = \sqrt{\xi^2 u^2(t) + [Js(t) - \xi v(t)]^2} \leq |\xi u(t)| + |Js(t) - \xi v(t)| \quad (\text{P54})$$

and then bound the two contributions separately. The first term gives

$$\int_{t_1}^{t_2} ds |\xi u(s)| = |\Re(\nu)| (e^{-\xi t_1} - e^{-\xi t_2}), \quad (\text{P55})$$

while the second term leads to exponentially decaying envelopes in the underdamped and overdamped regimes. In the underdamped case, Eqs. (P47)–(P48) imply

$$Js(t) - \xi v(t) = e^{-\zeta t} [a_u \cos(\omega t) + b_u \sin(\omega t)], \quad (\text{P56})$$

with

$$a_u := J(\mu_A - \mu_D) - \xi \Im(\nu), \quad (\text{P57})$$

$$b_u := \frac{\Im(\nu)(\xi\gamma_\varphi - 8J^2) - J(\mu_A - \mu_D)(\gamma + \xi)}{2\omega}, \quad (\text{P58})$$

such that

$$|Js(t) - \xi v(t)| \leq e^{-\zeta t} R_u, \quad R_u := \sqrt{a_u^2 + b_u^2}. \quad (\text{P59})$$

In the overdamped case one similarly finds

$$Js(t) - \xi v(t) = e^{-\zeta t} [a_o \cosh(\kappa t) + b_o \sinh(\kappa t)], \quad (\text{P60})$$

with

$$b_o := \frac{\Im(\nu)(\xi\gamma_\varphi - 8J^2) - J(\mu_A - \mu_D)(2\gamma + \gamma_\varphi)}{2\kappa}. \quad (\text{P61})$$

Since  $k, t \geq 0$ , we can use in the overdamped case  $\sinh(x)^2 + \cosh(x)^2 = \cosh(2x) \leq e^{2x}$  for  $x \geq 0$  and apply Cauchy-Schwarz inequality to obtain

$$\begin{aligned} |a \cosh(x) + b \sinh(x)| &\leq \sqrt{a^2 + b^2} \sqrt{\cosh(2x)} \\ &\leq e^x \sqrt{a^2 + b^2}, \end{aligned} \quad (\text{P62})$$

which leads to

$$|Js(t) - \xi v(t)| \leq e^{(\kappa - \zeta)t} R_o, \quad R_o := \sqrt{a_o^2 + b_o^2}. \quad (\text{P63})$$

Below, we skip the critical case as it follows again from the other two cases by taking a suitable limit  $\omega \rightarrow 0/\kappa \rightarrow 0$ . We then eventually obtain for the variation bound

$$|\Delta \mathcal{C}_M| \leq \int_{t_1}^{t_2} ds \Gamma_M(s) \leq \Re(\nu) (e^{-\xi t_1} - e^{-\xi t_2}) + \begin{cases} \frac{R_u}{\zeta} (e^{-\zeta t_1} - e^{-\zeta t_2}) & \text{if } \gamma_\varphi < 4|J| \\ \frac{R_o}{\zeta - \kappa} (e^{(\kappa - \zeta)t_1} - e^{(\kappa - \zeta)t_2}) & \text{if } \gamma_\varphi > 4|J| \end{cases}. \quad (\text{P64})$$

The variation bound on  $|\Delta \mathcal{C}_M|$  (P64) is valid for any  $M$  of the form in Eq. (100).

To obtain uniform time bounds analytically, we consider in the following again the special case  $M = |A\rangle\langle A|$  as then the first term on the right-hand side in Eq. (P64) vanishes and we can solve for an anticipated  $|\Delta \mathcal{C}_{|A\rangle\langle A}|^*$  for the

minimal time  $\Delta\tau^* \geq 0$ :

$$\Delta\tau^* \geq \begin{cases} \frac{1}{\zeta} \ln \left( 1 - \frac{\zeta |\Delta C_{|A\rangle\langle A|}^*| e^{\zeta t_1}}{R_u} \right)^{-1} & \text{if } \gamma_\varphi < 4|J| \\ \frac{1}{\zeta - \kappa} \ln \left( 1 - \frac{(\zeta - \kappa) |\Delta C_{|A\rangle\langle A|}^*| e^{(\zeta - \kappa) t_1}}{R_o} \right)^{-1} & \text{if } \gamma_\varphi > 4|J| \end{cases}. \quad (\text{P65})$$

In analogy to Sec. P1, the time bound eventually yields a hard constraint on the maximal possible magnitude of the yield change in terms of the respective system parameters, namely

$$|\Delta C_{|A\rangle\langle A|}| < \begin{cases} \frac{R_u}{\zeta} e^{-\zeta t_1} & \text{if } \gamma_\varphi < 4|J| \\ \frac{R_o}{\zeta - \kappa} e^{-(\zeta - \kappa) t_1} & \text{if } \gamma_\varphi > 4|J| \end{cases}, \quad (\text{P66})$$

which constitutes a strict feasibility bound for finite times  $t_2 \geq 0$ .

- 
- [1] M. R. Wasielewski, M. D. E. Forbes, N. L. Frank, K. Kowalski, G. D. Scholes, J. Yuen-Zhou, M. A. Baldo, D. E. Freedman, R. H. Goldsmith, T. I. Goodson, M. L. Kirk, J. K. McCusker, J. P. Ogilvie, D. A. Shultz, S. Stoll, and K. B. Whaley, Exploiting chemistry and molecular systems for quantum information science, *Nat. Rev. Chem.* **4**, 490 (2020).
- [2] G. D. Scholes, A molecular perspective on quantum information, *Proc. R. Soc. A: Math. Phys. Eng. Sci.* **479**, 20230599 (2023).
- [3] W. Wu and G. D. Scholes, Foundations of quantum information for physical chemistry, *J. Phys. Chem. Lett.* **15**, 4056 (2024).
- [4] Y. Zhang, C. P. Oberg, Y. Hu, H. Xu, M. Yan, G. D. Scholes, and M. Wang, Molecular and supramolecular materials: From light-harvesting to quantum information science and technology, *J. Phys. Chem. Lett.* **15**, 3294 (2024).
- [5] G. D. Scholes, A. Olaya-Castro, S. Mukamel, A. Kirrander, K. K. Ni, G. J. Hedley, and N. L. Frank, The quantum information science challenge for chemistry, *J. Phys. Chem. Lett.* **16**, 1376 (2025).
- [6] J. Rissler, R. M. Noack, and S. R. White, Measuring orbital interaction using quantum information theory, *Chem. Phys.* **323**, 519 (2006).
- [7] K. Boguslawski, P. Tecmer, Ö. Legeza, and M. Reiher, Entanglement measures for single- and multireference correlation effects, *J. Phys. Chem. Lett.* **3**, 3129 (2012).
- [8] Y. Zhao, K. Boguslawski, P. Tecmer, C. Duperrouzel, G. Barcza, Ö. Legeza, and P. W. Ayers, Dissecting the bond-formation process of d<sup>10</sup>-metal-ethene complexes with multireference approaches, *Theor. Chem. Acc.* **134**, 120 (2015).
- [9] C. Duperrouzel, P. Tecmer, K. Boguslawski, G. Barcza, Ö. Legeza, and P. W. Ayers, A quantum informational approach for dissecting chemical reactions, *Chem. Phys. Lett.* **621**, 160 (2015).
- [10] K. Boguslawski and P. Tecmer, Orbital entanglement in quantum chemistry, *Int. J. Quantum Chem.* **115**, 1289 (2015).
- [11] J. Brandejejs, L. Veis, S. Szalay, G. Barcza, J. Pittner, and Ö. Legeza, Quantum information-based analysis of electron-deficient bonds, *J. Chem. Phys.* **150**, 204111 (2019).
- [12] L. Ding, S. Mardazad, S. Das, S. Szalay, U. Schollwöck, Z. Zimborás, and C. Schilling, Concept of orbital entanglement and correlation in quantum chemistry, *J. Chem. Theory Comput.* **17**, 79 (2021).
- [13] L. Ding, S. Knecht, Z. Zimborás, and C. Schilling, Quantum correlations in molecules: from quantum resourcing to chemical bonding, *Quantum Sci. Technol.* **8**, 015015 (2022).
- [14] L. Ding, G. Dünneweber, and C. Schilling, Physical entanglement between localized orbitals, *Quantum Sci. Technol.* **9**, 015005 (2024).
- [15] K. Liao, L. Ding, and C. Schilling, Quantum information orbitals (QIO): Unveiling intrinsic many-body complexity by compressing single-body triviality, *J. Phys. Chem. Lett.* **15**, 6782 (2024).
- [16] D. Aliverti-Piuri, K. Chatterjee, L. Ding, K. Liao, J. Liebert, and C. Schilling, What can quantum information theory offer to quantum chemistry?, *Faraday Discuss.* **254**, 76 (2024).
- [17] Y. Zhao, D. Zhao, C. Rong, S. Liu, and P. W. Ayers, Information theory meets quantum chemistry: A review and perspective, *Entropy* **27**, 10.3390/e27060644 (2025).
- [18] L. Ding, E. Matito, and C. Schilling, From entanglement to bonds: Chemical bonding concepts from quantum information theory, *arXiv preprint* (2025), [arXiv:2501.15699 \[quant-ph\]](https://arxiv.org/abs/2501.15699).
- [19] G. Greene-Diniz, C. N. Self, M. Krompiec, L. Coopmans, M. Benedetti, D. Muñoz Ramo, and M. Rosenkranz, Measuring correlation and entanglement between molecular orbitals on a trapped-ion quantum computer, *Sci. Rep.* **15**, 28409 (2025).
- [20] N. Glaser, A. Baiardi, A. Z. Lieberherr, and M. Reiher, Vibrational entanglement through the lens of quantum information measures, *J. Phys. Chem. Lett.* **15**, 6958 (2024).
- [21] Y. Wang, A. Benny, B. Le Dé, A. W. Chin, and G. D. Scholes, A numerically exact description of ultrafast vibra-

- tional decoherence in vibration-coupled electron transfer, *Proc. Natl. Acad. Sci. U.S.A.* **122**, e2416542122 (2025).
- [22] R. O. Esquivel, M. Molina-Espíritu, A. R. Plastino, and J. S. Dehesa, Quantum information from selected elementary chemical reactions: Maximum entangled transition state, *Int. J. Quantum Chem.* **115**, 1417 (2015).
- [23] G. S. Engel, T. R. Calhoun, E. L. Read, T.-K. Ahn, T. Mančal, Y.-C. Cheng, R. E. Blankenship, and G. R. Fleming, Evidence for wavelike energy transfer through quantum coherence in photosynthetic systems, *Nature* **446**, 782 (2007).
- [24] M. B. Plenio and S. F. Huelga, Dephasing-assisted transport: quantum networks and biomolecules, *New J. Phys.* **10**, 113019 (2008).
- [25] E. Collini, C. Y. Wong, K. E. Wilk, P. M. G. Curmi, P. Brumer, and G. D. Scholes, Coherently wired light-harvesting in photosynthetic marine algae at ambient temperature, *Nature* **463**, 644 (2010).
- [26] G. Panitchayangkoon, D. Hayes, K. A. Fransted, J. R. Caram, E. Harel, J. Wen, R. E. Blankenship, and G. S. Engel, Long-lived quantum coherence in photosynthetic complexes at physiological temperature, *Proc. Natl. Acad. Sci. U.S.A.* **107**, 12766 (2010).
- [27] A. Ishizaki and G. R. Fleming, Quantum superpositions in photosynthetic light harvesting: delocalization and entanglement, *New J. Phys.* **12**, 055004 (2010).
- [28] S. Mukamel, Communications: Signatures of quasiparticle entanglement in multidimensional nonlinear optical spectroscopy of aggregates, *J. Chem. Phys.* **132**, 241105 (2010).
- [29] A. Olaya-Castro and G. D. Scholes, Energy transfer from Förster–Dexter theory to quantum coherent light-harvesting, *Int. Rev. Phys. Chem.* **30**, 49 (2011).
- [30] G. S. Engel, Quantum coherence in photosynthesis, *Procedia Chem.* **3**, 222 (2011).
- [31] N. Christensson, H. F. Kauffmann, T. Pullerits, and T. Mančal, Origin of long-lived coherences in light-harvesting complexes, *J. Phys. Chem. B* **116**, 7449 (2012).
- [32] E. Harel and G. S. Engel, Quantum coherence spectroscopy reveals complex dynamics in bacterial light-harvesting complex 2 (LH2), *Proc. Natl. Acad. Sci. U.S.A.* **109**, 706 (2012).
- [33] E. Romero, R. Augulis, V. I. Novoderezhkin, M. Ferretti, J. Thieme, D. Zigmantas, and R. van Grondelle, Quantum coherence in photosynthesis for efficient solar-energy conversion, *Nat. Phys.* **10**, 676 (2014).
- [34] A. Chenu and G. D. Scholes, Coherence in energy transfer and photosynthesis, *Annu. Rev. Phys. Chem.* **66**, 69 (2015).
- [35] H.-G. Duan, V. I. Prokhorenko, R. J. Cogdell, K. Ashraf, A. L. Stevens, M. Thorwart, and R. J. D. Miller, Nature does not rely on long-lived electronic quantum coherence for photosynthetic energy transfer, *Proc. Natl. Acad. Sci. U.S.A.* **114**, 8493 (2017).
- [36] A. Streltsov, G. Adesso, and M. B. Plenio, Colloquium: Quantum coherence as a resource, *Rev. Mod. Phys.* **89**, 041003 (2017).
- [37] G. D. Scholes, G. R. Fleming, L. X. Chen, A. Aspuru-Guzik, A. Buchleitner, D. F. Coker, G. S. Engel, R. van Grondelle, A. Ishizaki, D. M. Jonas, J. S. Lundeen, J. K. McCusker, S. Mukamel, J. P. Ogilvie, A. Olaya-Castro, M. A. Ratner, F. C. Spano, K. B. Whaley, and X. Zhu, Using coherence to enhance function in chemical and biophysical systems, *Nature* **543**, 647 (2017).
- [38] J. Cao, R. Cogdell, D. F. Coker, H.-G. Duan, J. Hauer, U. Kleinekathöfer, T. L. C. Jansen, T. Mančal, R. J. D. Miller, J. P. Ogilvie, V. Prokhorenko, T. Renger, H.-S. Tan, R. Tempelaar, M. Thorwart, E. Thyryhaug, S. Westenhoff, and D. Zigmantas, Quantum biology revisited, *Sci. Adv.* **6**, eaaz4888 (2020).
- [39] C. Chuang and P. Brumer, LH1–RC light-harvesting photocycle under realistic light–matter conditions, *J. Chem. Phys.* **152**, 154101 (2020).
- [40] A. E. Sifain, F. Fassioli, and G. D. Scholes, Toward witnessing molecular exciton entanglement from spectroscopy, *Phys. Rev. A* **104**, 042416 (2021).
- [41] T. Jiang, J. Ren, and Z. Shuai, Unified definition of exciton coherence length for exciton–phonon coupled molecular aggregates, *J. Phys. Chem. Lett.* **14**, 4541 (2023).
- [42] L. F. Calderón, C. Chuang, and P. Brumer, Electronic–vibrational resonance does not significantly alter steady-state transport in natural light-harvesting systems, *J. Phys. Chem. Lett.* **14**, 1436 (2023).
- [43] D. F. E. Bajac, A. D. Zapata Escobar, and G. A. Aucar, Molecular response properties, electron correlation, and quantum entanglement, *J. Chem. Theory Comput.* **21**, 4674 (2025).
- [44] S. M. Harvey and M. R. Wasielewski, Photogenerated spin-correlated radical pairs: From photosynthetic energy transduction to quantum information science, *J. Am. Chem. Soc.* **143**, 15508 (2021).
- [45] T. Mani, Molecular qubits based on photogenerated spin-correlated radical pairs for quantum sensing, *Chem. Phys. Rev.* **3**, 021301 (2022).
- [46] T. P. Fay, L. P. Lindoy, D. E. Manolopoulos, and P. J. Hore, How quantum is radical pair magnetoreception?, *Faraday Discuss.* **221**, 77 (2020).
- [47] E. Chitambar and G. Gour, Quantum resource theories, *Rev. Mod. Phys.* **91**, 025001 (2019).
- [48] G. Gour, *Quantum Resource Theories* (Cambridge University Press, Cambridge, 2025).
- [49] C. Napoli, T. R. Bromley, M. Cianciaruso, M. Piani, N. Johnston, and G. Adesso, Robustness of coherence: An operational and observable measure of quantum coherence, *Phys. Rev. Lett.* **116**, 150502 (2016).
- [50] R. Takagi, B. Regula, K. Bu, Z.-W. Liu, and G. Adesso, Operational advantage of quantum resources in sub-channel discrimination, *Phys. Rev. Lett.* **122**, 140402 (2019).
- [51] R. Takagi and B. Regula, General resource theories in quantum mechanics and beyond: Operational characterization via discrimination tasks, *Phys. Rev. X* **9**, 031053 (2019).
- [52] M. Oszmaniec and T. Biswas, Operational relevance of resource theories of quantum measurements, *Quantum* **3**, 133 (2019).
- [53] C. Napoli, T. R. Bromley, M. Cianciaruso, M. Piani, N. Johnston, and G. Adesso, Robustness of coherence: An operational and observable measure of quantum coherence, *Phys. Rev. Lett.* **116**, 150502 (2016).
- [54] L. Li, K. Bu, and Z.-W. Liu, Quantifying the resource content of quantum channels: An operational approach, *Phys. Rev. A* **101**, 022335 (2020).
- [55] Z.-W. Liu, X. Hu, and S. Lloyd, Resource destroying maps, *Phys. Rev. Lett.* **118**, 060502 (2017).
- [56] G. Gour, Quantum resource theories in the single-shot

- regime, *Phys. Rev. A* **95**, 062314 (2017).
- [57] M. Sarkis and A. Tkatchenko, Are molecules magical? Non-stabilizerness in molecular bonding, [arXiv:2504.06673](https://arxiv.org/abs/2504.06673) (2025).
- [58] N. Yunger Halpern and D. T. Limmer, Fundamental limitations on photoisomerization from thermodynamic resource theories, *Phys. Rev. A* **101**, 042116 (2020).
- [59] D. Siciliano, R. B. P. Pietsch, G. Spaventa, S. F. Huelga, and M. B. Plenio, Correlated dynamics as a resource in molecular switches, *Phys. Rev. A* **112**, 042411 (2025).
- [60] J. J. Omiste, J. Floß, and P. Brumer, Coherent control of penning and associative ionization: Insights from symmetries, *Phys. Rev. Lett.* **121**, 163405 (2018).
- [61] A. Devolder, T. V. Tschersbul, and P. Brumer, Leveraging reactant entanglement in the coherent control of ultracold bimolecular chemical reactions, *Phys. Rev. Lett.* **135**, 233401 (2025).
- [62] P. Zanardi, C. Zalka, and L. Faoro, Entangling power of quantum evolutions, *Phys. Rev. A* **62**, 030301 (2000).
- [63] F. Galve, F. Plastina, M. G. A. Paris, and R. Zambrini, Discording power of quantum evolutions, *Phys. Rev. Lett.* **110**, 010501 (2013).
- [64] A. Mani and V. Karimipour, Cohering and decohering power of quantum channels, *Phys. Rev. A* **92**, 032331 (2015).
- [65] K. Bu, A. Kumar, L. Zhang, and J. Wu, Cohering power of quantum operations, *Phys. Lett. A* **381**, 1670 (2017).
- [66] K. Ben Dana, M. García Díaz, M. Mejatty, and A. Winter, Resource theory of coherence: Beyond states, *Phys. Rev. A* **95**, 062327 (2017).
- [67] Q. Zhuang, P. W. Shor, and J. H. Shapiro, Resource theory of non-Gaussian operations, *Phys. Rev. A* **97**, 052317 (2018).
- [68] G. Styliaris, L. Campos Venuti, and P. Zanardi, Coherence-generating power of quantum dephasing processes, *Phys. Rev. A* **97**, 032304 (2018).
- [69] P. Zanardi and L. Campos Venuti, Quantum coherence generating power, maximally abelian subalgebras, and Grassmannian geometry, *J. Math. Phys.* **59**, 012203 (2018).
- [70] J. R. Seddon and E. T. Campbell, Quantifying magic for multi-qubit operations, *Proc. R. Soc. A* **475**, 20190251 (2019).
- [71] T. Theurer, D. Egloff, L. Zhang, and M. B. Plenio, Quantifying operations with an application to coherence, *Phys. Rev. Lett.* **122**, 190405 (2019).
- [72] S. Mandal, M. Narozniak, C. Radhakrishnan, Z.-Q. Jiao, X.-M. Jin, and T. Byrnes, Characterizing coherence with quantum observables, *Phys. Rev. Res.* **2**, 013157 (2020).
- [73] K. Kuroiwa, R. Takagi, G. Adesso, and H. Yamasaki, Every quantum helps: Operational advantage of quantum resources beyond convexity, *Phys. Rev. Lett.* **132**, 150201 (2024).
- [74] A. A. Clerk, M. H. Devoret, S. M. Girvin, F. Marquardt, and R. J. Schoelkopf, Introduction to quantum noise, measurement, and amplification, *Rev. Mod. Phys.* **82**, 1155 (2010).
- [75] M. Hawton, Photon position measure, *Phys. Rev. A* **82**, 012117 (2010).
- [76] B. Hellenkamp, S. Schmid, O. Doroshenko, O. Opanasyuk, R. Kühnemuth, S. Rezaei Adarini, B. Ambrose, M. Aznauryan, A. Barth, V. Birkedal, M. E. Bowen, H. Chen, T. Cordes, T. Eilert, C. Fijen, C. Gebhardt, M. Götz, G. Gouridis, E. Gratton, T. Ha, P. Hao, C. A. Hanke, A. Hartmann, J. Hendrix, L. L. Hildebrandt, V. Hirschfeld, J. Hohlbein, B. Hua, C. G. Hübner, E. Kallis, A. N. Kapanidis, J.-Y. Kim, G. Krainer, D. C. Lamb, N. K. Lee, E. A. Lemke, B. Levesque, M. Levitus, J. J. McCann, N. Naredi-Rainer, D. Nettle, T. Ngo, R. Qiu, N. C. Robb, C. Röcker, H. Sanabria, M. Schlierf, T. Schröder, B. Schuler, H. Seidel, L. Streit, J. Thurn, P. Tinnefeld, S. Tyagi, N. Vandenberk, A. M. Vera, K. R. Weninger, B. Wünsch, I. S. Yanez-Orozco, J. Michaelis, C. A. M. Seidel, T. D. Craggs, and T. Hugel, Precision and accuracy of single-molecule FRET measurements—a multi-laboratory benchmark study, *Nat. Methods* **15**, 669 (2018).
- [77] L. Leppäjärvi and M. Sedlák, Postprocessing of quantum instruments, *Phys. Rev. A* **103**, 022615 (2021).
- [78] T. Heinosaari, M. A. Jivulescu, and I. Nechita, Order preserving maps on quantum measurements, *Quantum* **6**, 853 (2022).
- [79] E. Haapasalo, Minimal sufficient positive-operator valued measure on a separable Hilbert space, *J. Math. Phys.* **56**, 102205 (2015).
- [80] T. Heinosaari, T. Miyadera, and M. Ziman, An invitation to quantum incompatibility, *J. Phys. A* **49**, 123001 (2016).
- [81] R. Beneduci, Positive operator valued measures and Feller Markov kernels, *J. Math. Anal. Appl.* **442**, 50 (2016).
- [82] R. T. Rockafellar, *Convex Analysis* (Princeton University Press, 1997).
- [83] A. Barvinok, *A Course in Convexity*, Graduate Studies in Mathematics, Vol. 54 (American Mathematical Society, Providence, RI, 2002) p. 366.
- [84] M. J. W. Hall, J. D. Cresser, L. Li, and E. Andersson, Canonical form of master equations and characterization of non-Markovianity, *Phys. Rev. A* **89**, 042120 (2014).
- [85] S. Scopa, G. T. Landi, A. Hammoumi, and D. Karevski, Exact solution of time-dependent lindblad equations with closed algebras, *Phys. Rev. A* **99**, 022105 (2019).
- [86] M. M. Taddei, B. M. Escher, L. Davidovich, and R. L. de Matos Filho, Quantum speed limit for physical processes, *Phys. Rev. Lett.* **110**, 050402 (2013).
- [87] A. del Campo, I. L. Egusquiza, M. B. Plenio, and S. F. Huelga, Quantum speed limits in open system dynamics, *Phys. Rev. Lett.* **110**, 050403 (2013).
- [88] I. Marvian, R. W. Spekkens, and P. Zanardi, Quantum speed limits, coherence, and asymmetry, *Phys. Rev. A* **93**, 052331 (2016).
- [89] S. Deffner and S. Campbell, Quantum speed limits: from Heisenberg’s uncertainty principle to optimal quantum control, *J. Phys. A* **50**, 453001 (2017).
- [90] G. Lindblad, On the generators of quantum dynamical semigroups, *Comm. Math. Phys.* **48**, 119 (1976).
- [91] D. Chruściński and S. Maniscalco, Degree of non-Markovianity of quantum evolution, *Phys. Rev. Lett.* **112**, 120404 (2014).
- [92] H.-P. Breuer, E.-M. Laine, J. Piilo, and B. Vacchini, Colloquium: Non-Markovian dynamics in open quantum systems, *Rev. Mod. Phys.* **88**, 021002 (2016).
- [93] Alternatively, one could replace the inner  $\max_{\pi(\rho) \in \mathcal{P}(\rho)}$  by a min (conservative scenario) or fix a particular selection rule for  $\pi(\rho)$ . In case the minimiser of  $D(\cdot \| \cdot)$  is

- unique, all these conventions coincide on the level of the resource impact functional. However, for the variation bound in terms of  $\Gamma_M(t)$  below it is required to either work with twice a maximum (i.e., over  $\rho$  and  $\pi(\rho)$ ) or twice a minimum.
- [94] C. W. Helstrom, *Quantum Detection and Estimation Theory* (Academic Press, New York, 1976).
- [95] M. A. Nielsen and I. L. Chuang, *Quantum Computation and Quantum Information: 10th Anniversary Edition* (Cambridge University Press, 2010).
- [96] J. Watrous, *The Theory of Quantum Information* (Cambridge University Press, Cambridge, 2018).
- [97] F. Hiai and D. Petz, The proper formula for relative entropy and its asymptotics in quantum probability, *Commun. Math. Phys.* **143**, 99 (1991).
- [98] T. Ogawa and H. Nagaoka, Strong converse and Stein's lemma in quantum hypothesis testing, *IEEE Trans. Inf. Theory* **46**, 2428 (2000).
- [99] O. Mülken and T. Schmid, Environment-assisted quantum transport and trapping in dimers, *Phys. Rev. E* **82**, 042104 (2010).
- [100] A. Thilagam, Non-hermitian exciton dynamics in a photosynthetic unit system, *J. Chem. Phys.* **136**, 065104 (2012).
- [101] E. J. O'Reilly and A. Olaya-Castro, Non-classicality of the molecular vibrations assisting exciton energy transfer at room temperature, *Nat. Commun.* **5**, 3012 (2014).
- [102] P.-Y. Yang and J. Cao, Steady-state analysis of light-harvesting energy transfer driven by incoherent light: From dimers to networks, *J. Phys. Chem. Lett.* **11**, 7204 (2020).
- [103] Y.-C. Cheng and G. R. Fleming, Dynamics of light harvesting in photosynthesis, *Annu. Rev. Phys. Chem.* **60**, 241 (2009).
- [104] A. Ishizaki and G. R. Fleming, Theoretical examination of quantum coherence in a photosynthetic system at physiological temperature, *Proc. Natl. Acad. Sci. U. S. A.* **106**, 17255 (2009).
- [105] A. Ishizaki and G. R. Fleming, On the adequacy of the Redfield equation and related approaches to the study of quantum dynamics in electronic energy transfer, *J. Chem. Phys.* **130**, 234110 (2009).
- [106] A. Ishizaki and G. R. Fleming, Unified treatment of quantum coherent and incoherent hopping dynamics in electronic energy transfer: reduced hierarchy equation approach, *J. Chem. Phys.* **130**, 234111 (2009).
- [107] M. Sarovar, A. Ishizaki, G. R. Fleming, and K. B. Whaley, Quantum entanglement in photosynthetic light-harvesting complexes, *Nat. Phys.* **6**, 462 (2010).
- [108] A. Ishizaki and G. R. Fleming, Quantum coherence in photosynthetic light harvesting, *Annu. Rev. Condens. Matter Phys.* **3**, 333 (2012).
- [109] M. K. Lee, P. Huo, and D. F. Coker, Semiclassical path integral dynamics: Photosynthetic energy transfer with realistic environment interactions, *Annu. Rev. Phys. Chem.* **67**, 639 (2016).
- [110] T. Mirkovic, E. E. Ostroumov, J. M. Anna, R. van Grondelle, Govindjee, and G. D. Scholes, Light absorption and energy transfer in the antenna complexes of photosynthetic organisms, *Chem. Rev.* **117**, 249 (2017).
- [111] A. Jha, F. Zheng, Z. Liu, S. Mukamel, M. Thorwart, R. J. D. Miller, and H.-G. Duan, Quantum coherent dynamics in photosynthetic protein complexes, *Chem. Soc. Rev.* [10.1039/D5CS00948K](https://doi.org/10.1039/D5CS00948K) (2026), advance Article.
- [112] F. A. Pollock, C. A. Rodríguez-Rosario, T. Frauenheim, M. Paternostro, and K. Modi, Non-Markovian quantum processes: Complete framework and efficient characterization, *Phys. Rev. A* **97**, 012127 (2018).
- [113] F. A. Pollock, K. Modi, C. A. Rodríguez-Rosario, T. Frauenheim, and M. Paternostro, Operational markov condition for quantum processes, *Phys. Rev. Lett.* **120**, 040405 (2018).
- [114] S. Milz, F. A. Pollock, and K. Modi, Completely positive divisibility does not mean Markovianity, *Phys. Rev. Lett.* **123**, 040401 (2019).
- [115] M. R. Jørgensen and F. A. Pollock, Exploiting the causal tensor network structure of quantum processes to efficiently simulate non-Markovian path integrals, *Phys. Rev. Lett.* **123**, 240602 (2019).
- [116] S. Milz and K. Modi, Quantum stochastic processes and quantum non-Markovianity, *PRX Quantum* **1**, 010301 (2020).
- [117] R. de Wit, J. Keeling, B. W. Lovett, and A. W. Chin, Process tensor approaches to modeling two-dimensional spectroscopy, *Phys. Rev. Res.* **7**, 013209 (2025).
- [118] M. Cygorek and E. M. Gauger, Understanding and utilizing the inner bonds of process tensors, *SciPost Phys.* **18**, 024 (2025).
- [119] J. Keeling, E. M. Stoudenmire, M.-C. Bañuls, and D. R. Reichman, Process tensor approaches to non-Markovian quantum dynamics, [arXiv:2509.07661](https://arxiv.org/abs/2509.07661) (2025).
- [120] M. Shubrook, M. Cygorek, E. Gauger, J. Iles-Smith, and A. Nazir, Numerically exact open quantum system work statistics with process tensors, [arXiv:2512.16823](https://arxiv.org/abs/2512.16823) (2025).
- [121] J. Yuen-Zhou and A. Aspuru-Guzik, Quantum process tomography of excitonic dimers from two-dimensional electronic spectroscopy. i. general theory and application to homodimers, *J. Chem. Phys.* **134**, 134505 (2011).
- [122] J. Yuen-Zhou, J. J. Krich, M. Mohseni, and A. Aspuru-Guzik, Quantum state and process tomography of energy transfer systems via ultrafast spectroscopy, *Proc. Natl. Acad. Sci. U.S.A.* **108**, 17615 (2011).
- [123] L. Chuntonov and J. Ma, Quantum process tomography quantifies coherence transfer dynamics in vibrational exciton, *J. Phys. Chem. B* **117**, 13631 (2013).
- [124] L. A. Pachón, A. H. Marcus, and A. Aspuru-Guzik, Quantum process tomography by 2D fluorescence spectroscopy, *J. Chem. Phys.* **142**, 212442 (2015).
- [125] K. Gururangan and E. Harel, Coherent and dissipative quantum process tensor reconstructions in two-dimensional electronic spectroscopy, *J. Chem. Phys.* **150**, 164127 (2019).
- [126] A. Rivas, S. F. Huelga, and M. B. Plenio, Entanglement and non-Markovianity of quantum evolutions, *Phys. Rev. Lett.* **105**, 050403 (2010).
- [127] D. Chruściński and A. Kossakowski, Non-Markovian quantum dynamics: Local versus nonlocal, *Phys. Rev. Lett.* **104**, 070406 (2010).
- [128] I. de Vega and D. Alonso, Dynamics of non-Markovian open quantum systems, *Rev. Mod. Phys.* **89**, 015001 (2017).
- [129] R. Bhatia, *Matrix Analysis*, Graduate Texts in Mathematics, Vol. 169 (Springer-Verlag, New York, 1997).
- [130] A. Y. Kitaev, Quantum computations: algorithms and error correction, *Russ. Math. Surv.* **52**, 1191 (1997).
- [131] J. Watrous, Notes on super-operator norms induced by

- Schatten norms, [arXiv:quant-ph/0411077](#) (2004).
- [132] J. Watrous, Semidefinite programs for completely bounded norms, [Theory of Computing](#) **5**, 217 (2009).
- [133] G. Benenti and G. Strini, Computing the distance between quantum channels: usefulness of the Fano representation, [J. Phys. B: At. Mol. Opt. Phys.](#) **43**, 215508 (2010).
- [134] M. Tomamichel, *Quantum Information Processing with Finite Resources: Mathematical Foundations*, Springer-Briefs in Mathematical Physics, Vol. 5 (Springer, Cham, 2016).
- [135] R. Bhatia and F. Kittaneh, Commutators, pinchings, and spectral variation, [Operators and Matrices](#) **2**, 143 (2008).
- [136] J. Neyman and E. S. Pearson, IX. On the problem of the most efficient tests of statistical hypotheses, [Philos. Trans. R. Soc. A](#) **231**, 289 (1933).
- [137] W. Hoeffding, Probability inequalities for sums of bounded random variables, [J. Am. Stat. Assoc.](#) **58**, 13 (1963).
- [138] R. Kannan and C. K. Krueger, Dini derivatives, in *Advanced Analysis*, Universitext (Springer, New York, NY, 1996) pp. 55–80.